ELECTRONIC STRUCTURE STUDIES ON SOME MAIN GROUP COMPOUNDS AND ORGANOMETALLICS

A Thesis
Submitted for the Degree of
DOCTOR OF PHILOSOPHY

by

Gantasala Naga Srinivas

School of Chemistry
University of Hyderabad
Hyderabad 500 046
INDIA

July 1996

*Dedicated to
my father,   mother,
sister and brother.*

Contents

Chapter 3: Studies on Si_3H_3X and A4H4 Molecules.

Chapter 4: Studies on Ti_xC_{12} Cluster and Transition Metal-Containing
            Poly-ynes.

Statement

I hereby declare that the work embodied in the thesis is the result of investigations carried out by me in the School of Chemistry, University of Hyderabad, Hyderabad, India under the supervision of **Professor Eluvathingal D. Jemmis.**

In keeping with the general practice of reporting scientific observations, due acknowledgements have been made wherever the work described is based on the findings of other investigators.

G. Naga Srinivas

July 1996

Certificate

Certified that the work contained in the thesis entitled **Electronic Structure Studies on Some Main Group Compounds and Organometallics** has been carried out by Mr. G. Naga Srinivas under my supervision and the same has not been submitted elsewhere for any degree.
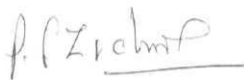
Eluvathingal D. Jemmis

Thesis Supervisor

Dean

School of Chemistry

Acknowledgements

With great pleasure I wish to thank my supervisor Professor E.D. Jemmis for providing me the opportunity to study the chemical problems theoretically. His valuable guidance in both academic and personal sphere was highly inspiring throughout my tenure as a research student.

I express my sincere thanks to the Dean and the faculty members of the school of chemistry. Special thanks are due to Professor K. D. Sen and Dr. M. Durga prasad.

I am very fortunate to have a group of highly co-operative lab-mates, both past and present, who made me feel very comfortable all these days.

I would like to avail this opportunity to thank Professors P.v.R. Schleyer, J. Leszczynski and Dr. A. A. Korkin for their help in calculations.

I thank the non-teaching staff of the School of Chemistry for their help.

I greatly acknowledge the financial assistance from UGC, New Delhi throughout my tenure.

I am indebted to my family members who always stood by me, providing a strong support to rely on.

G. Naga Srinivas

Abbreviations

MO	: Molecular Orbital
HOMO	: highest occupied molecular orbital
LUMO	: lowest unoccupied molecular orbital
EH	: extended Huckel
FMO	: fragment molecular orbital
xz, yz, etc.	: xz, yz etc are used instead of d_{xz}, d_{yz}, etc
eV	: electron volts
DOS	: density of states
COOP	: crystal orbital overlap population
H_b	: bridging hydrogen
H_t	: terminal hydrogen
Bu	: butyl
t-Bu	: tertiary butyl
Me	: methyl
Et	: ethyl
C_p	: cyclopentadienyl anion
Ph	: phenyl
2c-2e	: two centre-two electron
3c-2e	: three centre-two electron
HF	: Hartree-Fock
MP2	: second order M0ller-Plesset perturbation
NBO	: natural bond orbital

Introduction

The trends in chemical and physical properties of the elements are enshrined in the periodic table. All of chemistry involves various combinations of these elements. The synthesis of new molecules with novel structures and properties is the most exciting area in chemistry. Detailed understanding of molecular shapes and reactivity helps in the progress of chemistry. Often compounds formed from elements in the same group do not have a general pattern of chemical behaviour. It is necessary to know how properties differ within broad classes of molecules.

Quantum chemistry provides a basis for the understanding of the molecular structure, thermodynamic stabilities and chemical reactivities of the molecules. Computational theoretical chemistry is able today to provide reliable information on any reasonably small system, independent of the limitations inherent in the experimental approach, such as the inability to observe short lived species. One of the most practical approaches for the quantitative application of quantum chemistry is through the molecular orbital approximation. This thesis deals with the molecular orbital calculations on some main group compounds and organometallics selected for specific characteristics that they are anticipated to demonstrate. Several of these are awaiting synthesis. A brief description of the problems studied is given below.

Cyclopropenium ion (C3H3+) is the smallest *2n* aromatic system known so far. The all-boron analog $(B_3H_6^+)$ and the all-silicon analog $(Si_3H_3^+)$ of $C_3H_3^+$ are studied in chapter 1. In section 1 we describe the

study of potential energy surface of $B_3H_6^+$. The cyclobutadiene dication has paved way for nonplanar 2π aromatic compounds. The boron substituted 1,3-diborocyclobutadiene has been characterised experimentally. Therefore, the study of a systematic boron substitution in $C_3H_3^+$ leading to $C2BH3$, $CB2H4$, $B3H5$ and $B_3H_6^+$ has been considered in this chapter. The cyclic aromatic compounds and their acyclic counterparts are also studied and analysed in detail. The nonplanar structure of $B_3H_6^+$, where three bridging and three terminal hydrogens are on the opposite sides of B3 plane is found to be the global minimum. Section 2 describes the study of potential energy surface of the $Si_3H_3^+$. In spite of silicon belonging to the same group as carbon, there are many anomalies between carbon chemistry and silicon chemistry, as Josef Michl expresses *"Silicon and Carbon - are they kissing cousins? They are alike in so many ways and yet, they are so different"}* In this regard there are many studies on anions and cations of silicon compounds.

The ion molecular reactions in silane produced $Si_3H_3^+$ along with many other cations. This cation is isoelectronic to $C_3H_3^+$ and the study of the potential energy surface of $Si_3H_3^+$ will be interesting to see how the *2n* aromaticity effects these silicon cations. Due to the diagonal relationship between silicon and boron, and the isolobal analogy between divalent silicon and trivalent boron, various bridged isomers have also been studied along with the classical isomers in this chapter. Though the classical *2n* electron delocalized trisilacyclopropenium is the global minimum for $Si_3H_3^+$, there are many bridged structures which are close to the global minimum and these are more stable than the other classical structures.

After the analysis of aromatic systems in chapter 1, corresponding saturated compounds are studied in chapter 2. This chapter mainly deals with the heavier analogs of cyclopropane and cyclobutane. Though all the elements in the group 14 have some common properties, there are many differences in their chemistry. For example, ethene A_2H_4 (A = C) is a planar molecule; the heavier analogs (A = Si and Ge) are non planar. Moving still further, the Sn_2H_4 and Pb_2H_4 have bridged structures. This shows how each element differs from the other within the group. It is also known that the heavier elements in this group show the divalency compared to carbon which is tetravalent. These differences lead to the study of the strained ring systems in group 14, and change in their behaviour on descending the group has been studied. Various H-bridged alternatives are also considered in this study.

The cyclopropenium ion is a versatile 2-electron ligand for various main group as well as for organometallic fragments. The section 1 of chapter 3 is devoted to the study of similar patterns for the newly detected silicon analog $Si_3H_3^+$. Various capping fragments (X) are considered for Si_3H_3X molecules and their bonding properties have been studied in detail. The experience gained in chapter 1 and 2 on bridged isomers allowed to study the triply H-bridged Si_3H_3X, which, interestingly, was found to be more stable than the classical systems. These structures were related to the various organometallic complexes through isolobal and isosynaptic analogies. If one applies these analogies to tetrametal tetrahedranes, one arrives at various kinds of tetrahedranes in group 14, which is the main theme in section 2 of this chapter. Different kinds of hydrogen environment in $H_4M_4(L)_{12}$ leads to variety of structures for A4H4 (A = C, Si, Ge, Sn

and Pb). Despite the strain, the substituted tetrahedrane of carbon C_4R_4 (R = t-Bu) was prepared experimentally. However, the same could be achieved for Si_4R_4 only when the R group is very bulky (super silyl). Hence, the classical tetrahedranes in group 14 and their analogs derived from organometallic chemistry lead to an interesting study. The findings in this chapter strengthen the relation between organometallic compounds and their main group analogs.

Hence from $C_3H_3^+$ to $B_3H_6^+$, $Si_3H_3^+$ and then to the saturated alicyclic compounds A_3H_6 and A_4H_8 are studied in chapters 1 and 2. The chapter 3 is devoted to study the 2-electron ligand nature of $Si_3H_3^+$ in a similar fashion to $C_3H_3^+$ and then extended to tetrahedranes in group 14 (A_4H_4). The relation between these studies is summarised in Scheme 1.

Chapter 4 consists of two sections. Section 1 deals with the study of reaction centres in Metallacarbohedrenes. These new clusters are first introduced by Castleman, the first example being Ti_8C_{12}. These compounds lead to another field in cluster chemistry and the clusters are named as Met-Cars (the abbreviated form of Metallacarbohedrenes). Various experimental groups have extended the work on Met-Cars and prepared M_8C_{12} clusters with a variety of metal, M, ranging from early transition metal Sc to the late transition metal Fe. Different kinds of geometries are suggested for these clusters. The most important ones are the T_h and D_{2d} structures based on dodecahedrene. The third one which is stable than the above two is derived as tetracapped tetrahedrane structure. In the present chapter, we have studied possible reaction centres in these varieties of geometries.

Scheme 1
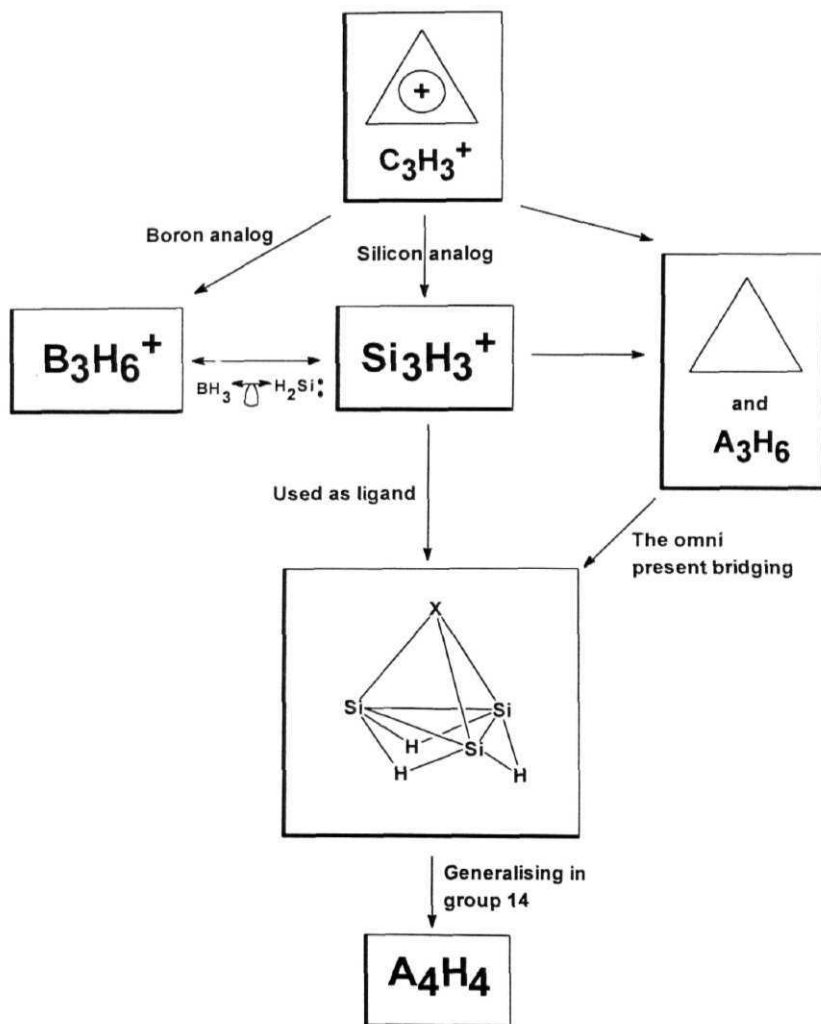
Section 2 describes the electronic structure study of polymers. The metal containing poly-yne polymers are one of the important fields in the polymer chemistry. There were many experiments with various metal and carbon chains to get the low band gap polymer. These low band gap polymers will help in developing various materials viz. non-linear optical devices and conducting molecular wires. The main aim in this study is to scan the various metals and carbon chains to decrease the band gap. This is achieved for Iron which will also be cost effective for experimental preparation. Not only the metal and the carbon chain but also the topology of the substituents in the carbon chain are also found to be playing significant roles in band gap alteration.

Different theoretical methods are chosen depending on the problem under study and the available facilities. For higher level of calculations with a large amount of computational time, collaborations are sought from the people with better computer facilities and their contributions are acknowledged. A brief introduction of the theoretical methods used in this thesis is given below.

The molecular orbital calculations are approximate solutions to the time-independent Schrodinger equation.[2]

$$\mathbf{H\psi = E\psi}$$

where

H   is the Hamiltonian operator.

ψ is the molecular wavefunction.

E   is the energy of the system.

The Hamiltonian, H, is made up of kinetic and potential energy terms. That is

$$H = T + V$$

where the kinetic energy represents the summation of ∇^2 over all the particles in molecule

$$T = -(h2/87r2) \; \Sigma(1/m_k) \; (\partial^2/\partial x^2 + \partial^2/\partial y^2 + \partial^2/\partial z^2)$$

and the potential energy is the coulomb repulsion between each pair of charged entities (approximating each atomic nucleus to be a single charged mass).

$$V = \sum_i \sum_I \left(\frac{Z_I e^2}{r_{iI}} \right) + \sum_i \sum_{j<i} \left(\frac{e^2}{r_{ij}} \right) + \sum_I \sum_{J<I} \left(\frac{Z_I Z_J e^2}{R_{IJ}} \right)$$

and r, R are distances. In this equation, the first term is electron-nuclei attraction, second term is electron-electron repulsion and the third term is nucleus-nucleus repulsion.

To solve the Schrodinger equation with the complete hamiltonian describing a system is a very complicated process. Therefore, some approximations are necessary to simplify the hamiltonian and the Born-

Oppenheimer approximation is the first of this kind.[3] According to this approximation, the nuclear and electronic kinetic energies are separated and the nuclear kinetic energy is neglected as the mass of nucleus is enormously greater than that of an electron.

$$H = T_{elec} + V_{nucl-elec} + V_{elec} + V_{nucl}$$

The wave function ψ is a mathematical function. To describe a system meaningfully, ψ must be single-valued, finite and continuous at any point in the space under consideration.

Minimization of the total energy of the system with respect to the one electron functions are done using **Hartree-Fock method**.[1d] The Hartree-Fock theory is based on the variational **method**.[4] According to this, a basis set will be selected for orbital expansion and then the coefficients C_{ui} which are adjusted to minimize the expectation value of the energy (E_{expt}).

$$(\partial E_{expt}/\partial C_{ui}) = 0 \quad (all\ u,\ i)$$

When the Hartree-Fock equations are derived using the linear combination of atomic orbitals (LCAO) for the Molecular Orbitals, these are called Roothaan MO equations which are relatively simpler to solve.[5] Solving the Hartree-Fock-Roothaan equations without any empirical parameters is known as *ab initio* MO theory.[6]

In general, the molecular orbital is expanded in terms of a set of atomic orbitals (χ).[7]

$$\phi_i = \sum_u^n c_{ui} \chi_u$$

where

ϕ_i is the i th molecular orbital

C_{ui} are coefficients of linear combinations

χ_u is the u th atomic orbital

n   is the number of atomic orbitals

These atomic orbitals are also called `basis functions'. In the earlier days, Slater Type Orbitals (STO's) were used as basis functions due to their similarity with atomic orbitals of the hydrogen atom.[8] The STO's are represented by

$$\chi_i(\xi, n, l, m; r, \theta, \phi) = N r^{n-1} e^{-\xi r} Y_{lm}(\theta, \phi)$$

where

N   is the normalization constant

ξ is the exponent

r, θ, Φ are the spherical coordinates

Y_{lm} is the angular momentum part (function describing the shape)

n,l,m   are the principal, angular and magnetic quantum numbers
        respectively.

The evaluation of two-electron integrals is the most time consuming for STO's, and hence these STO's are found to be not suitable for fast calculations.[7] To overcome this problem, Gaussian Type Orbitals (GTO's) are introduced.[9] The shape of the STO function can be approximated by taking summation of various GTO's with different exponents and coefficients. The GTO is expressed as

$$g(a,l,m,n;x,y,z) = Ne^{-\alpha r^2} x^l y^m z^n$$

where
N   is normalization constant
a   is an exponent
x,y,z   are cartesian coordinates
l,m,n   are integral exponents at cartesian coordinates
$r^2 = x^2 + y^2 + z^2$

Strictly speaking, the GTO's are not really atomic orbitals, but are simpler functions. Hence, these are referred as primitives. There fore, for molecular calculations a linear combination of gaussian primitives is to be used as basis functions.[10]

In general, the gaussian contractions are obtained by least square fit to slater atomic orbitals. The accuracy of the set depends on the number of

contractions used to represent a single STO (i.e. zeta). Single zeta (SZ), double zeta (DZ), triple zeta (TZ) and quadruple zeta (QZ) etc. represent the number of contractions per STO. In the minimal basis set (i.e. SZ), only one contraction per STO is used. DZ set will have two contractions per STO and so on. Since the valence orbitals are more affected while forming a bond than the inner (core) orbitals, more contractions are employed frequently to describe the valence orbitals. This leads to the development of split-valence (SV) basis sets.

The most popular minimal basis sets are denoted by STO-nG, where n is the number of primitives in the contraction. These sets are obtained by least square fit of the combinations of n gaussian functions to an STO of the same type with £= 1.0. Later, to specify the number of primitives and contractions, the parentheses method has been used: where $(12,9,1) \rightarrow [5,4,1]$ means that 12 s-type and 9 p-type primitives are contracted to form 5 s-type, 4 p-type basis functions respectively and 1 d-primitive is used as a basis function by itself. However, this notation does not tell the number of primitives used in each contraction. The more elaborate notation should list the number of primitives in each contraction. e.g. $(63111,4311,1)$ means that there are 5 s-type contractions consisting of 6,3,1,1 and 1 primitives respectively. The p-shell consists of 4 basis functions with 4,3,1 and 1 primitives and d-shell has 1 uncontracted primitive.

Pople and co-workers have introduced different types of conventions for basis sets.[11] Symbols like n-ijG or n-ijkG have been used. These can be encoded as: n-number of primitives for the inner shells; ij or ijk-number of primitives for contractions in the valence shell. The ij notations describe

sets of valence double zeta quality and ijk sets of triple zeta. For example, the 6-311G set for H_2O represents (6311,311) and (311) contractions for oxygen and hydrogen respectively (can also be written as (6311,311)/(311)). Later, these contractions are augmented with other functions for better description. The most popular method of augmentation are the polarization and diffuse functions.[6,7] Addition of functions having higher values of L (angular quantum number) than the occupied atomic orbitals for the atoms gives polarized functions. For example the d-functions are considered polarization functions for Si, but the p-type functions are not considered as polarization functions for Li. The exponents for polarization functions cannot be derived from Hartree-Fock calculations for the atom, since they are not populated. In practice, these are estimated by explicit optimization using correlated methods. In general, the polarization information is given in parenthesis along with the basis set. For example, 6-31G(d,p), also represented as 6-31G**, uses d-functions as polarization on heavy atoms and p-functions as polarization on H-atom. The 6-311G(3d2f,2p) represents 6-311G set augmented with 3 functions of type d and 2 functions of type f on heavy atoms, and 2 functions of type p on hydrogens, i.e. (6311,311,111,11)/(311,11). Polarization functions are, as a rule, used uncontracted.

Augmentation of basis sets with diffuse functions are necessary for correct description of anions, weak bonds (e.g. hydrogen bonds) and for calculation of properties like dipole moments, polarizabilities etc.[12] Diffuse functions are usually of s and p type. These gaussians have very small exponents and decay slowly with increasing distance from the nucleus. The following notation is used for diffuse functions: n-ij+G or n-ijk+G when 1

diffuse s-type and p-type gaussians (each with the same exponent) are added to a standard basis set on heavy atoms. The n-ij++G or n-ijk++G are obtained by adding 1 diffuse s-type and p-type gaussian on heavy atoms and 1 diffuse s-type gaussian on hydrogens. For example, 6-311++G (2d1f,2p1d) represents (63111,3111,11,1)/(311,11,1).

In most of the cases, the chemical bonding can be described using the valence orbitals of the atoms involved, leaving the core (inner) shell unaffected. This leads to the development of Effective Core Potential (ECP) or Effective Potential (EP) approaches, where the inner shell electrons are treated as averaged potential rathei than actual particles. The ECP's are not orbitals but modification to the hamiltonian, and are very efficient for computational purposes. It is also very easy to incorporate relativistic effects into ECP, which are very important in describing heavier atoms. The core potentials can only be specified for shells that are filled. For rest of the electrons (i.e. valence electrons) one has to provide basis functions, which are optimized for use with the ECP's.

The drawback of the Hartree-Fock theory is that the correlation between the motions of electrons is not treated fully.[13] The inter-electronic interaction is represented by coulomb and exchange terms. The coulomb term represents direct interaction of the electron with the averaged charge of all the others obtained by squaring the one electron wave functions. But, the exchange interaction involves electrons with the same spin only. In reality, an electron in an atom will have instantaneous interactions with all the other electrons. This is the origin of the correlation-energy error.[14] Generally, there are two methods used to estimate the correlation effects

viz. Configuration Interaction (CI) and **Møller-Plesset** perturbation theory.[15,16]

In the CI the wave function is constructed from many Slater determinants. Each of these determinants represent an individual electron configuration. The determinants are constructed by replacing one or more of the occupied orbitals ϕ_i, ϕ_j, ... with virtual spin orbitals ϕ_a, ϕ_b,.....

If one virtual orbital ϕ_a replaces an occupied orbital ϕ_i within the determinant, it is called single substitution ($\psi_i{}^a$). Similarly, in double substitution ($\psi_{ij}{}^{ab}$), two occupied orbitals are replaced by virtual orbitals. Therefore, in full CI, the wave function ψ consists of a linear combination of the **Hartree-Fock** determinants and all substituted determinants. But the full CI is impractical for large molecules and also the correlation effects of inner-shell will be insensitive to chemical environment. The excitations to very high virtual orbitals tend to be less significant than lower energy excitations. Due to these reasons, for all practical purposes only the limited set of substitutions are taken by truncating the CI expansion at some level. For example, if single excitations are added to the HF determinant it is called CIS method. The **CID** adds the double excitations and the CISD adds the singles and doubles. But the limited CI is not size-consistent which can be achieved by Quadratic Configuration Interaction **(QCI)**. For example, QCISD(T) adds triple substitution to QCISD to provide greater accuracy.

The second method to estimate the correlation effects is the **Møller-plesset** perturbation theory,[16] which is mainly derived from many-body perturbation theory.[17] In the limited CI, the hamiltonian matrix is truncated

at some level. But in perturbation model, the hamiltonian is treated as the sum of two parts, the second being a perturbation on the first. Thus, in general, the Hamiltonian is expressed as,

$$H = \mathbf{H}^0 + \mathbf{k}\mathbf{H}^1 + \mathbf{k}^2\mathbf{H}^2 + ...$$

where, k indicates the order of magnitude of the perturbating operator H^1 relative to H^0. The main assumption of perturbation theory is that the eigenstates of H can still be written as a combination of the eigen states in the absence of the perturbation (i.e. eigenstates of H^0).

Therefore, the E and ψ are expressed in the form of power series.

$$E = \mathbf{E}^0 + \mathbf{k}\mathbf{E}^1 + \mathbf{k}^2\mathbf{E}^2 + ...$$
$$\psi = \psi^0 + \mathbf{k}\psi^1 + \mathbf{k}^2\psi^2 + ...$$

The truncation of the series leads to various orders of correlation effects. In the MP2 method the series is truncated at the second order and for MP3 it is truncated at 3rd order and so on. The perturbation methods are more satisfactory than the CID or CISD methods for determining the correlation energy as the size-consistency can be achieved by the termination of the Hamiltonian at any order. The MP2 level of calculations have widely been used in the present study.

It is very difficult to carryout the computations routinely for large polyatomic molecules using the *ab initio* method. Different approximations are made to Hartree-Fock equations to overcome the computational

15

difficulties. The simplest form of approximations is the extended Hückel theory,[18] which is used in the present thesis to study the Metallacarbohedrene clusters. This approximation starts with the Roothaan equation, leaving the Hamiltonian undefined.

$$H \sum_n c_{in} \chi_n = \varepsilon_i \sum c_{in} \chi_n$$

The coefficients c_{in} and the orbital energies ε_i are obtained by solving the secular determinant

$$\left| H_{nm} - \varepsilon\, s_{nm} \right| = 0$$

The explicit form of H_{nm} is never sought and nearly all integrals are represented by empirical parameters. Matrix elements H_{mm} are taken as measures of the electron attracting power of particular atoms. The H_{nm} are approximated as

$$H_{nm} = 0.5k\left(H_{nn} + H_{mm}\right)s_{nm}$$

k is a parameter and the S_{nm} are computed from analytic atomic orbitals centred on the appropriate atoms. Now the matrix elements are fixed, and a simple diagonalization of the determinant yields the ej and coefficients c_{in} of the molecular orbitals. There is no self-consistency as the resulting orbitals are not used in computing the matrix elements again. The total Hückel energy is taken as $\Sigma 2\varepsilon_i$ for a closed-shell molecule. Since the electron-electron interaction is not specifically considered, there is no

concept of exchange and singlet and triplet states are not distinguished. Despite the crude nature of the method very large number of studies concerning geometry and reaction mechanisms are reported in the literature.[9]

All the above discussed methods rely on the wave function of the system. However, Kohn, Hohenberg and Sham have developed an alternative method.[20] According to their method, the electron density could be used as a fundamental quantity to develop a rigorous many-body theory applicable to any atomic, molecular or solid state system. This approach is known as the density functional method.

The Density Functional Theory (DFT) begins with the postulate that the total energy is a functional of the total electron density (p) for given positions of the atomic nuclei (R_α).[21]

$$\mathbf{E} = \mathbf{E}\big[\rho, \mathbf{R}_\alpha\big]$$

Therefore, unlike HF theory, DFT uses a physical observable, the electron density, as fundamental quantity. The total energy is then decomposed into a kinetic energy term T[p], an electrostatic or Coulomb energy term, U[p] and a many-body term $E_{xc}[\rho]$, which contains all the exchange and the correlation effects similar to HF theory.

$$\mathbf{E} = \mathbf{T}\big[\rho\big] + \mathbf{U}\big[\rho\big] + \mathbf{E}_{xc}\big[\rho\big]$$

Then, the total density is decomposed into single-particle densities which originate from one-particle wave functions, ψ_i.

$$\rho(\mathbf{r}) = \sum_{occ} \left| \psi_i(\mathbf{r}) \right|^2$$

Also, the total energy should assume a minimum upon variation of the total electron density.

$$\partial E / \partial \rho = 0$$

From this, **Kohn-Sham** equations arrive as one particle wavefunctions in the form of effective one-particle Schrodinger equations.

$$\left[-\frac{1}{2}\nabla^2 + \mathbf{V}_c(\mathbf{r}) + \mu_{xc}(\mathbf{r}) \right] \psi_i = \varepsilon_i \psi_i$$

The **Hamiltonian** in this equation is an effective one-electron operator. It contains a **one-electron** kinetic energy operator, a Coulomb potential operator, $\mathbf{V}_c$, which includes all electrostatic interactions (electron-electron, electron-nuclei, nuclei-nuclei), and the exchange-correlation potential operator (μ_{xc}). **The** kinetic energy and Coulomb potential operator are identical to those in HF theory. Approximations in DFT are introduced in the exchange-correlation potential operator, while, in principle, there are no conceptual approximations made in the wave functions or in any other place. The most commonly used approximation is local density approximation (**LDA**).[20]

$$E_{xc}[\rho] = \int \rho(\mathbf{r})\varepsilon_{xc}[\rho(\mathbf{r})]d\mathbf{r}$$

That is, the $\varepsilon_{xc}[\rho]$ is the exchange-correlation energy per electron in an interacting electron system of constant density p. For metallic and strongly delocalized systems where the electron density is nearly constant, the LDA gives solutions very close to the exact ones.

Another type of approximation gives rise to a hybrid method called B-LYP/HF procedure.[22] This method was developed by the mixing of DFT and HF methods. According to this procedure, the total energy at HF is first determined.

$$\mathbf{E_{HF}} = \mathbf{E_T} + \mathbf{E_v} + \mathbf{E_j} + \mathbf{E_k}$$

where E_T is the kinetic energy, E_v is the potential energy and E_j and E_k are Coulomb and exchange energy parts. The exchange energy E_k is replaced by an exchange-correlation functional from Becke and Lee-Yang-Parr approximations using the electron density from HF.

$$\mathbf{E_k} = \mathbf{E_{xc}^{B-LYP}}[\rho_{HF}]$$

The functional $\mathbf{E_{XC}^{B-LYP}}$ is derived from the sum of parallel-spin ($\alpha\alpha$ PP) and antiparallel-spin ($\alpha\beta$) parts.

$$\mathbf{E_{xc}^{B-LYP}} = \mathbf{E_P}[\rho_\alpha] + \mathbf{E_P}[\rho_\beta] + \mathbf{E_A}[\rho_\alpha, \rho_\beta]$$

where the parallel spin part, $\mathbf{E_P}$, is known as Becke exchange function[23] and the anti parallel part, $\mathbf{E_A}$, is known as Lee, Yang and Parr correlation function.[24] If Becke's 3 parameter functionals are used, this method is known as Becke3LYP or B3LYP method.[23]

This hybrid method has been widely tested and found to give good results comparable to those obtained from the MP2 method.[25] However, the time taken for computations using this hybrid method is found to be very less compared to MP2 methods. In chapter 3, we have used this method, as implemented in the Gaussian92 program, to compare the relative stabilities of pyramidal Si_3H_3X molecules and tetrahedranes (A4H4).

Study of polymers is also one of the important areas of applied theoretical chemistry. Since the bonds in polymers are not much different from the bonds in molecules, the LCAO approximation used in molecular quantum chemistry can also be applied for polymers. The LCAO Bloch form which describes the delocalized polymer orbitals $\phi_n(k,r)$ as a periodic-combination of functions centred at the atomic nuclei of polymers is expressed as

$$\phi_n(\mathbf{k},\mathbf{r}) = N^{-\frac{1}{2}} \sum_{j=1}^{N} \sum_{p=1}^{\omega} e^{(i_k R_j)} c_{np}(\mathbf{k}) \chi_p(\mathbf{r} - \mathbf{R}_j)$$

where

n   is the bond index

k   is the position vector in the first Brillouin zone

N   is the number of cells

ω is the basis set length describing the wave function within the cell.

j refers the set of the three cell indices (j_1, j_2, j_3)

R_j defines the position vector

$C_{np}(k)$ is the expansion coefficient of the linear combination

According to tight binding approximation,[26] the polymer can be considered as a large molecule. Hence, a general **Hamiltonian** of electrons and nuclei can be constructed. By using the variational expression, the total energy can be derived, in straight forward analogy to the SCF closed-shell formalism.

$$E = N\left[\sum_j h(j)d(j) + \frac{1}{2}\sum_j g(j)d(j)\right]$$

where $h(j)$ and $d(j)$ represent the one electron submatrix and density sub matrix respectively. The g(j) is a repulsion submatrix.

Different degrees of sophistications can be obtained in the study of polymers also, in a fashion similar to that of molecular quantum chemistry, by various approximations. If all electrons are considered and all necessary integrals are calculated, the method is called *ab initio*. On the other hand, the *semi-empirical* methods use the experimental data to reduce the number of integrals to be calculated. One of such empirical methods is **Hückel** method, where only π-**electrons** of purely conjugated organic molecules are taken into account, and all interactions except for the nearest neighbours are neglected. Hoffmann extended the parameterization of this method to σ-bonded systems also and applied it to a large variety of organic and

inorganic systems.[27] This is well known as the *extended Hückel* method, which is used in chapter 4, to study the electronic structure of one dimensional poly-yne systems.

In recent years, the natural bond orbital (NBO) method to understand the bonding in molecules has been popularized due to the limitations in the population analyses due to Mulliken and Lowdin. The NBO method is useful to understand the bonding in molecules. The NBO method extracts the information in the first-order density matrix of the *ab initio* calculations. Then develops a unique set of atomic hybrids and bond orbitals for a given molecule, thereby leading to "Lewis structure" which is easy to understand. The general procedure follows as shown below.[28]

It consists of a sequence of transformations from the given input basis set χ_i. First, the atomic orbitals are transferred to Natural Atomic Orbitals (NAOs) by weighted symmetric orthogonalization procedure. The NAOs are divided into three parts, viz. the core part consisting of inner orbitals, the valence orbitals and the third part consisting solely of the residual portions. The second step is to form Natural Bond Orbitals (NBOs) by optimal orthonormal set of direct hybrids and polarization coefficients from NAOs. These NBOs will have maximum occupancy properties and will be localized on one or two atomic centres rather than being delocalized over the entire molecule. Hence this analysis leads to Lewis structures.

References

1. Michl, J. in introduction to the special issue dealing with "Silicon Chemistry" in *Chem. Rev.* **1995,** *95,* No. 5.

2.(a) Schrodinger, E. *Ann. Physik.* **1926,** *79,* 361.

  (b) Pilar, F.L. *Elementary Quantum Chemistry,* McGraw-Hill: New York, 1968.

  (c) McQuarrie, D.A. *Quantum Chemistry,* Oxford University Press: California, 1983.

  (d) Szabo, A.; Ostlund, N.S. *Modern Quantum Chemistry,* McGraw-Hill: New York, 1982.

  (e) Levine, I.N. *Quantum Chemistry,* .2nd,.ed., Allyn and Bacon: Boston, 1977.

3. Born, M.; Oppenheimer, J. R. *Ann. Physik.* **1927,** *84,* 457.

4.(a) Epstein, S. *The Variation Method in Ouantum Chemistry,* Academic Press: New York, 1974.

  (b) Mikhlin, S.G. *Variational Methods in Mathematical Physics,* Pergamon: Oxford, 1964.

  (c) Schaefer III, H.F. *The Electronic Structure of Atoms and Molecules,* Addison-Wesley, Reading: Massachusetts, 1972.

5.(a) Roothaan, C.C.J. *Rev. Mod. Phys.* **1951,** *23,* 69.

  (b) Hall, G.G. *Proc. Roy. Soc.* **1951,** *A205,* 541.

  (c) Roothaan, C.C.J. *Rev. Mod. Phys.* **1960,** *32,* 179.

6. Hehre, W.J.; Radom, L.; Schleyer, P.v.R.; Pople, J.A. *Ab Initio Molecular Orbitals Theory,* John Wiley and Sons: New York, 1986.

7. Carsky, P.; Urban, M. *Lecture Notes in Chemistry,* Vol. 16, Spinger-Verlog: Berlin Heidelberg, 1980.

8.(a) Slater, J.C. *Phys. Rev.* **1930,** *36,* 57.

  (b) Zener, C. *Phys. Rev.* **1930,** *36,* 51.

9. Boys, S.F. *Proc. Roy. Soc.* **1950,** *A200,* 542.

10.(a)Foster, J.M.; Boys, S.F. *Rev. Mod. Phys.* **1960,** *32,* 303.

  (b) Boys, S.F.; Shavitt, I. *Proc. Roy. Soc.* **1960,** *A254,* 487.

  (c) Huzinaga, S. *J. Chem. Phys.* **1965,** *42,* 1293.

11.(a)Hehre, W.J.; Stewart, R.F.; Pople, J.A. *J. Chem. Phys.* **1969,** *51,* 2657.

  (b) Hehre, W.J.; Ditchfield, R.; Stewart, R.F.; Pople, J.A. *J. Chem. Phys.* **1970,** *52,* 2769.

   (c) Binkley, J.S.; Pople, J.A.; Hehre, W.J. *J. Am. Chem. Soc.* **1980,** 702, 939.

   (d) Gordon, M.S.; Binkley, J.S.; Pople, J.A.; Pietro, W.J.; Hehre, W.J. *J. Am. Chem. Soc.* **1982,** *104,* 2797.

12.(a) Radom, L. *Modern Theoretical Chemistry,* Schaefer III, H.F. ed., Plenum: New York, 1977.

   (b) Simsons, J. *Ann. Rev. Phys. Chem.* **1977,** *28,* 15.

   (c) Hopkinson, A.C. *Progress in Theoretical Organic Chemistry,* Csizmada, I.G. ed., Elsevier: New York, **1977,** vol.2.

13.(a) McWeeny, R. *Int. J. Quant. Chem.* **1967,** 75, 351.

   (b) Herigonte, P.V. *Structure and Bonding* **1972,** 72, 1.

14. McWeeny, R. *The New World of Quantum Chemistry,* Pullman, B.; Parr, R. eds., D. Reidel Publishing Company: Dordrecht, Holland, 1976.

15.(a) Hurley, A.C. *Electron Correlation in Small Molecules,* Academic Press: London, 1977.

   (b) Buenker, R.J.; Peyerimhoff, S.D. *Theoret. Chim. Acta.* **1974,** *35,* 33.

16.   Møller, C; Plesset, M.S. *Phys. Rev.* **1934,** *46,* 618.

17.   Hubac, I.; Carsky, P. *Topics Curr. Chem.* **1978,** *75,* 97.

18.(a) Hoffmann, R.; Lipscomb, W.N. *J. Chem. Phys.* **1962,** *36,* 2179.

   (b) Hoffmann, R. *J. Chem. Phys.* **1963,** *39,* 1397.

19.   Hoffmann, R. *Angew. Chem. Int. Ed. Engl.* **1982,** *21,* 711.

20.(a) Hohenberg, P.; Kohn, W. *Phys. Rev.* **1964,** *B136,* 864.

   (b) Kohn, W.; Sham, L.J. *Phys. Rev.* **1965,** *A140,* 1133.

21. Parr, R.G.; Yang, W. *Density Functional Theory of Atoms and Molecules,* Oxford University Press: O.:ford, 1989.

22.(a) Johnson, B.G.; Gill, P.M.W.; Pople, J.A. *J. Chem. Phys.* **1993,** *98,* 5612.

   (b) Gill, P.M.W.; Johnson, B.G.; Pople, J. A.; Frisch, M.J. *Int. J. Quant. Chem. Symp.* 1992,26,319.

   (c) Gill, P.M.W.; Johnson, B.G.; Pople, J.A.; Frisch, M.J. *Chem. Phys. Lett.* **1992,** 797, 499.

23.(a) Becke, A.D. *Phys. Rev.* **1988,** *A38,* 3098.

   (b) Becke, A.D. *J. Chem. Phys.* **1993,** *98,* 5648.

24.   Lee, C; Yang, W.; Parr, R.G. *Phys. Rev.* **1988,** *B37,* 785.

25.   Johnson, B.G.; Gill, P.M.W.; Pople, J.A. *Chem. Phys. Lett.* **1994,** *220,* 377 and references therein.

26.(a) Andre, J.-M. *Electronic Structure of Polymers and Molecular Crystals,* Andre, J.-M.; Ladik, J. eds., Plenum Press: New York, 1974.

   (b) Andre, J.M. *J. Chem. Phys.* **1969,** *50,* 1536.

27.   Hoffmann, R. *Angew. Chem. Int. Ed. Engl.* **1987,** *26,* 846.

28.(a) Foster, J.P.; Weinhold, F. *J. Am. Chem. Soc.* **1980,** *102,* 7211.

   (b) Weinhold, F.; Reed, A.E. *J. Chem. Phys.* **1983,** *78,* 4066.

   (c) Reed, A.E.; Weinstock, R.B.; Weinhold, F. *J. Chem. Phys.* **1985,** *83,* 735.

   (d) Reed, A.E.; Curtiss, L.A.; Weinhold, F. *Chem. Rev.* **1988, 88,** 899.

Chapter 1: **B$_3$H$_6$$^+$and Si$_3H_3$$^+$:** The Cyclopropenyl Cation
Analogs in Boron and Silicon Chemistry.

[1.0] *Abstract*

The all boron analog, $B_3H_6^+$, and all silicon analog, $Si_3H_3^+$, of $C_3H_3^+$ have been studied in chapter 1.

Molecular orbital studies at MP2/631G* level on the isomers $C_3H_3^+$ (5) and its boron analogs C2BH3 (7), CB2H4 (11), B3H5 (15) and $B_3H_6^+$ (18) indicate that 5 to 15 prefer cyclic planar *2n* aromatic structures. $B_3H_6^+$ (18, D_{3h}) distorts to a C_{3v} structure, 19, lower in energy by 41.1 kcal/mol, with the three bridged hydrogens and three terminal hydrogens on opposite side of the B3 plane. The aromatic stabilization energy of 19 is determined using isodesmic equations. The factors responsible for the C_{3v} distortion in $B_3H_6^+$ are to be found in several contexts including lithiocarbons and metallaboranes.

The potential energy surface of $Si_3H_3^+$ has been investigated theoretically at the MP2/6-31G* level. The global minimum is the planar aromatic D_{3h} structure (11). Except for the trisilacyclopropenyl cation, all other $Si_3H_3^+$ analogs of known $C_3H_3^+$ isomers are not stable. There are twelve other minima within a range of 45 kcal/mol from the global minimum. Five isomers (**11**, 13, 14, 20 and 24) display planar cyclic 3c-2e π delocalization and eight isomers (13, 18, 19, 20, 24, 25, 26 and 27) have 3c-2e SiHSi bridged bonds. Four (13, 14, 25 and 26) and five (20 and 31) coordinated silicons are also represented among the computed isomers.

[1.1] *B₃H₆⁺: The Smallest Nonplanar 2K Aromatic*

Three membered ring boron hydrides are known to play an important role in the mechanism of diborane pyrolysis.[1] The cations of these rings have attained great interest in recent years due to their detection in mass spectra, and their relation with carbocations.[2-3] The electron impact mass-spectrometric studies on B_4H_8CO was found to produce among others the cation $B_3H_6^+$.[2] Interestingly, $B_3H_6^+$ is isoelectronic with the $C_3H_3^+$, inviting comparison to the 2π aromatic character of cyclopropenyl cation.[4,5] The boranes are known to form multicentre bonding.[6,1a] Diborane [6] is the classic example which contains two bridging hydrogens.[7] Similar structures are anticipated for $B_3H_6^+$ as well.

1   **2**   **3**

4
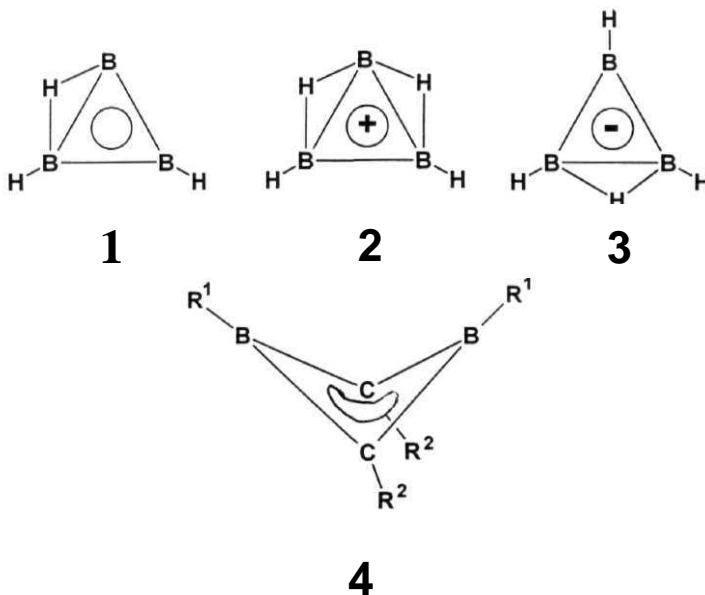
Among the triboranes, B3H3 (1, C_s), with one bridging hydrogen and 2π electron delocalization, is found to be the global minimum.[6,8] Similarly, the global minimum of $B_3H_4^+$ (2, C_{2v}) vvith two bridging hydrogens and of B3H4- (3 C_{2v}) with one bridging hydrogen also contain the *2n* electron delocalization.[6,8] Thus, the *2n* aromaticity is expected to play an important role in the structures of the cyclic three membered boron hydrides. On the other hand the cyclobutadiene dication is also a *2n* aromatic system.[9] This cation came as a revelation to chemists showing that 2π aromaticity no longer requires planarity. The neutral boron analog, 1,3-diborocyclobutadiene has been structurally characterized to be nonplanar.[10] By keeping these factors in view this chapter deals with systematic comparison of the $C_3H_3^+$ (the carbon chemistry) to $B_3H_6^+$ (the boron chemistry) via various combinations of carbon and boron in three membered rings (the carborane chemistry).

The standard 6-31G* basis was employed initially to compute the equilibrium geometries (within the given symmetry restriction) at HF level.[11] Thc effect of electron correlation on the structure was estimated by optimizing the HF/6-31G* structures at the MP2/6-31G* level.[12] The relative energies of some of the isomers are further determined at the QCISD(T)/6-31G* level.[13] Vibrational frequencies were computed from analytical second derivatives at the MP2/6-31G* level to characterize the nature of the stationary points.[14] GAUSSIAN90 series of programs were used for the present study.[15] The zero point energies (ZPE) were scaled by 0.9.[11] The energy comparisons are at MP2/6-31G*//MP2/6-31G* +ZPE

5   **6**
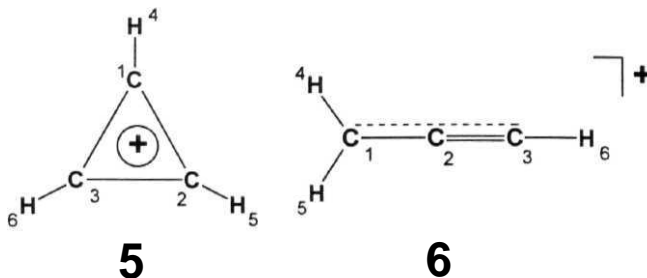
The $C_3H_3^+$ is known to be more stable as cyclopropenyl cation (5, D_{3h}), the smallest $2n$ aromatic compound.[4] There are many theoretical calculations available on $C_3H_3^+$ potential energy surface.[5] Some of the important points will be presented here for comparison.

The C-C bond length (1.367A) in 5 is shorter than the C-C single bond length (1.504A in cyclopropane)[16] and longer than the C-C double bond (1.301Å in cyclopropene).[17,8b] The HOMO is a delocalized π-orbital ($1a_2''$) over the planar C3 ring. The 7r-overlap population between the two carbons is 0.059. The Mulliken charge analysis shows the positive charge to be localized on hydrogens (charge on C is -0.03 and on H is 0.36) due to their

electronegativity differences. Resonance stabilization energy (RSE) of 5 has been estimated using the isodesmic equations 1 and 2.[5] The RSE in equation 1 represents total 3c-2e delocalization, while those in equation 2 show the extra cyclic n delocalization. Many experimental evidences established the D_{3h} structure of 5.[4] Derivatives of 5 were also prepared. X-ray diffraction studies on derivatives of 5 showed that the CC bonds are equal, supporting the $2n$ delocalization in **5**.[18]
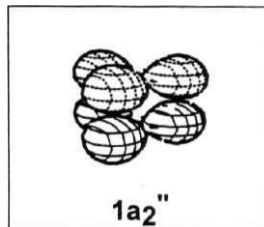
Table 1

Total energies (hartrees) and Relative energies (kcal/mol) for the structures studies. The zero point energies ZPE (kcal/mol) are given at MP2/6-31G* level. The values in parentheses are number of imaginary frequencies.

| Structure No. | Total energy | | Relative energy | | ZPE |
	HF/6-31G*	MP2/6-31G*	MP2/6-31G*	QCISD(T)/6-31G*	
5	-115.00702	-115.36365(0)	0.0		28.83
6	-114.95110	-115.31130(0)	31.6		27.41
7	-102.10240	-102.43539(0)	0.0		26.80
8	-102.08907	-102.42045(0)	7.3		24.47
11	-89.51186	-89.81481(0)	0.0		31.70
12	-89.44787	-89.72983(2)	50.8		28.93
13	-89.45225	-89.75973(0)	33.2		29.91
14	-89.47381	-89.74148(0)	42.7		27.97
15	-76.86511	-77.14840(0)	0.0	0.0	35.71
16	-76.86727	-77.14694(0)	0.6	0.5	35.37
17	-76.88221	-77.10984(0)	21.9	16.7	33.20
19	-77.19351	-77.45969(0)	0.0	0.0	43.73
18	-77.09289	-77.39040(1)	41.1	44.7	41.03
20	-76.94539	-77.25464(1)	120.3		34.41
21	-77.09579	-77.32133(3)	81.8		38.11
22	-77.16865	-77.41222(2)	26.0		39.53
$C_2BH_6^-$		-104.22105			
$C_2BH_4^-$		-102.99692			
C_2BH_5		-103.60558			
$CB_2H_7^-$		-91.62116			
$CB_2H_5^-$		-90.34554			
CB_2H_6		-90.91327			
$B_3H_8^-$		-78.96816			
$B_3H_6^-$		-77.70095			
$(\mu\text{-H})_2B_3H_5$		-78.28504			
$(\mu\text{-H})_3B_3H_4$		-78.31503			
B_3H_9		-79.48513			
$B_3H_8^+$		-78.57802			
B_2H_6		-53.00228[a]			

[a]from ref. 33.

Table 2

Optimized geometric parameters of the structures at MP2/6-31G* level. Distances are in angstroms and the angles are in degrees.

Structure	Parameter	MP2/6-31G*
5	C-C	1.367
	C-H	1.083
6	C(1)-C(2)	1.232
	C(2)-C(3)	1.357
	C(1)-H	1.091
	C(3)-H	1.078
	HC(1)C(2)	120.8
7	C-C	1.359
	C-B	1.473
	C-H	1.083
	B-H	1.182
	HCC	139.0
8	C-C	1.227
	C-B	1.511
	C-H	1.068
	B-H	1.192
	HBC	120.0
11	C-B	1.438
	B-B	1.709
	C-H	1.075
	B-H	1.185
	$B-H_b$	1.320
	H_tBB	155.8
12	C-B	1.552
	B-B	1.653
	B-H	1.186
	C-H	1.097
	HBB	160.7
13	C-B	1.586
	B-B	1.484
	B-H	1.179
	C-H	1.084
	HBB	176.6
14	C-B	1.430
	B-H	1.194
	HBC	118.8
15	B(1)-B(2)	1.578
	B(2)-B(3)	1.606
	$B(2)-H_t$	1.179
	$B(2)-H_b$	1.233
	$B(1)-H_b$	1.429
	$B(1)B(2)H_b$	59.6
	$B(3)B(2)H_t$	127.8

Structure	Parameter	MP2/6-31G*
16	B(1)-B(2)	1.637
	B(2)-B(3)	1.526
	B(1)-H	1.186
	$B(2)-H_b$	1.292
	$B(3)B(2)H_b$	166.4
	HB(1)H	118.0
17	B(1)-B(2)	1.646
	B(2)-B(3)	2.946
	B(1)-H	1.205
	B(2)-H	1.197
	HB(2)B(3)	118.1
	HB(2)B(3)B(1)	105.2
18	B-B	1.620
	$B-H_t$	1.185
	$B-H_b$	1.289
19	B-B	1.649
	$B-H_t$	1.177
	$B-H_b$	1.329
	Z_b	0.678
	Z_t	0.385
20	B-B	1.529
	B-H	1.252
	HBB	127.5
21	B-B	2.004
	B-H	1.183
	HBH	133.0
22	B(1)-B(2)	1.696
	B(2)-B(3)	1.778
	$B(1)-H_t$	1.197
	$B(2)-H_t$	1.177
	$B(1)-H_b$	1.216
	$B(1)B(2)H_b$	63.3
	$B(2)B(3)H_t$	118.9

Z_b, Z_t represents the nonplanarity of the bridging and terminal hydrogens.

The acyclic isomer of $C_3H_3^+$ is propargyl cation 6 (C_{2v}). It is 31.6 kcal/mol higher in energy than the *2n* aromatic system 5 (Table 1).[5] The π-overlap population between C(l)-C(2) is 0.076 and between C(2)-C(3) is 0.224 in 6. The Mulliken charge analysis shows the posititve charge to be distributed on C(2) (0.08) and on Hydrogens (H(4) = H(5): 0.35, H(6): 0.43). Experimental studies also support the relative stability of the two isomers; 6 is 24.9 kcal/mol higher in energy than **5**.[19] The existence of propargyl cation has been established in the gas phase by mass spectrometric methods.[4]

$\Delta E = 78.0$ kcal/mol (1)

$\Delta E = 35.7$ kcal/mol (2)
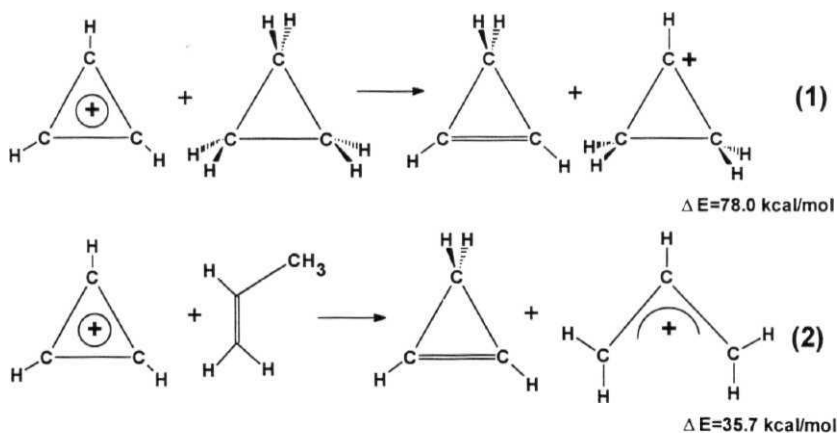
Replacement of CH^+ in the $C_3H_3^+$ by an isolobal BH leads to the neutral C2BH3. Our results agree well with the previous predictions on borirene (7, C_{2v}).[10,20] The BC bond length is shortened by 0.172Å, compared to the corresponding BC bond length in C2BH5 (1.531A, Table 2)[8b,10]. Similarly the CC bond length is 0.035Å longer than the CC double bond length (1.324Å) in $C_2BH_4^-$.[10]

7

8
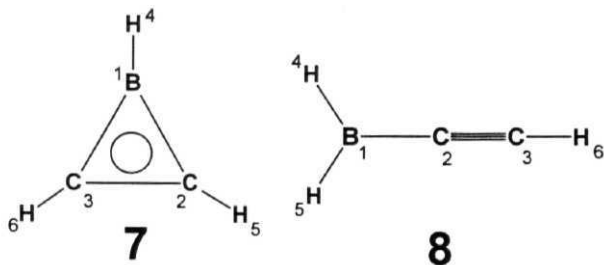
Interestingly, the CC bond length in 7 is 0.008A shorter than that in cyclopropenyl cation (1.367A). The B-C σ-bonding walsh orbital ($3b_2$) is the HOMO in 7, in contrast to 5 where the HOMO is a delocalized π orbital. The H0M0-1 is traced to be a π orbital in 7. The 7r-overlap population between the two carbons (0.094) in 7 is more than that in the cyclopropenyl cation resulting in the shortening of the CC bond. The B-C π-overlap population is found to be 0.045. The Mulliken

$3b_2$

charge on carbon in 7 is -0.26. Compared to that in 5, there is a charge transfer by an amount 0.23. This is mainly attributed to the higher electronegative character of C (though BH is a π acceptor). The resonance stabilization energy (RSE) of the borirene has been calculated using the equation 3, which is derived from equation 1.


(3)

$\Delta E = 33.9$ kcal/mol
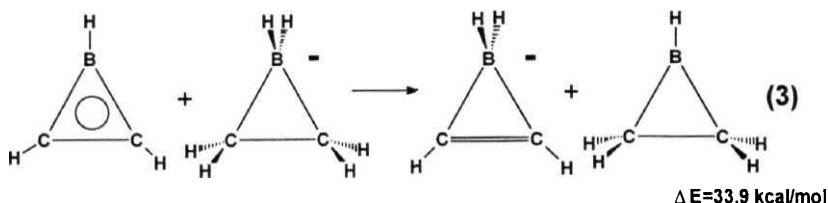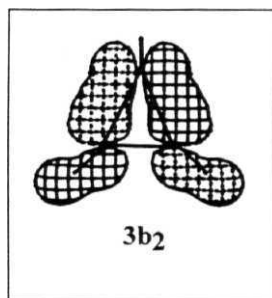
The propargyl cation analog of C_2BH_3 (8, C_{2v}) is 7.3 kcal/mol higher in energy than the cyclic aromatic system 7. The C-C bond distance in 8 is (1.227A) shorter than the C(2)-C(3) bond distance in propargyl cation (6). Therefore, the rc-overlap population between C-C (0.277) has been increased compared to that in 6. Hence, CH_2^+ is appears to be a better n acceptor compared to the isolobal fragment BH_2. Substituted analogs of 7 and 8 have been prepared experimentally; and their structures were established by X-ray diffraction methods.[10,21-22] For example, C_2BR_3 (R = 2,4,6-trimethyl phenyl) shows both the cyclic structure 7 and the acyclic structure 8.[21] Though the structures have been established by X-ray diffraction methods, there was a controversy on cyclic C2BR3; is it a trialkylborocyclopropenyl (9) or a closo-carborane (10).[23] However, Williams et al have established by NMR methods that 10 is the more appropriate representation of C2BR3. The comparable [11]B and ^{13}C chemical shifts, and the correlation graphs between them support 10 instead of 9. One of the important findings in these experiments is the almost exact equivalence of the ^{13}C chemical shift values of the ring carbons in (CR)2BR' (R=Bu, R'=Me) and $C_3R_3^+$.[23]

9   10
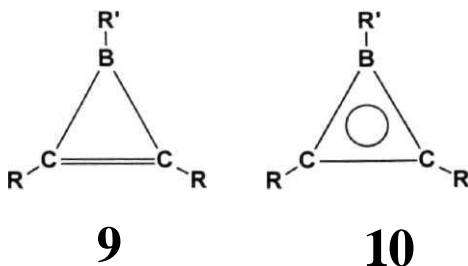
In continuation, the replacement of a C in C_2BH_3 by an isoelectronic BH leads to CB2H4. The hydrogen bridged structure 11 (C_{2v}) is found to be a minimum and more stable than the van't Hoff structure (12, C_{2v}) and the anti-van't Hoff structure (13, C_{2v}).[8b,24] The van'tHoff structure is 50.8 kcal/mol higher in energy than 11 and is a second order saddle point. Whereas, the anti van't Hoff structure 13 is a minimum and 33.2 kcal/mol higher in energy than 11. Previous calculations have predicted that the hydrogen bridged structure (11) is 31.7 kcal/mol (at 4-31G//STO-3G level) more stable than the anti van't Hoff structure (13).[25]


11   **12**   **13**   **14**
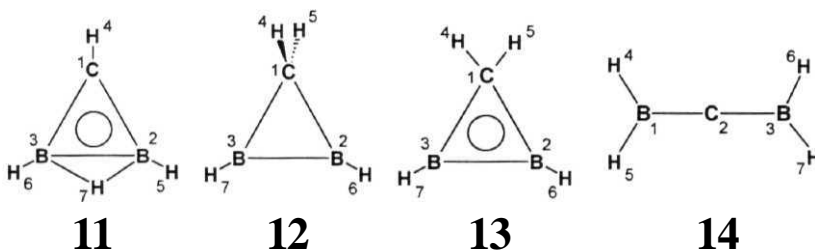
The MO analysis shows the 3c-2e B-H-B bonding, 2c-2e B-C bonding and a 3c-2e π delocalization in 11. Structure 12 has a classical 2c-2e B-B bond. But, structure 13 has a 3c-2e σ-bond between B-C-B, a 2c-2e bond between B-B and a 3c-2e % delocaliztion. Thus, the B-C bond distance in 13 (1.586A) is longer than the corresponding distance in 11. The B-C bond distance in 11 (1.438A) is shorter than the corresponding distance in 7. The rc-overlap population between B-C in 11 (0.076) and 13 (0.065) are found to be slightly higher than that in 7 (0.045). The Mulliken charge at C in 11 (-0.35) is more than the charge at C in 7 (-0.26). Resonance stabilization energy (RSE) of 11 has been estimated using the equation 4.

$$\Delta E = 45.6 \text{ kcal/mol} \tag{4}$$
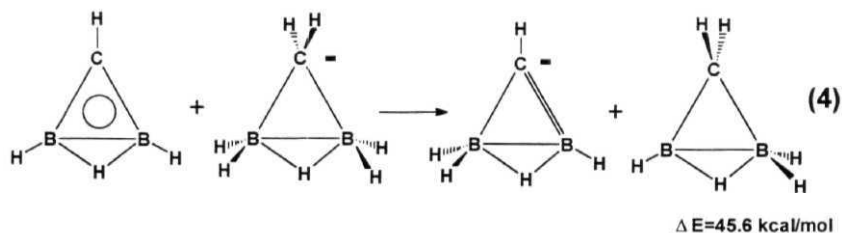
The acyclic structure 14 (C_{2v}) is a minimum and 42.7 kcal/mol higher in energy than 11. The B-C bond distance in 14 (1.430A) is shorter than the corresponding distance in 8 (1.511 A). The B-C rc-overlap population increases from 8 (0.027) to 14 (0.069). However, the Mulliken charge analysis shows the positive charge at central C (0.02) in 14, whereas negative charge (-0.13) in 8. The substituted analogs of 11, $B_2(\mu\text{-H})R_2CR'$ (R = $C(CH_3)$, R' = $CH(Si(CH3)3)2$),[26] $B_2(\mu\text{-H})RR'CR''$ (R = $CH(SiMe_3)2$, R' = $2,3,5,6\text{-Me4C6H}$ and R" = $SiMe_2(2,3,5,6\text{-Me4C6H}))$[27] and $B_2(\mu\text{-H})R_2CR'$ (R = $2,3,5,6\text{-Me4C6H}$ and R' = $C(SiMe3)(BEt2)$[27] were prepared experimentally, and their structures have been established by NMR spectrometric and X-ray diffraction methods.

The all boron neutral analog of $C_3H_3{}^+$ is B3H5, obtained by replacing the C by BH in CB2H4. Isomer 15 (C_{2v}) with two bridging hydrogens is found to be a minimum and 0.6 kcal/mol more stable than 16, which contains only one bridging hydrogen. Previous studies on the isomers of B3H5 using the 4-31G basis set gave the open structure 17 (C_{2v}) to be the most stable.[8c] Our calculations at the 6-31G* level agree with this result, but calculations at the MP2/6-31g* level change this picture. 15 and 16, with two π electrons each were found to lie lower in energy than 17 by

21.9 and 21.3 kcal/mol respectively. These are further confirmed at the QCISD(T)/6-31G* level. Later, theoretical study on the potential energy surface of B3H5 has also confirmed 15 to be the global minimum.[6]


15 **16** **17**
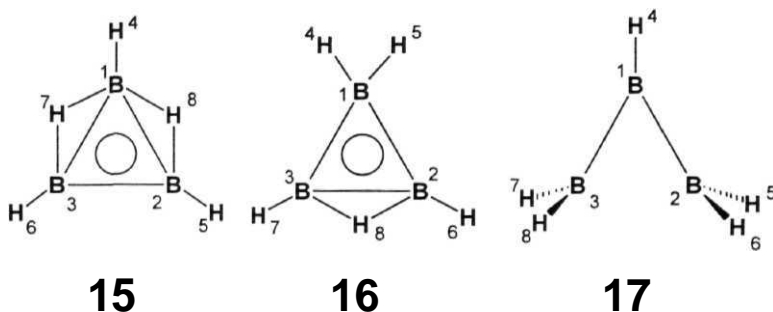
The B-B distances in 15, 1.606A (bridged) and 1.578A (unbridged) are considerably shorter than the standard single bond distances in $B_3H_8^-$ and longer than double bond distances in B_2H_2 (1.525Å at MP2/6-31G* level).[6] But, in 16, the B-B distances 1.526A (bridged) and 1.637A (unbridged) are different from 15. The B-B (bridged) distance in 11 is found to be (1.709A) longer than that in 16. There is an interesting variation in the distance of the bridging hydrogens to the two borons in 15. The $B(2)H_b$ distance is 1.233Å while the B(1)Hb distance is 1.429A. This is due to the unequal disposition of the two degenerate Walsh orbitals of the B3H3 group along the B(l)-B(2) bond.[28] The interaction of the two bridging hydrogens with the B3H3 destroys the degeneracy. The symmetric combination of the bridging hydrogens can increase the interaction by shifting itself towards B(2) and B(3). The rest of the skeleton reorganizes to accommodate this change. The HtB(2)B(3) bond angle correspondingly decreases to 127.8°. The B-B (unbridged) π-overlap population is nearly

equal in 15 (0.056) and 16 (0.057), and it is more compared to 13 (0.040). However the B-B (bridged) π-overlap population in 15 (0.075) is less than that in 16 (0.090), and more than that in 11 (0.043). The isodesmic equation 5 gives the RSE for 15.[6] All the structures in equation 5 are boron counterparts of the structures in equation 1.

$$\Delta E = 81.9 \text{ kcal/mol} \qquad (5)$$
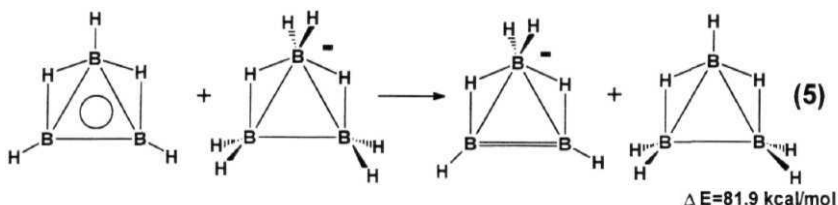
Protonation of the B-B bond in 15 leads to $B_3H_6^+$ (18, D_{3h}), the cationic all boron analog of $C_3H_3^+$. But the frequency analysis has shown that 18 is a transition state. The negative frequency corresponds to the motion of three bridging hydrogen atoms in a direction perpendicular to the B3 plane and three terminal hydrogen atoms in an opposite direction. Optimization along this distortion coordinate leads to 19 (C_{3v}) which is calculated to be a minimum, 61.7 kcal/mol below 18 at the $6\text{-}31G^*$ level. Optimization at the MP2/6-31G* and QCISD(T)/6-31G* levels decreases the energy difference between 18 and 19 to 41.1 and 44.7 kcal/mol respectively. The bridging hydrogens are 0.678A above the B3 plane and the terminal hydrogens are 0.385Å below the B3 plane. The other D_{3h} structures on the $B_3H_6^+$ potential energy surface that we could find corresponds to 20 and 21, lies 120.3 and 81.8 kcal/mol higher in energy than 19 respectively. Structure 22 (C_{2v}) is calculated to be 26 .0 kcal/mol higher in energy than 19. These results are in direct contrast to the planar 2

π-aromatic structures that were studied above (viz. $C_3H_3^+$ (5), C_2BH_3 (7), CB_2H_4 (11), B_3H_5 (15)).
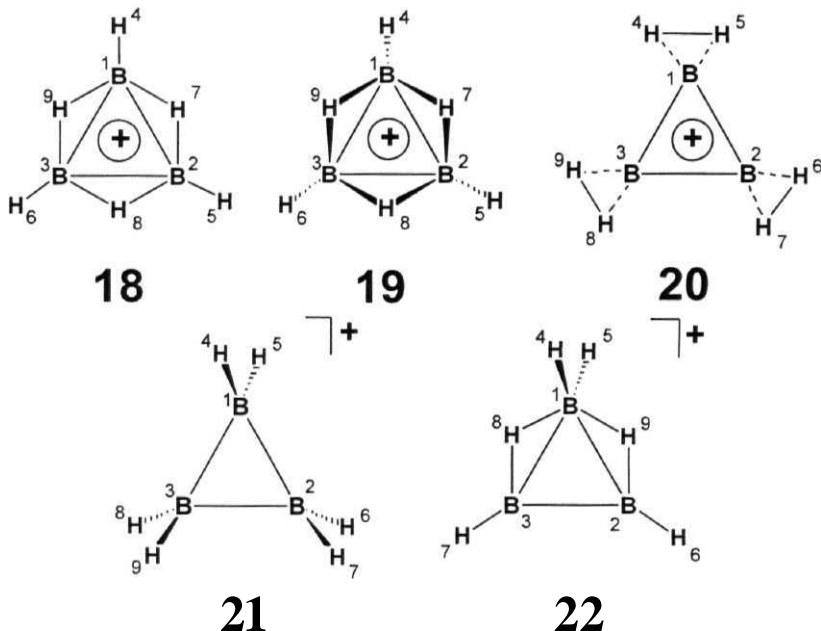

The electronic structure of 18 and 19 may provide a better understanding for the observed deformation (Fig.1). Description of the bonding in 18 is familiar in terms of the Walsh orbitals of cyclic B3H3 and H_3^+.[28] The degenerate MOs of H_3^+ (1e') interact with B-H bonding MOs (1e') and B-B bonding MOs (2e') of B3H3 fragment leading to 1e' and 2e' bonding MOs in $B_3H_6^+$ (18). The all symmetric MO (1a$_1$') of H_3^+ can interact with two MOs (viz. 1a$_1$' and 2a$_1$') of B3H3. But the energy difference between 1a]' of H_3^+ and 1a$_1$' of B3H3 leads to only a weak bonding. The 2a$_1$' of B3H3 mainly corresponds to B-H bonding and is not effective in bonding with 1a$_1$' of H_3^+. This bond strain destabilizes the

$B_3H_6^+$ in its D_{3h} symmetry. The HOMO is the expected π MO in 18. Under C_{3v} symmetry the $1a_2''$ (HOMO) and $3a_1'$ of 18 belong to the same irreducible representation in 19 and hence mix. Fig.2 shows the dramatic effect of this σ-π mixing. There is still substantial n delocalization in 19 as evidenced by the marginally longer B-B distance of 1.649A compared to that in 18. However, the aromaticity of 19 is expected to be less than that of 18 for the following reason. Under the C_{3v} symmetry the π-antibonding orbitals mix with the B-B bonding orbitals leading to stabilization of 3e in 19 (Fig.2). This decreases the aromatic delocalization in 19 compared to 18, in which only $1a_2''$ contributes to aromaticity.

Recently Korkin et al studied the potential energy surface of $B_3H_6^+$ in detail and confirmed that 19 is, in fact, the global minimum.[6] The $B_3H_6^+$ (19) is a highly favoured ion. The absolute value of protonation leading to it from B3H5 is exothermic by 191.1 kcal/mol at the QCISD(T)/6-31G* level. Equation 6 gives the RSE of isomer 19,[6] whereas equations 7 and 8 compare the stability of 19 against the cyclopropenium ion, 5.

A more general way of looking at the preference of 19 over 18 for $B_3H_6^+$ involves the steric congestion between bridging hydrogens and the terminal hydrogens. The formally non-bonding H_t-H_b distance in 11 (2.026A) and 15 (2.013A) are decreased to 1.882A in 18. This is an unusually short H-H nonbonded distance.[29] Structure 19 is an attempt to increase this distance to 2.093Å.

Fig. I: Interaction diagram between H_3^+ and B3H3 leading to $B_3H_6^+$ (18).
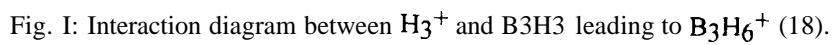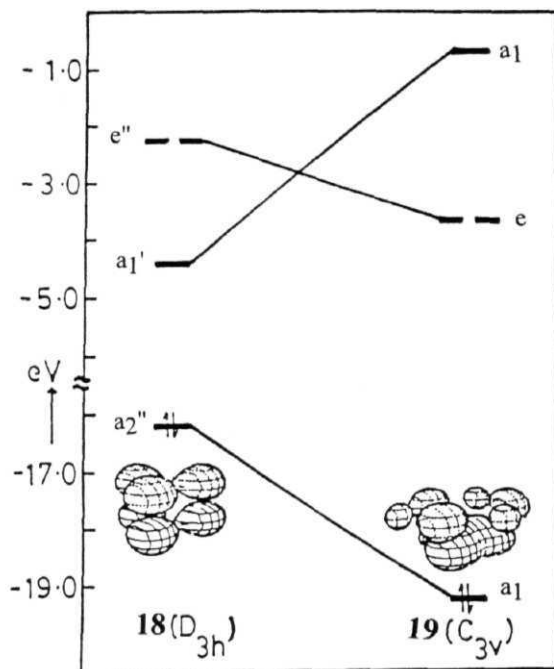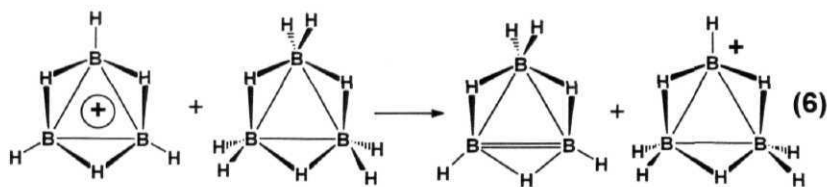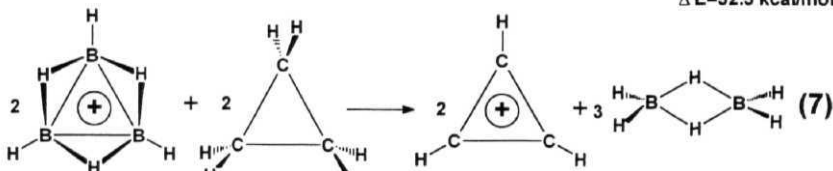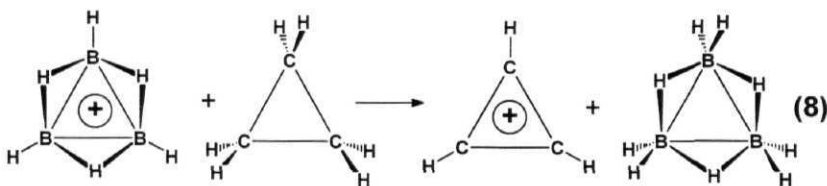
Fig. 2: Correlation diagram between 18 and 19 showing the dramatic stabilization of HOMO.

$$\Delta E = 32.5 \text{ kcal/mol} \quad (6)$$

$$\Delta E = 58.7 \text{ kcal/mol} \quad (7)$$

$$\Delta E = 41.6 \text{ kcal/mol} \quad (8)$$

If the H_t-H_b interactions are strong enough to cause a distortion of 18 to 19, similar distortions in increased magnitude should have been seen in the *4n* and 6π systems B_4H_8 and $B_5H_{10}^-$ which are common ligands. Even though B_4H_8 and $B_5H_{10}^-$ do not have independent existence, there are several well characterized complexes in which these appear as π ligands.[30] The metals prefer to attach to that face of the B_nH_{2n} ligand which has the π-orbitals oriented towards the C_n axis.[30] A *%* complex involving $B_3H_6^+$ as the ligand is not known so far. However, theoretical calculation shows that, B_3H_6 is an interesting 7r-ligand for various main

group fragments (viz. CH, SiH, NH^+, PH^+, NO and PO) as well as for transition metal fragments $(Co(CO)3)$.[31] It is observed that some of these fragments force the both bridging and terminal hydrogens of B_3H_6 ring to be one side.[31] similarly, an isolobal analog $[(CO)_3Fe]_3(\mu\text{-}H)_3CR$, where the BH is replaced by $Fe(CO)_3$ and a CR group takes the place of a d^9 ML3 fragment, is well known.[32] Therefore, a n complex of $B_3H_6^+$ is certainly a target within reach.
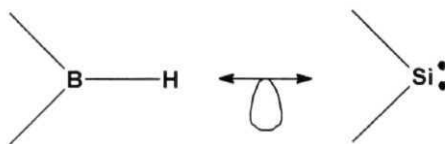
23

The isolobal analogy between trivalent boron and divalent silicon (23) leads to a cation $Si_3H_3^+$ from the $B_3H_6^+$.[34] The study of the potential energy surface of $Si_3H_3^+$ is interesting due to the diagnal relation between boron and silicon and the group trends from carbon to silicon. Hence section 2 of this chapter is devoted to the isomer study of $Si_3H_3^+$.

References:

1 .(a) *Boron Hydride Chemistry,* Muetteries, E.L., Ed. Academic Press: New York, 1975.

(b) Lipscomb, W.N.; Stanton, J.F.; Connick, W.B.; Magers, D.H. *Pure. Appl. Chem.* **1991,** *63,* 335.

2. Rosenstock, H.M.; Draxl, K.; Steiner, B.W.; Herron, J.T. *J. Phys. Chem. Ref. Data.* 1977, *6,* suppl. No. 1.

3.(a) Sakai, S. *Chem. Phys. Lett.* **1994,** *217,* 288.

(b) Buhl, M.; Schaefer III, H.F.; Schleyer, P.v.R.; Boese, R. *Angew. Chem. Int. Ed. Engl.* **1993,** *32,* 1154.

(c) Baudler, M.; Rockstein, K.; Oelert, W. *Chem. Ber.* **1991,** *124,* 1149.

(d) Grützmacher, H. *Angew. Chem. Int. Ed. Engl* **1992,** *32,* 1329.

(e) Glore, J.D.; Rathke, J.W.; Schaeffer, R. *Inorg. Chem.* **1973,** /.?, 2175.

4.(a) Lossing, F.P. *Can. J. Chem.* **1972,** *50,* 3973.

(b) Holmes, J.L.; Lossing, F.P. *Can. J. Chem.* **1979***, 57,* 249.

5.(a) Radom, L.; Hariharan, P.C.; Pople, J.A.; Schleyer, P.v.R. *J. Am. Chem. Soc. 1976,98,* 10.

(b) Li, W.-K.; Riggs, N.V. *J. Mol. Struct. (THEOCHEM)* **1992,** *257,* 189, and references therein.

(c) Wong, M.W.; Radom, L. *J. Am. Chem. Soc.* **1993** *115*, 1507.

(d) Lopez, R.; Sordo, J.A.; Sordo, T.L. *J. Chem. Soc, Chem. Commun.* **1993**, 1751.

(e) Maluendes, S.A.; McLean, A.D.; Yamashita, K.; Herbst, E. *J. Chem. Phys.* **1993**, *99*, 2812.

6. Korkin, A.A.; Schleyer, P.v.R.; McKee, M.L. *Inorg. Chem.* **1995,** *34,* 961.

7.(a) Williams, R.E. *Chem. Rev.* **1992,** *92,* 177, and references therein.

(b) Longuest-Higgins, H.C. *J. Chim. Phys.* **1949,** *46,* 268.

(c) Lipscomb, W.N. *Boron Hydrides;* Benjamin: New York, 1963.

8.(a) Krempp, M.; Damrauer, R.; DePuy, C.H.; Keheyan, Y. *J. Am. Chem. Soc.* **1994,** *116*, 3629.

(b) Liang, C; Allen, L.C. *J. Am. Chem. Soc.* **1991**, *113*, 1878.

(c) Bigot, B.; Lequan, R.M.; Devaquet, A. *Nouv. J. Chem.* **1978,** 2, 449.

9.(a) Krogh-Jesperson, K.; Schleyer, P.v.R.; Pople, J.A.; Cremer, D. *J. Am. Chem. Soc. 1978,700,4301.*

  (b) Chandrasekhar, J.; Schleyer, P.v.R.; Krogh-Jesperson, K. *J. Comput. Chem.* **1981,** *2,* 356.

10.(a) Krogh-Jesperson, K.; Cremer, D.; Dill, J.D.; Pople, J.A.; Schleyer, P.v.R. J. *Am. Chem. Soc.* **1981,** *103,* 2589.

  (b) Schleyer, P.v.R.; Budzelaar, P.H.M.; Cremer, D.; Kraka, K. *Agew. Chem., Int. Ed. Engl.* **1984,** *23,* 374.

  (c) Hildenbrand, M.; Pritzkow, H.; Zenneck, U.; Siebert, W. *Angew. Chem. Int. Ed Engl.* **1984,** *23,* 371.

  (d) van der Kerk, G.J.M.; Budzelaar, P.H.M.; van der Kerk-van Hoof, A.; Schleyer, P.v.R. *Angew. Chem. Int. Ed. Engl.* **1983,** *22,* 48.

11.(a) Hariharan, P.C.; Pople, J.A. *Chem. Phys. Lett.* **1972,** *66,* 217.

  (b) Francl, M.M.; Pietro, W.J.; Hehree, W.J.; Binkley, J.S.; Gordon, M.S.; DeFrees, D.J.; Pople, J.A. *J. Chem. Phys.* **1982,** *77,* 3654.

  (c) Hehre, W.J.; Radom, L.; Schleyer, P.v.R.; Pople, J.A. *Ab initio Molecular Orbital Theory.* Wiley: New York, 1986.

12.   Møller, C.; Plesset, M.S. *Phys. Rev.* **1934,** *46,* 618.

13.   Pople, J. A.; Head-Gordon, M.; Raghavachari, K. *J. Chem. Phys.* **1987,** *87,* 5968.

14.   Pople, J.A.; Raghavachari, K.; Schlegel, H.B.; Binkley, J.S. *Int. J. Quantum. Chem. Symp.* **1979,** *13,* 255.

15.   Frisch, M.J.; Head-Gordon, M.; Trucks, G.W.; Foresman, J.B.; Schlegel, H.B.; Raghavachari, K.; Robb, M.A.; Binkley, J.S.; Gonzalez, C; DeFrees, D.J.; Fox, D.J.; Whiteside, R.A.; Seeger, R.; Mellius, C.F.; Baker, J.; Martin, R.L.; Kahn, L.R.; Stewart, J.J.P.; Topiol, S.; Pople, J.A. GAUSSIAN 90, Gaussian Inc.: Pittsburgh, PA, 1990.

16.(a) Inagaki, S.; Yoshikawa, K.; Hayano, Y. *J. Am. Chem. Soc.* **1993,** *115,* 3706.

  (b) Horner, D.A.; Grev, R.S.; Schaefer III, H.F. *J. Am. Chem. Soc.* **1992,** *114,* 2093.

  (c) Nagase, S.; Kobayashi, K.; Nagashima, M. *J. Chem. Soc, Chem. Commun.* **1992,** 1302.

  (d) Cremer, D.; Gauss, J.; Cremer, E. *THEOCHEM,* **1988,** *46,* 531.

  (e) Cox, J.D.; Pilcher, G. *Thermochemistry of Organic and Organometallic compounds,* Academic: New York, 1970.

17(a) Wong, M.W.; Radom, L. *J. Am. Chem. Soc.* **1993,** *115,* 1507.

  (b) Domnin, I.N.; Kopf, J.; Keyaniyam, S.; De Meijere, A. *Tetrahedron* **1985,** *41,* 5377.

    (c) Ammon, H.L.; Sherrer, C; Agranat, I. *Chem. Scr.* **1978**, *11*, 39.

    (d) Starova, G.L.; Domnin, I.N.; Markin, V.N. *Vest. Leningr. U., Fiz. Khim.* **1984,** 58.

18.(a) Sundaralingam, M; Jensen, L.H. *J. Am. Chem. Soc.* **1966,** *88,* 198.

    (b) Ku, A.T.; Sundaralingam, M. *J. Am. Chem. Soc.* **1972,** *94,* 1688.

19.   Lias, S.G.; Bartmess, J.E.; Liebman, J.F.; Holmes, J.L.; Levin, R.D.; Mallard, W.G. *J. Phys. Chem.* Ref. Data Suppl. **1988,** *17.*

20.(a) Budzelaar, P.H.M.; Kos, A.J.; Clark, T.; Schleyer, P.v.R. *Organometallics*. **1985,** *4,* 429.

    (b) Volpin, M.E.; Koreskov, Y.D.; Dulova, V.G.; Kursanov, D.N. *Tetrahedron.* **1962,** *18,* 107.

21.   Eisch, J.J.; Shafii, B.; Odom, J.D.; Rheingold, A.L. *J. Am. Chem. Soc.* **1990,** *112,* 1847.

22.   Pues, C; Berndt, A. *Angew. Chem. Int. Ed. Engl.* **1984,** *23,* 313.

23.   Fehlner, T P. in *Advances in Boron and Boranes,* Liechman, J.F.; Greenberg, A.; Williams, R.E. Ed.; VCH: New York, 1968.

24.   Fau, S.; Frenking, G. *THEOCHEM* **1995** (in press).

25.(a) Collins, J.B.; Dill, J.D.; Jemmis, E.D.; Apeloig, Y.; Schleyer, P.v.R.; Seeger, R.; Pople, J.A. *J. Am. Chem. Soc.* **1976,** *98,* 5419.

    (b) Krogh-Jesperson, K.; Crether, D.; Poppinger, D.; Pople, J.A.; Schleyer, P.v.R.; Chandrasekhar, J. *J. Am. Chem. Soc.* **1979,** *101,* 4843.

    (c) Farras, J.; Olivella, S.; Sole, A.; Vilarrasa, J. *J. Comput. Chem.* **1986,** 7, 428.

26.   Wehrmann, R.; Meyer, H.; Berndt, A. *Angew. Chem. Int. Ed. Engl.* **1985,** *24,* 788.

27.   Menzel, M.; Steiner, D.; Winkler, H-J.; Schwikart, D.; Mehle, S.; Fau, S.; Frenking, G.; Massa, W.; Berndt, A. *Angew. Chem. Int. Ed. Engl.* **1995,** *34,* 327.

28. Jorgenson, W.L.; Salem, L. *The Organic Chemists Book of Orbitals*; Academic Press: New York, 1973.

29.   Tsuzuki, S.; Schafer, L.; Goto, H.; Jemmis, E.D.; Osaya, H.; Siam, K.; Tanabe, K.; Osawa, E. *J. Am. Chem. Soc.* **1991,** *113*, 4665.

30.(a) Greenwood, N.N.; Savory, C.G.; Grimes, R.N.; Sneddon, L.G.; Davison, A.; Wreford, S.S. *J. Chem. Soc, Chem. Commun.* 1974,718.

    (b) Miller, V.R.; Grimes, R.N. *J. Am. Chem. Soc.* **1973,** *95,* 5078.

   (c) Weiss, R.; Grimes, R.N. *J. Am. Chem. Soc.* **1977,** *99,* 8087.

31. Jemmis, E.D.; Subramanian, G.; Srinivas, G.N. *Inorg. Chem.* **1994,** 55, 2317.

32. Wong, K.S.; Haller, K.J.; Dutta, T.K.; Chipman, D.M.; Fehlner, T.P. *Inorg. Chem.* **1982,** 2/, 3197.

33. Buhl, M.; Schleyer, P.v.R. *J. Am. Chem. Soc.* **1992,** *114*, 477.

34. (a) Jemmis, E.D.; Prasad, B.V.; Prasad, P.V.A.; Tsuzuki, S.; Tanabe, K. *Proc. Ind. Acad. Sci. (Chem. Sci.).* **1990,** *102,* 107.

   (b) Jemmis, E.D.; Prasad, B.V.; Tsuzuki, S.; Tanabe, K. *J. Phys. Chem.* **1990,** *94,* 5530.

[1.2] *Isomer Study of $Si_3H_3^+$*

Reactive silicon compounds have drawn considerable attention due to the interest in the Chemical Vapour Deposition (CVD) of silicon.[1] Along with these, studies on the kinetics and thermochemistry of small silicon compounds have grown rapidly.[2] Ion-molecule reactions of silane have produced, among others, $Si_3H_3^+$, which has been detected by ICR spectrometric methods.[3] Silicon hydrides (or hydrosilicons) are of additional interest in view of the striking contrast they provide to the structures of hydrocarbons.[4] The silicon analog (1) of ethylene (2) is nonplanar and the structures of Si_2H_2 (3), and C_2H_2 (4) differ dramatically.[5,6] Similarly, a trigonal prismatic structure (5) was calculated to be more favourable for Si_6H_6 than the traditional planar 6π aromatic structure, known to be the global minimum for benzene (6).[7]
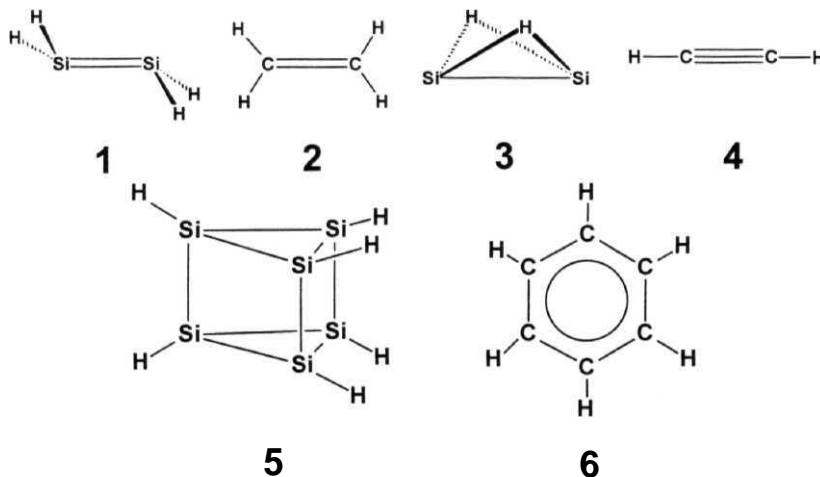
Recently, the prismatic structure for Si_6R_6 (R - 2,6-diisopropylphenyl) has been determined by X-ray analysis.[8] These structural alternatives available to hydrosilicons prompted us to study the potential energy surface of $Si_3H_3^{+}$,[9] isoelectronic to $C_3H_3^{+}$. The minimum energy structures for $C_3H_3^{+}$ are 7, 8, 9 and 10 with cyclopropenyl cation, 7 being the global minimum.[10] We find that the classical *2n* aromatic structure (11) is the global minimum for $Si_3H_3^{+}$ also.[9] However in contrast to $C_3H_3^{+}$ isomers there are several low energy structures with 3c-2e bonds, H- and Si- bridging and cyclic *n* delocalization on the $Si_3H_3^{+}$ potential energy surface.
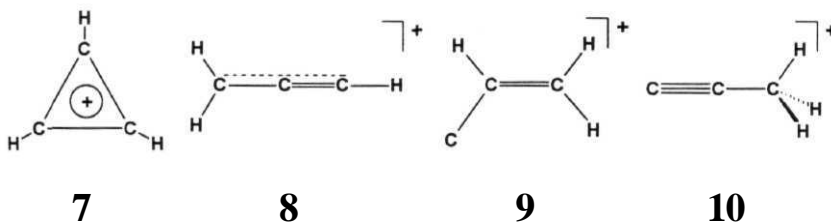
**7**   **8**   **9**   **10**

The geometries of all the structures considered were optimized initially at the Hartree-Fock (HF) and the MP2 levels of theory with the polarized 6-31G* basis set.[11-13] For open shell species, the unrestricted SCF reference function (UHF or UMP2) was used. The nature of the calculated stationary points were then determined by analytical evaluation of the harmonic force constants and vibrational frequencies at the HF level for all structures as well as at the MP2 level.[14] All the calculations were carried out using GAUSSIAN92 program package.[15] The energy comparisons are at MP2/6-31G*//MP2/6-31G* + ZPE (HF/6-31G*). Zero point energies were scaled by 0.9 as recommended.[11] The MP2/6-31G*

geometries and NBO analysis at HF level are used in the discussion (Table 1 and Fig. 1).[16,17]

The trisilacyclopropenyl cation, 11 (Fig. 1)[9], an analog of cyclopropenyl cation, is found to be the global minimum on the potential energy surface of $Si_3H_3^+$. The SiSi bond length of 2.198A is slightly longer than the standard double bond length (2.138Å in the D_{2h} planar and 2.165Å in the C_{2h} bent structures of disilene)[6] but much shorter than the normal SiSi single bond length (SiSi distance in trisilacyclopropane is 2.327A and in disilane 2.335Å).[18] HOMO of 11 is the delocalized n-orbital. Mulliken charge analysis shows the positive charge to be localized on the Si (charge on Si is 0.31 and on H is -0.01). On the other hand in $C_3H_3^+$, the reversed electronegativity differences of C and H makes the positive charge to be localized on H's (C is -0.03; H is 0.36). The isodesmic equations (1) and (2) provide estimates of the resonance stabilization energy (RSE) in 11 and in the cyclopropenyl cation (values in parantheses). The RSE in equation 1 represent total 3c-2e delocalization, while those in equation 2 show the extra cyclic π-delocalization or aromaticity.

X=Si (C)
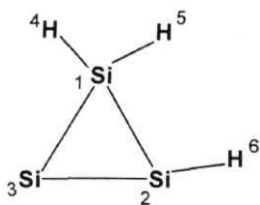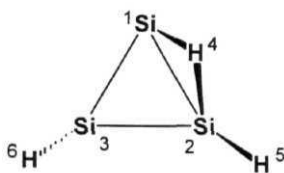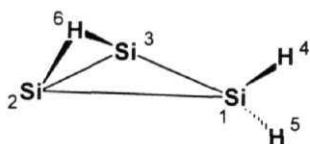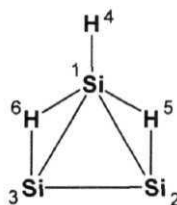$\Delta E = 38.1 (78.0)$ kcal/mol **(1)**
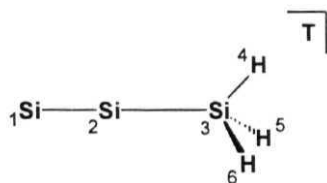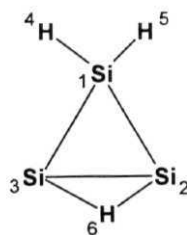

X=Si (C)
$\Delta E = 16.1 (35.7)$ kcal/mol **(2)**
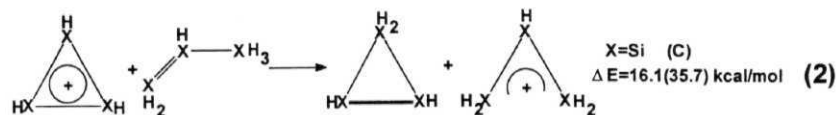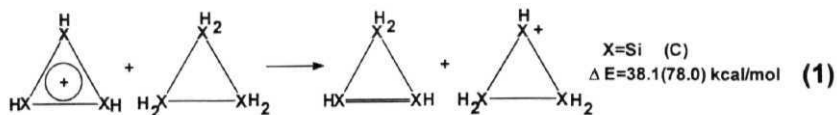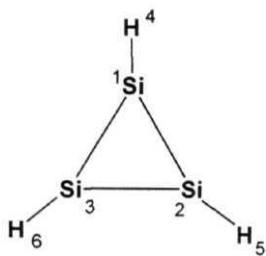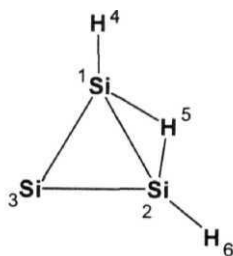
Fig. 1: The optimized structures of $Si_3H_3^+$, which are minimum at MP2/6-31G* level.

22

24
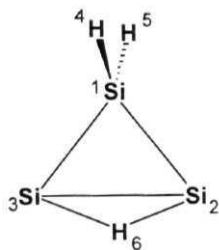
25
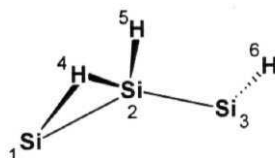
26
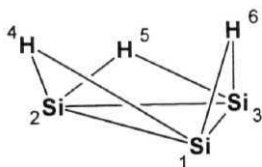
27
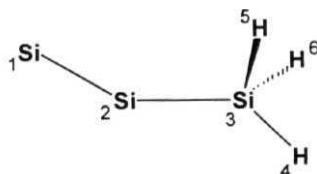
30
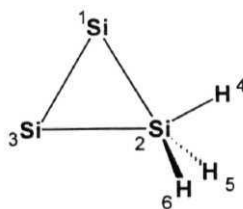
31

Fig. 1: (Continued)

Table 1

Total Energy (hartrees), Relative Energies (kcal/mol), Zero Point Energy (ZPE, kcal/mol), and number of imaginary frequencies (NIM) at MP2/6-31G* level for the structures considered.

Structues	Total Energy	ZPE	Relative Energy	NIM
11	-868.40970	16.52	0.0	0
12	-868.33205	16.44	48.7	0
13	-868.38719	16.85	14.4	0
14	-868.38559	16.22	15.1	0
15	-868.38244	15.66	17.1	1
16	-868.37405	16.36	22.4	1
17	-868.37866	15.96	19.5	1
18	-868.38010	16.88	18.6	0
19	-868.37549	16.51	21.5	0
20	-868.377033	15.86	24.7	0
22	-868.36858	17.80	25.7	0
24	-868.36528	16.89	27.8	0
25	-868.34521	14.66	40.4	0
26	-868.34002	14.91	42.3	0
27	-868.34226	16.24	42.4	0
29	-868.32297	16.46	54.5	0
30	-868.34043	17.80	43.4	0
31	-868.33846	17.75	44.7	0
32	-868.32400	16.55	53.8	2
33	-868.29513	17.84	71.9	2
34	-868.29661	17.76	70.9	2
35	-868.33440	13.67	47.2	1

Table 2:

Important geometrical parameters of the optimized structures at MP2/6-31G* level (distances in A and angles in degrees).

S.No.	Parameter	Calc. Value
11	Si(1)-Si(2)	2.198
	Si(1)-H(4)	1.479
12	Si(1)-Si(2)	2.343
	Si(2)-Si(3)	2.237
	Si(2)-H(5)	1.498
	Si(1)-H(4)	1.482
	Si(2)-Si(1)-H(4)	103.28
	Si(1)-Si(2)-H(5)	149.28
	Si(3)-Si(2)-Si(1)-H(4)	-97.37
	Si(3)-Si(1)-Si(2)-H(5)	138.72
13	Si(2)-Si(3)	2.269
	Si(1)-Si(2)	2.248
	Si(1)-H(4)	1.478
	Si(1)-H(5)	1.659
	Si(2)-Si(1)-H(4)	141.36
	Si(1)-Si(3)	2.386
	Si(1)-Si(2)	2.339
14	Si(2)-Si(3)	2.168
	Si(1)-H(5)	1.477
	Si(1)-H(4)	1.490
	Si(2)-H(6)	1.487
	Si(3)-Si(2)-H(6)	175.15
	Si(2)-Si(1)-H(4)	86.92
	Si(2)-Si(1)-H(5)	162.72
	Si(1)-Si(2)	2.295
	Si(2)-Si(3)	2.209
15	Si(1)-Si(3)	2.291
	Si(1)-H(4)	1.476
	Si(1)-H(5)	1.531
	Si(2)-H(6)	1.482
	H(4)-Si(1)-Si(2)	170.80
	H(5)-Si(1)-Si(2)	64.45
	H(6)-Si(2)-Si(l)	123.52
	Si(1)-Si(3)	2.262
	Si(2)-Si(3)	2.096
16	Si(1)-H(4)	1.478
	Si(2)-H(6)	1.480
	Si(3)-Si(2)-H(6)	166.45
	H(4)-Si(1)-Si(2)-Si(3)	111.31

S.No.	Parameter	Calc. Value
17	Si(1)-Si(2)	2.661
	Si(1)-Si(3)	2.282
	Si(2)-Si(3)	2.135
	Si(1)-H(4)	1.747
	Si(2)-H(4)	1.570
	Si(2)-H(5)	1.474
	Si(3)-H(6)	1.470
	Si(3)-Si(2)-H(5)	161.77
	Si(2)-Si(3)-H(6)	134.92
18	Si(1)-Si(2)	2.582
	Si(2)-Si(3)	2.145
	Si(1)-Si(3)	2.308
	Si(1)-H(4)	1.746
	Si(2)-H(4)	1.582
	Si(2)-H(5)	1.475
	Si(3)-H(6)	1.473
	Si(3)-Si(2)-H,5)	160.73
	Si(2)-Si(3)-H(6)	131.05
	Si(3)-Si(2)-Si(1)-H(4)	-24.33
	H(5)-Si(2)-Si(3)-Si(1)	187.38
	H(6)-Si(3)-Si(1)-Si(2)	132.44
19	Si(2)-Si(3)	2.231
	Si(1)-Si(3)	2.225
	Si(1)-Si(2)	**2.911**
	Si(2)-H(6)	1.726
	Si(3)-H(6)	1.643
	Si(1)-H(4)	1.474
	Si(1)-H(5)	1.476
	H(6)-Si(2)-Si(3)-Si(1)	90.50
20	Si(1)-Si(2)	2.287
	Si(2)-Si(3)	2.385
	Si(1)-H(4)	1.472
	Si(1)-H(5)	1.700
	Si(2)-H(5)	1.638
22	Si(1)-Si(2)	2.244
	Si(2)-Si(3)	2.390
	Si(3)-H(4)	1.460
	Si(2)-Si(3)-H(4)	102.24

Continued..

Table 2: (Continued)

S.No.	Parameter	Calc. Value
23	Si(1)-Si(2)	2.043
	Si(2)-Si(3)	**2.587**
	Si(3)-H(4)	**1.462**
	Si(2)-Si(3)-H(4)	**96.70**
24	Si(l)-Si(2)	2.326
	Si(2)-Si(3)	2.512
	Si(1)-H(4)	**1.482**
	Si(2)-H(6)	**1.618**
	H(4)-Si(l)-H(5)	115.26
25	Si(1)-Si(2)	2.372
	Si(2)-Si(3)	**2.953**
	Si(1)-H(4)	**1.481**
	Si(2)-H(6)	1.741
	H(4)-Si(l)-H(5)	117.55
26	Si(l)-Si(2)	2.254
	Si(2)-Si(3)	2.416
	Si(1)-H(4)	1.685
	Si(2)-H(4)	1.714
	Si(2)-H(5)	**1.499**
	Si(3)-H(6)	1.517
	Si(l)-Si(2)-H(5)	**96.61**
	H(5)-Si(2)-Si(3)	115.92
	Si(2)-Si(1)-H(4)	**49.0**
	H(6)-Si(3)-Si(2)	**83.84**
27	Si(l)-Si(2)	2.502
	Si(1)-H(4)	1.665
	Si(l)-Si(2)-Si(3)-H(5)	-130.78
29	Si(l)-Si(2)	2.302
	Si(1)-H(4)	1.721
30	Si(l)-Si(2)	2.295
	Si(2)-Si(3)	2.380
	Si(3)-H(4)	**1.479**
	Si(3)-H(5)	1.473
	Si(l)-Si(2)-Si(3)	158.19
	Si(2)-Si(3)-H(4)	99.80
	Si(2)-Si(3)-H(5)	107.51
31	Si(l)-Si(2)	2.732
	Si(2)-Si(3)	2.338
	Si(l)-Si(3)	2.373

S.No.	Parameter	Calc. Value
32	Si(1)-Si(2)	2.184
	Si(2)-Si(3)	2.015
	Si(3)-H(6)	1.471
	Si(l)-H(4)	1.467
	Si(2)-Si(l)-H(4)	120.29
33	Si(1)-Si(2)	2.525
	Si(l)-H(4)	1.512
	Si(l)-Si(2)-Si(3)	126.04
	Si(2)-Si(l)-H(4)	88.26
	Si(l)-Si(2)-H(5)	116.98
34	Si(1)-Si(2)	2.515
	Si(2)-Si(3)	2.534
	Si(l)-H(4)	1.514
	Si(2)-H(5)	1.491
	Si(3)-H(6)	1.512
	Si(l)-Si(2)-Si(3)	132.26
	H(4)-Si(l)-Si(2)	88.42
	H(5)-Si(2)-Si(3)	116.15
	Si(2)-Si(3)-H(6)	88.20
35	Si(l)-Si(2)	2.309
	Si(l)-Si(4)	1.580
	Si(2)-H(5)	1.495
	H(4)-Si(l)-Si(2)	60.86
	Si(l)-Si(2)-H(5)	106.48
	H(4)-Si(l)-Si(2)-H(5)	79.28

The stabilization in 11 is nearly half of that of the cyclopropenyl cation. A C_S excited state ($^3A'$, 12) (obtained by transferring an electron from SiSi σ-bonding orbital (a") of 11 to π^*-antibonding orbital (a')), is also found to be a minimum, 48.7 kcal/mol higher in energy than 11.


12
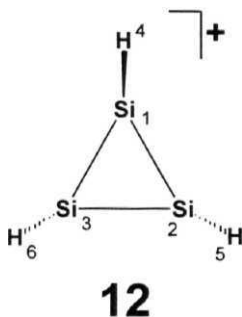
The nearest low energy C_{2v} isomer 13 (Fig. 1), with one hydrogen bridging the Si(l)Si(2) bond, is 14.4 kcal/mol higher in energy than 11. The Si(l)Si(2) bond distance is shorter than the SiSi distance (2.373Å at SCF/DZP level) in tribridged $Si_2H_3^+$.[19] But, it is longer than SiSi distance (2.185Å at SCF/DZP level) in dibridged Si_2H_2 (3).[5d] The electronic structure of 13 is quite remarkable with a cyclic π-delocalized MO, a lone pair on the divalent Si and an H-bridged SiSi bond. The Si(2)-Si(3) *n*-overlap population (0.099) is less than that found in 11 (0.110), due to the longer SiSi bond length (2.269A, Table 2). 13 can be considered as an analog of the most stable structure of CB_2H_4[20] and of $B_3H_4^-$.[21] A related structure with a divalent Si has been characterized experimentally for C_2SiH_2.[22] Similar structure with two divalent silicons and an H-bridged SiSi bond is calculated to be the global minimum for CSi_2H_2.[23]

The C_s planar minimum, 14, (Fig. 1) close in energy to 13 (Table 1) is obtained by shifting its bridging hydrogen to the terminal position. Dramatic changes in the Si-Si bond lengths in 14 is in accord with the following bonding description: a 3c-2e bond (Si(3)-Si(l)-Si(2)) in the σ-framework, a 3c-2e π-bond and a σ-lone pair. The positive charge is more localized on Si(l) in 14 (NBO charges are Si(l): 0.508, Si(2): 0.441, Si(3): 0.360) than in 13 (NBO charges are Si(l) = Si(2): 0.465, **Si(3): 0.388**). The symmetry allowed interconversion of 13 and 14, has a transition state 15 (2.0 kcal/mol above 14). A similar transition state is found for Si_3H_2.[24]

15   **14a**
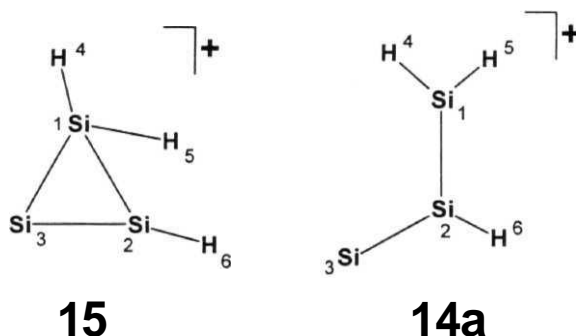
The dramatic effect of electron correlation is seen in the collapse of **14a,** which is a minimum at HF, into **14** at MP2 with the transformation of the localized Si(l)-Si(2) bond in **14a** to a SiH2-bridged bond in **14.** However, the carbon analog (9) of **14a** has been detected mass spectrometrically.[25] Rotation of SiH_2 group in **14** out of the SiSiSi plane leads to the C_s transition structure 16, in which a pair of π-electrons are localized in the Si(2)Si(3) bond.

The planar C_s structure 17 with unsymmetrical H-bridged bond has a bonding pattern similar to that of the C_{2v} minimum 13, but is 5.1 kcal/mol higher in energy and is a transition state. The non-planar minimum, 18 (Fig.l), arising from 17 on optimization without any symmetry constraint,[9a] is only 1.0 kcal/mol more stable than 17. The bridging hydrogen in 18 is 0.65A above the SiSiSi plane.

16   **17**
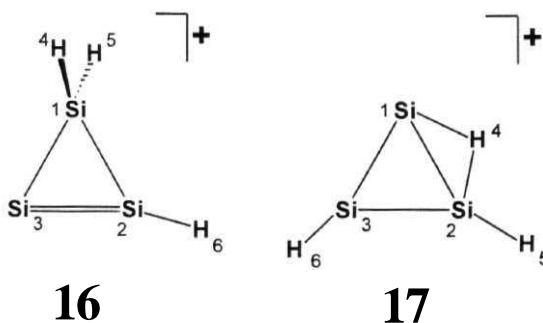
The next isomer 19 (Fig.l), with C_1 symmetry,[9a] is 21.5 kcal/mol higher in energy than 11. The MO analysis reveals the following features: a 2c-2e bond between Si(1) and Si(3), a 3c-2e hydrogen bridged bond between Si(2) and Si(3), and lone pair orbitals on Si(2) and Si(3). The charge is found to be mainly delocalized between Si(1) (q_{NBO} =0.793) and Si(3) (q_{NBO} =0.635). Though the **Si(l)-Si(2)** bond distance (2.911A) is much longer than the normal Si-Si single bond distance, there is a weak bonding interaction between the p_π-orbital on Si(1) and the lone pair on Si(2), as supported by the small positive Mulliken overlap population (0.046). This interaction arises mainly due to electron correlation effect, as at HF the Si(l)Si(2) distance is much larger (3.268A).

21   **20a**   **23**
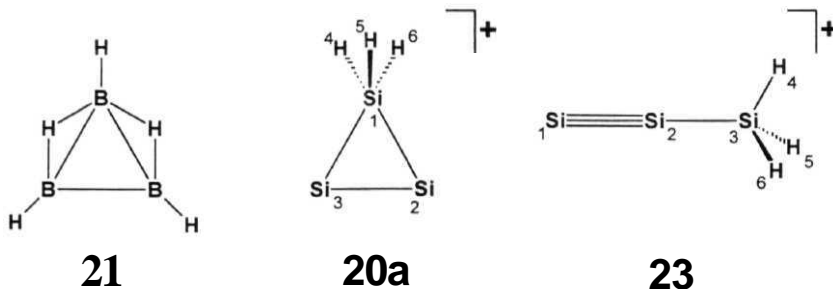
Isomer 20 (Fig.1), with the energy 24.7 kcal/mol above **11**, is related to the global B3H5 (21) minimum.[21,25] **21** and 20 have the same number of valence electrons and trivalent boron is isolobal with the divalent Si with a lone pair.[23] Electron correlation favours the 3c-2e delocalization present in the H-bridged structure, as the C_s minimum 20a, calculated at HF, collapses to the planar C_{2v} (20) at MP2.

The most stable acyclic structure obtained in this study is the triplet isomer, 22 (Fig.1), 25.7 kcal/mol higher in energy than 11. The *n*-bond in 22 is formed by two equivalent one-electron half bonds in perpendicular planes. The corresponding triple bonded structure, 23, with empty σ-hybrid orbital on Si(l) has high energy (99.2 kcal/mol above **11**) and shows an instability towards UHF. However, the carbon analog (10) is known experimentally.[26]

Comparison of 24 and 25 (Fig.l) provides an interesting example of the preference for a planar tetracoordinated Si over the tetrahedral arrangement and 3c-2e delocalized bonding (SiH2-bridged and cyclic π-orbitals in 24) over localized bonds. Both 24 and 25 have two H-bridged

divalent silicons. The H-bridged SiSi bond in **24** (2.512Å), as expected, is much shorter than that in **25** (2.953 A) because of the bonding p_π-p_π overlap and a reduced electron repulsion in the σ-frame in **24.** Structure **24** is an analog of the doubly H-bridged isomer of Si_2H_2.[5] This analogy is even more evident for the non-planar C_S minimum **24a** established at HF, which optimizes to 24 at MP2 level.


24a   **28**   **29**
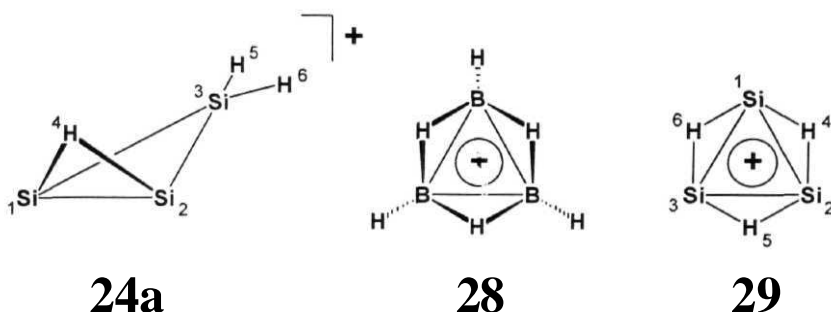
Isomer 26 (Fig.l), with $C\backslash$ symmetry is another acyclic minimum on the potential energy surface of $Si_3H_3^+$. The MO analysis of 26 reveals the following features: A 2c-2e bond between Si(1)Si(2), **Si(2)Si(3), Si(2)H(5)** and Si(3)H(6) and a 3c-2e bond between Si(1)H(4)Si(2). Two lone pairs are traced one each on Si(1) and Si(3). The positive charge is localized on Si(1) (qNBO = 0.846) and **Si(3)** (qNBO = 0.715).

The isolobal analogy between trivalent boron and divalent silicon[23] relates the triply H-bridged nonplanar C_{3v} minimum 27 (Fig.l) (42.4 kcal/mol above 11) to the C_{3v} global minimum of $B_3H_6^+$, **28**.[21,25] The SiSi distance is close to that of hydrogen bridged SiSi bond distances found in 18 and **24.** Similarly, the SiH_b bond distance is close to that in 13 and

24. The bridging hydrogens lie 0.833A above the Si_3 plane. The HOMO, HOMO-1 and HOMO-2 are traced to be the three lone pair orbitals on Si. The HOMO-3 is a π-orbital on Si_3 ring plane, and has a substantial contribution from the hydrogen 1s orbital also. This leads to a six orbital cyclic delocalization similar to that observed in $B_3H_6^+$ (Fig.2 in Chapter 1.1). The planar D_{3h} structure 29 is 12.1 kcal/mol above 27, and is a minimum at MP2/6-31G*. However, 29 is a higher order saddle point at other levels of theory.[9] The corresponding triply bridged structures for $C_3H_3^+$ are not minima.[9]

The singlet C_s isomer 30 (Fig. 1) has an electronic structure similar to that of the triplet 22. In accordance with the Hund's rule, electron pairing is energetically unfavourable in the C_{3v} symmetrical singlet electron state compared to the triplet state. Isomer 31 (Fig. 1) is characterised to be a minimum, 44.7 kcal/mol higher in energy than the global minimum 11. Two lone pairs, one each on Si(1) and Si(3), were traced from the MO pattern. The charge is localized mostly on Si(1)

32   **33**

34   **35**
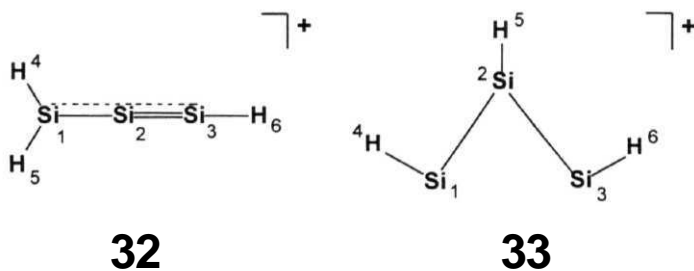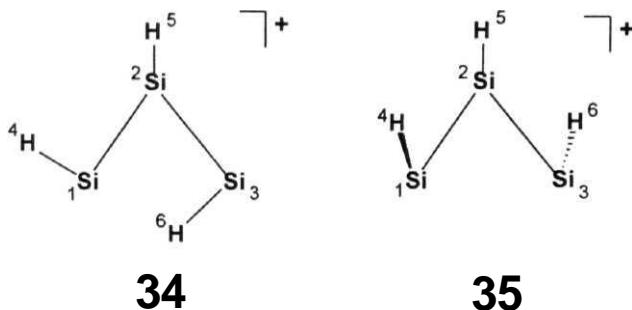
Several other acyclic structures considered here turned out to be not minima. The trisilapropargyl cation, 32, is characterized to be a second order saddle point. 32 is 53.8 kcal/mol higher in energy than 11. The analogous propargyl cation 8 is only 27.5 kcal/mol above the cyclopropenyl cation,[10b] and is known experimentally.[27]

The three open chain HSiSi(H)SiH structures 33, 34 and 35 do not correspond to minima (Table 1). Planar structures, 33 (C_{2v}) and 34 (C_S), with delocalized 2π-electrons and with two lone pairs on terminal silicons, are substantially higher in energy than 35. Nonplanar 35 also has two lone pairs on the terminal silicons (below and above Si_3 plane). The positive charge is localized more on the terminal Si atoms than on the central Si due to hyperconjugation. This is also responsible for decrease in the bond angle H(6)Si(3)Si(2) and H(4)Si(1)Si(2) to 60.0. Further optimization of 35 with the relaxed symmetry constrains led to 26.

Thus, the potential energy surface of $Si_3H_3^+$ contrasts dramatically with that of $C_3H_3^+$. Apart from the classical cyclopropenyl cation, $C_3H_3^+$ does not have any low energy cyclic structure. On the other hand, we have

characterized nine cyclic structures with varying numbers of bridging hydrogens within a range of 45 kcal/mol from the classical trisilacyclopropenyl cation, the global minimum, **11**. The silicon analogs of the acyclic structures prop-2en-l-yl-3-ylidene cation and 1-propynyl cation are not minima. The trisilaprop-2-en-l-yl-3-ylidene cation collapse to 14 on further optimization at the MP2/6-31G* level. Trisila-1-propynyl cation (23) is a minimum but unstable to UHF; whereas, the triplet state (22) is found to be a minimum. The planar tetracoordinated silicon is stabilized through π-delocalization in 13, 14 and 24. Isomers 20 and 27, derived from B3H5 and $B_3H_6^+$ using the isolobal analogy between trivalent boron and divalent silicon, are also minima. In general, the hydrogen bridged structures and the structures with divalent silicon dominate the potential energy surface of $Si_3H_3^+$; even though the global minimum is the classical aromatic structure.

References:

1.(a) Boo, H.B.; Armentrout, P.B. *J. Am. Chem. Soc,* **1987,** *109,* 3549.

  (b) Elkind, J.L.; Armentrout, P.B. *J. Phys. Chem.* **1984,** *88,* 5454.

  (c) Jasinski, J.M. *J. Phys. Chem.* **1986,** *90,* 555.

2.(a) Weber, M.E.; Armentrout, P.B. *J. Chem. Prhys.* **1988,** *88,* 6898.

  (b) Walsh, R. *J. Chem. Soc, Faraday Trans.* 1. **1983,** *1,* 2233.

  (c) Jasinski, J.M.; Chu, J.O. *J. Chem. Prhys.* **1988,** *88,* 1678.

  (d) Ignacio, E.W.; Schlegel, H.B. *J. Phys. Chem.* **1990,** *94,* 7439, and references therein.

3.   Stewart, G.W.; Henis, J.M.S.; Gaspar, P.P. *J. Chem. Phys.* **1973,** *58,* 890.

4.(a) Luke, B.T.; Pople, J.A.; Krogh-Jespersen, M.B.; Apeloig, Y.; Chandrasekhar, J.; Schleyer, P.v.R. *J. Am. Chem. Soc.* **1986,** *108,* 260.

  (b) Luke, B.T.; Pople, J.A.; Krogh-Jespersen, M.B.; Apeloig, Y.; Karni, M.; Chandrasekhar, J.; Schleyer, P.v.R. *J. Am. Chem. Soc.* **1986,** *108,* 270.

  (c) Sannigrahi, A.B.; Nandi, P.K. *Chem. Phys. Lett.* **1992,** *188,* 575, and references therein.

  (d) Trinquier, G. *J. Am. Chem. Soc.* **1990,** *112,* 2130, and references therein.

  (e) Somasundram, K.; Amos, R.D.; Handy, N.C. *Theoret. Chim. Acta.* **1986,** *70,* 393.

  (f) Nagase, S.; Kudo, T.; Aoki, M. *J. Chem. Soc, Chem. Commun.* **1985,** 1121.

  (g) Sax, A.F.; Kalcher, J.; Janoschek, R. *J. Comput. Chem.* **1988,** *9,* 564.

5.(a) Grev, R.S.; Schaefer III, H.F. *J. Chem. Phys.* **1992,** *97,* 7990 and, references therein.

  (b) Cordonnier, M.; Bogey, M.; Demuynck, C; Destombes, J.L. *J. Chem. Phys.* **1992,** *97,* 7984, and references therein.

  (c) Bogey, B.; Bolvin, H.; Demuynck. C; Destombes, J.L. *Phys. Rev. Lett.* 1991,66,413.

  (d) Brenda, T.C.; Schaefer III, H.F. *J. Phys. Chem.* **1990,** *94,* 5593.

6.(a) Windus, T.L.; Gordon, M.S. *J. Am. Chem. Soc,* **1992,** *114,* 9559.

  (b) Trinquier, G. *J. Am. Chem. Soc,* **1991,** *113,* 144.

  (c) Trinquier, G.; Malrieu, J.-P. *J. Am. Chem. Soc,* **1991,** *113,* 8634.

(d) Curtiss, L.A.; Raghavachari, K.; Deutsch, P.W.; Pople, J.A. *J. Chem. Phys.* **1991,** *95,* 2433.

(e) Karni, M.; Apeloig, Y. *J. Am. Chem. Soc.* 1990, 772, 8589.

(f) Grev, R.S.; Schaefer III, H.F.; Baines, K.M. *J. Am. Chem. Soc.* 1990, *112,* 9458.

(g) Schleyer, P.v.R.; Kost, D. *J. Am. Chem. Soc.* **1988,** *110*, 2105.

(h) Teramae, H. *J. Am. Chem. Soc.* 1987, *109,* 4140.

(i) Olbrich, G. *Chem. Phys. Lett.* **1986,** *130,* 115.

(j) Krogh-Jespersen, K. *J. Am. Chem. Soc.* **1985,** 707, 537.

(k) Krogh-Jespersen, K. *J. Phys. Chem.* **1982,** *86,* 1492.

7.   Nagase, S.; Nakano, M; Kudo, T. *J. Chem. Soc, Chem. Commun.* 1987, 60.

8.   Sekiguchi, A.; Yatabe, T.; Kabuto, C; Sakurai, H. *J. Am. Chem. Soc.* 1993, 775, 5853.

9.(a) Korkin, A.; Glukhovtsev, M; Schleyer, P.v.R *Int. J. Quantum. Chem.* **1993,** *46,* 137.

  (b) Glukhovtsev, M.N.; Kirienkova, T.V.; Simkin, B. Ya.; Minkin, V.I.; Yudilevich, I.A. *Zh. Org. Khim.* 1989, *25,* 196.

  (c) Jemmis, E.D.; Naga Srinivas, G.; Leszczynski, J.; Kapp, J.; Korkin, A.A.; Schleyer, P.v.R. *J. Am. Chem. Soc.* 1995, **117**, 11361.

10.(a) Radom, L.; Hariharan, P.C.; Pople, J. A.; Schleyer, P.v.R. *J. Am. Chem. Soc.* **1976,** *98,* 10.

  (b) Li, W.-K.; Riggs, N.V. *J. Mol. Struct.* (THEOCHEM) 1992, *257,* 189, and references therein.

  (c) Wong, M.W.; Radom, L. *J. Am. Chem. Soc.* 1993 775, 1507.

  (d) Lopez, R.; Sordo, J.A.; Sordo, T.L. *J. Chem. Soc, Chem. Commun.* 1993, 1751.

  (e) Maluendes, S.A.; McLean, A.D.; Yamashita, K.; Herbst, E. *J. Chem. Phys.* 1993, 99, 2812.

11.   Hehre, W.J.; Radom, L.; Schleyer, P.v.R.; Pople, J.A. *Ab initio Molecular Orbital Theory.* Wiley: New York, 1986.

12.(a) Hariharan, P.C.; Pople, J.A. *Chem. Phys. Lett.* 1972, *66,* 217.

  (b) Francl, M.M.; Pietro, W.J.; Hehre, W.J.; Binkley, J.S.; Gordon, M.S.; DeFrees, D.J.; Pople, J.A. *J. Chem. Phys.* **1982,** *77,* 3654.

13.   M0ller, C; Plesset, M.S. *Phys. Rev.* **1934,** *46,* 618.

14.   Pople, J.A.; Krishnan, R.; Schlegel, H.B.; Binkley, J.S. *Int. J. Quantum. Chem. Symp.* 1979, *13,* 255.

15. Gaussian 92, Revision A, Frisch, M.J.; Trucks, G.W.; Head-Gordon, M.; Gill, P.M.W.; Wong, M.W.; Foresman, J. B.; Johnson, B. G.; Schlegel, H. B.; Robb, M. A.; Replogle, E.S.; Gomperts, R.; Andres, J.L.; Raghavacharei, K.; Binkley, J.S.; Gonzalez, G.; Martin, R.L.; Fox, D. J.; DeFrees, D.J.; Baker, J.; Stewart, J.J.P; Pople, J.A. Gaussian, Inc., Pittsburgh PA, 1992.

16.(a) Reed, A.E.; Weinhold, F. *J. Chem. Phys*. **1985,** *83,* 1736.

   (b) Reed, A.E.; Curtiss, L.A.; Weinhold, F. *Chem. Rev.* **1988,** *88,* 899.

17. Reed, A.E.; Schleyer, P.v.R. *J. Am. Chem.Soc*. **1990,** *112,* 1434.

18. Schleyer, P.v.R.; Kaupp, M.; Bremer, H.M.; Mislow, K. *J. Am. Chem. Soc*. **1992,** 774,6791.

19. Brenda, T.C.; Schaefer III, H.F. *J. Chem. Phys.* **1990,** *93,* 7230.

20.(a) Collins, J.B.; Dill, J.D.; Jemmis, E.D.; Apeloig, Y.; Schleyer, P.v.R.; Seeger, R.; Pople, J.A. *J. Am. Chem. Soc.* **1976,** *98,* 5419.

   (b) Krogh-Jespersen, K.; Cremer, D.; Poppinger, D.; Pople, J.A.; Schleyer, P.v.R.; Chandrasekhar, J. *J. Am. Chem. Soc.* **1979,** *101,* 4843.

   (c) Farras, J.; Olivella, S.; Sole, A.; Vilarrasa, J. *J. Comput. Chem.* **1986,** 7, 428.

   (d) Fan, S.; Frenking, G. *J. Mol. Struct.* (THEOCHEM), in press.

21.(a) Mckee, M.L.; Buhl, M.; Charkin, O.P.; Schleyer, P.v.R. *Inorg. Chem.* **1993,** *32,* 4549.

   (b) Korkin, A.A.; Schleyer, P.v.R.; McKee, M.L. *Inorg. Chem.* **1995,** *34,* 961.

22. Maier, G.; Reisenauer, H.P.; Pacl, H. *Angew. Chem. Int. Ed. Engl. 1994 33,* 1248.

23.(a) Jemmis, E.D.; Prasad, B.V.; Prasad, P.V.A.; Tsuzuki, S.; Tanabe, K. *Proc. Ind. Acad. Sci. (Chem. Sci.).***1990,** *102,* 107.

   (b) Jemmis, E.D.; Prasad, B.V.; Tsuzuki, S.; Tanabe, K. *J. Phys. Chem.* **1990,** *94,* 5530.

24. Ernst, M.C.; Sax, A.F.; Kalcher, J.; Katzer, G. (to be published).

25. Jemmis, E.D.; Subramanian, G.; Naga Srinivas, G. *J. Am. Chem. Soc.* **1992,** *114,* 7939.

26. Burgers, P.C.; Homes, J.L.; Mommers, A.A.; Szulejko, J.E. *J. Am. Chem.Soc.* **1984,** *106,* 521.

27. Holmes, J.L.; Lossing, F.P. *Can J. Chem.* **1979,** *57,* 249.

The isomers study on $B_3H_6^+$ and $Si_3H_3^+$ revealed the following general conclusions.

$B_3H_6^+$:

i) The planar cyclic structures with 2π electron delocalization are found to be more stable than the acyclic structures for $C_3H_3^+$, C2BH3, CB2H4 and B3H5 molecules.

ii)   For $B_3H_6^+$ the planar structure 18 is a transition state whereas the nonplanar structure 19 is a minimum and is 41.1 kcal/mol lower in energy than 18.

iii)   The nonbonded repulsions between bridged and terminal hydrogens in 18 results the nonplanar structure 19.

iv)   The bridging hydrogens in 19 are found to have better bonding with the B3 ring compare to that in 18.

$Si_3H_3^+$:

i)   The potential energy surface of $Si_3H_3^+$ drastically differs with that of $C_3H_3^+$.

ii)   The trisialacyclopropenyl cation (11) is found to be the global minimum.

iii)   Several structures with H-bridging and divalent silicon are found to be minima.

iv)   Structures with planar tetracoordinated silicon (14 and 24), isomers derived from B3H5 and $B_3H_6^+$ (20 and 27) are also minima.

Chapter 2:   H-Bridged Alternatives to the Heavier Analogs
                of Cyclopropane and Cyclobutane.

Alternative H-bridged structures 9, 10, and **11** for homologues of cyclopropane (1) and 16, **17,** 18 and **19** for homologues of cyclobutane (2) have been calculated using ab initio MO methods at the MP2/6-31G* and MP2/LANL1DZ levels. The energy difference between the classical structure 1 and its bridged analogue 9 decreases in going from C to Pb (1 Vs 9: C 197.0, Si 84.0, Ge 36.0, Sn -1.7 and Pb -45.4 kcal/mol) for cyclopropane. The cyclobutane analogues have also shown similar trend (2 Vs **17:** C 184.9, Si 145.8, Ge 81.7, Sn 32.4 and Pb -28.4 kcal/mol). It has been observed that structures **9-C** and **17-C** are not minima, whereas **9-Pb** and **17-Pb** are the lowest energy minima. The nature of the bonding in these molecules has been analysed using NBO method. Strain energy of three- and four- membered rings are estimated using equations 1 and 2. Isolobal analogy connects 9 to B3H9 and $(C_pCoCO)_3$.

Alicyclic hydrocarbons are one of the important compounds in organic chemistry.[1] Cyclopropane (**1-C**) and cyclobutane (2-C) have invoked seminal interest both theoretically and experimentally, due to their unusual structure and chemical properties[2,3] (throughout this chapter the structure number is followed by the symbol of the atom 'A' to specify the species). Despite the strain, 1-C and 2-C can be explained in terms of tetravalent carbon.[4]

1   **2**
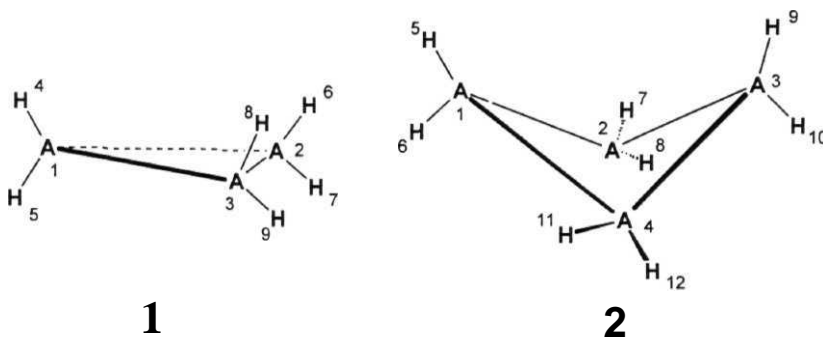
Do their homologues retain this classical structure? Experience with ethylene and acetylene points to marked differences in the structural arrangement on descending the group. A trans bent structure is found to be the global minimum for Si and Ge analogues (3-Si and 3-Ge) of ethylene.[5,6] 3 is a minimum for Sn and is a transition state for Pb.[7] The puckering of the hydrogens in 3 increases from Si to Pb. The H-bridged structure (4) is calculated to be lowest in energy for Sn and Pb.[7] Derivatives of Si_2H_4 and Ge_2H_4 have been found experimentally to have structures similar to **3**.[8,9] In the trans bent isomer 3, the pyramidalization angle θ_1 depends on the nature of the substituents.[9] For example, θ_1 is 18.0° in Si2(2,4,6-

$Me_3C_6H_2)_4$, whereas, it is $0.0°$ in $Si_2(2,6\text{-}Et_2C_6H_3)_4$.[10] Similarly, θ_1 is $32.0°$ in $Ge_2(CH(Me_3Si)_2)_4$.[11] The bistrimethylsilylmethyl derivative of Sn_2H_4 has the structure **3-Sn** with $\theta_1 = 41.0°$.[12] Derivatives of **4-Sn** are not yet known experimentally. Pb_2H_4 and its derivatives are also not known to the best of our knowledge.

A	θ_1
C	0.0
Si	11.2
Ge	36.5
Sn	48.9
Pb	56.3

3   **4**

H——A≡≡≡A——H

5   **6**
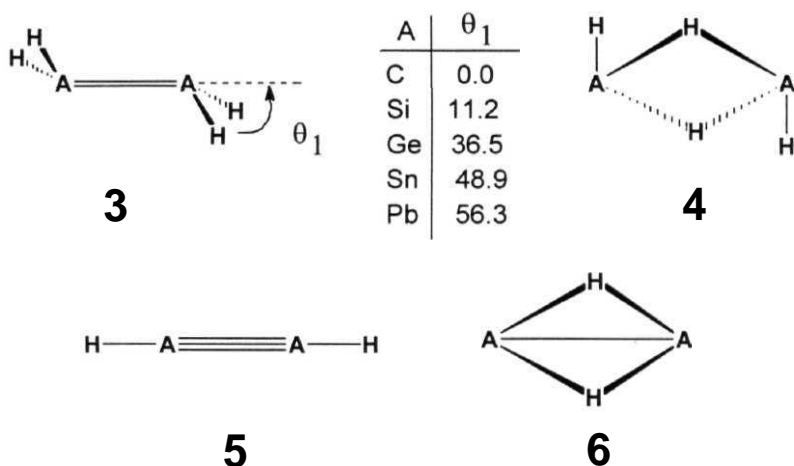
In contrast to acetylene **5-Si** and **5-Ge** analogues are calculated to prefer the doubly bridged structures **6**.[13,14] The structure of **6-Si** has been characterized experimentally.[15] The *2K* aromatic system, $A_3H_3^+$, also has shown similar trends. The classical 2π aromatic structure, 7-C, is the global minimum for $C_3H_3^+$.[16] In the case of $Si_3H_3^+$, **8-Si** is also a minimum and is higher in energy by **42.4 kcal/mol** than the global minimum, **7-Si** (Chapter 1).[17,18] The relative stabilities of 7 and 8 get reversed for Ge, Sn and Pb (7 Vs 8: Ge, -17.4; Sn, -32.4 and Pb, -63.3 kcal/mol at

Becke3LYP/TZ2P(+) level).[18] In fact, **7-Sn** is a transition state and **7-Pb** is a third order saddle point. These results indicate that alternative structures might indeed be possible for the strained ring compounds involving the heavier elements.

7   **8**
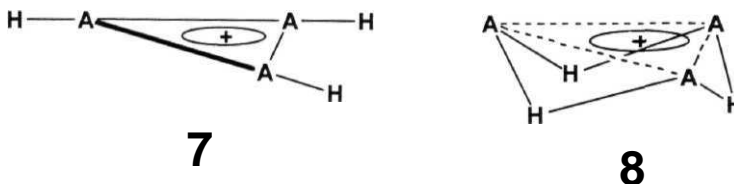
Derivatives of **1(C-Sn)**[19-22] and **2(C-Sn)**[23-26] with bulky substituents are known experimentally. Theretical studies are available on the parent structures **1(C-Pb)**[27-31] and **2(C-Pb)**.[27-33] None of these studies considered the H-bridged alternatives. In view of the results on 3-8, we reasoned that the bridged structures may be favourable for the homologues of cyclopropane and cyclobutane. This chapter deals with the studies on the bridged alternatives for heavier analogues of cyclopropane (section 2.1) and cyclobutane (section 2.2). The bridged alternatives are the lowest energy structures for Pb in both the 3-membered and the 4-membered rings.

The geometries of all the structures considered were optimized initially at the Hartree-Fock (HF) level.[34] These geometries were used for further optimization at the MP2 level to gauge the effect of electron correlation.[35] For C and Si, Pople's 6-31G* basis set was used.[36] Molecules involving Ge, Sn and Pb were optimized using the LANL1DZ basis set.[37] This basis set uses the valence **double-zeta** (DZ) basis on H and effective core potentials plus DZ on Ge, Sn and Pb. The nature of the

calculated stationary points was determined by evaluation of the harmonic force constants and vibrational frequencies at both the HF and MP2 levels.[38]   All the calculations were carrried out using the GAUSSIAN92 program package.[39]   The energy comparisons are at the MP2/6-31G*//MP2/6-31G* + ZPE level for C and Si and at the MP2/LANL1DZ//MP2/LANL1DZ + ZPE level for Ge, Sn and Pb. Zero point energies were scaled by 0.9.[34] The natural bond orbital (NBO) analysis at HF level and the geometries at the MP2 level are used in the discussion.[40]

The bridged structure, 4, of A_2H_4 suggested 9 (C_{3v}) as a possibility for A_3H_6. Similarly, 10 (D_{3h}) can be arrived at from the doubly bridged structure, 6. We also included 11 (D_{3h}), the planar alternative of 9. The total and relative energies are given in Table 1. The computed geometry of 9 is shown in Fig.1 and the important geometrical parameters are summarized in Table 2. The classical structure, 1, is found to be a minimum for all the Group 14 analogues from C to Sn. For Pb, however, 1 is calculated to be a transition state with the imaginary frequency leading to a C_{3h} structure, 12.31 For C_3H_6, all the bridged forms 9-C, **10-C** and **11-C** are calculated to be higher order saddle points, considerably higher in energy than **1-C** (Table 1).
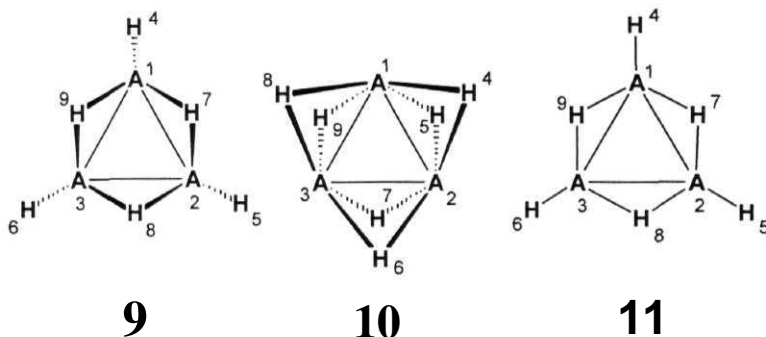

9   10   11

Table 1:

Total energies (in au), zero point energies (ZPE in Kcal/mol) and relative energies (RE in kcal/mol) of A_3H_6 system. The values in parentheses are the number of imaginary frequencies.

Molecule	Total energy (HF)	Total energy (MP2)	ZPE	RE
1-C (D_{3h})	-117.05887(0)	-117.44858(0)	52.6	0.0
9-C (C_{3v})	-116..71948(3)	-117.14976(3)	42.1	197.0
10-C (D_{3h})	-116.52135(5)	-116.99988(4)	35.5	297.0
11-C (D_{3h})	-116.31399(6)	-116.71343(6)	42.4	481.6
1-Si (D_{3h})	-870.18218(0)	-870.42320(0)	32.2	0.0
9-Si (C_{3v})	-870.05348(0)	-870.29100(0)	31.1	84.0
10-Si (D_{3h})	-869.98949(1)	-870.27715(0)	31.7	92.2
11-Si (D_{3h})	-869.80152(7)	-870.12780(4)	25.2	191.8
1-Ge (D_{3h})	-14.31686(0)	-14.46640(0)	29.0	0.0
9-Ge (C_{3v})	-14.26642(0)	-14.41152(0)	27.3	36.0
10-Ge (D_{3h})	-14.17173(3)	-14.35135(3)	24.7	76.1
11-Ge (D_{3h})				
1-Sn (D_{3h})	-13.13682(0)	-13.27329(0)	24.8	0.0
9-Sn (C_{3v})	-13.14752(0)	-13.27620(0)	24.6	-1.7
10-Sn (D_{3h})	-13.08659(3)	-13.23884(0)	24.0	22.3
11-Sn (D_{3h})	-12.90822(6)	-13.10830(4)	18.7	109.0
1-Pb (D_{3h})	-13.34036(1)	-13.48320(1)	22.8	0.0
9-Pb (C_{3v})	-13.42648(0)	-13.55559(0)	22.8	-45.4
10-Pb (D_{3h})	-13.37626(3)	-13.52474(2)	21.9	-25.3
11-Pb (D_{3h})	-13.19149(4)	-13.38549(1)	19.0	64.7
12-Pb (C_{3h})	-13.37018(0)	-13.50073(0)	??.A	-10.6
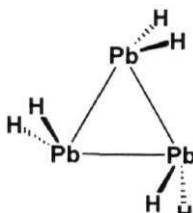
12

As we descend the group (Si-Pb), the preference for the classical structure 1 decreases. The triply H-bridged non-planar structure 9 is favoured and a minimum for all. The energy difference between 1 and 9 decreases from C to Pb (Table 1). In fact, for Sn and Pb, 9 is the lowest energy cyclic isomer that we have calculated, **(9-Sn < 1-Sn** by 1.7 kcal/mol and **9-Pb < 1-Pb** by 45.4 kcal/mol). 10 is calculated to be a higher order saddle point in each case, except for Sn and Si. The planar structure **11** is also a higher order saddle point for all except **11-Pb**, for which it is a transition state.

Scheme 1
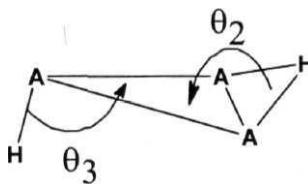
The classical structure 1 for C, Si, Ge and Sn has been discussed in literature.[27-30] Bond length comparisons were made typically with the

ethane like structures. The A-A distances in 1 are calculated to be slightly shorter than those in A_2H_6.[41] In contrast, the Pb-Pb distance in 1 is slightly longer than the distance in Pb_2H_6 (2.897A) (Table 2).[41] The bridged structure 9 has considerably elongated A-A distances compared to the cis-bridged A2H4, the cis analogue of 4.[7] The terminal $A\text{-}H_t$ distances increase uniformly in going from 1 to 9. The bridging hydrogens in 9 are only marginally out of the A3 plane (θ_2 in Table 2, Scheme 1). The angle between the A3 plane and the terminal A-H bonds (63, Scheme 1) is found to be unusual. 63 ranges from 80° to 84° (Table 2), with all three terminal hydrogens directed towards a converging point along the A-H direction except for 9-C (Fig. 1a, b). Thus, a projection of H_t onto the A3 plane falls inside the triangle. This type of arrangement is not seen in the classical structure, 1, where the hydrogens are directed away from each other. Similar trends have been noticed in 4 previously.

The bridging hydrogens in 9 are not far apart. The $H_b\text{-}H_b$ distances are 2.012A in 9-C, 2.411Å in **9-Si** and 2.464A in **9-Ge.** For **9-Sn** and **9-Pb,** the $H_b\text{-}H_b$ distances are clearly beyond the range of non-bonded repulsions (2.628A and 2.741A respectively).[42] Although the terminal A-H bonds are bent by a large angle (a projection of the hydrogens falls within the A3 triangle, Fig. 1), the distances between them is found to be relatively large except for 9-C (2.390, 2.653, 3.057, 3.384 and 3.522A in 9-C to **9-Pb** respectively). The extremely short $H_b...H_b$ non-bonded distances in 9-C contribute to its instability (Table 1).

Table 2:

Important geometric parameters of A_3H_6 systems.[a,b]

Molecule	A-A	$A-H_t$	$A-H_b$	θ_2	63
1-C[c]	1.504	1.085			
9-C	1.619	1.084	1.266	147.0	114.2
1-Si[c]	2.332	1.484			
9-Si	3.080	1.506	1.661	167.0	80.6
1-Ge	2.496	1.545			
9-Ge	3.417	1.602	1.777	172.6	82.5
1-Sn	2.860	1.719			
9-Sn	3.783	1.774	1.949	173.9	82.5
1-Pb	2.954	1.762			
9-Pb	3.889	1.824	2.007	174.3	83.3

[a]Distances are in Angstroms and angles are in degrees.
[b]θ_2 is the angle between A3 plane and AHA plane, θ_3 is the angle between A3 plane and AH_t axis (Scheme 1).
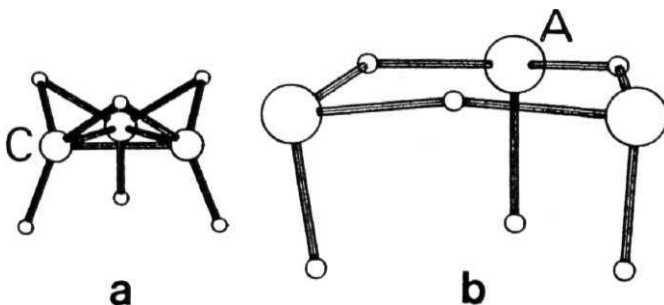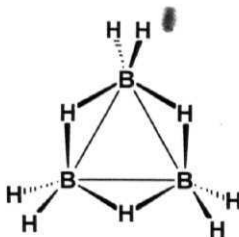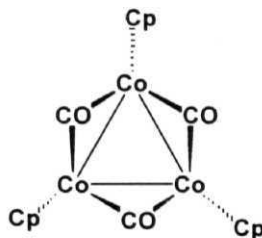[c]From ref. 27(c)

**Fig. 1**: Optimized geometries of (a) 9-C and (b) 9 (A is Si-Pb).

13　　　　**14**

The NBO analysis reveals the following bonding features for 9. The in-plane bonding in 9 can be described by three 3c-2e bonds involving the bridging hydrogens slightly outside the A3 plane and a lone pair on each A. The contribution of the p orbitals is higher in the 3c-2e bond; whereas the lone pairs have predominantly s character. The bonding of terminal hydrogens lying outside the A3 plane is best described by three 2c-2e bonds involving mainly the p orbitals of A3. In a formal way, the structure 9 can be derived from the structure of B3H9, 13, using the isolobal analogy between BH3 and SiH_2 (section 1.1 in Chapter 1)[43,44] and its heavier analogues. F01 example, if three terminal B-H bonds in 13 are replaced by Si with a lone pair, we obtain 9-Si. The lone pair on heavier atoms tends to have more s character, so that the remaining terminal A-H bonds have maximum p character leading to the calculated geometry, 9.

The isolobal analogy between main group elements and transition metal fragments[45] helps us to connect a recently reported trinuclear transition metal complex $Cp_3Co_3(CO)_3$, 14, to **9**.[46] CpCo is isolobal to B-H. The bridging carbonyls donate two electrons to skeletal bonding.

Ignoring the role played by the n^* molecular orbitals of CO, we can replace CO by H, with an electron added to the heavy atom. Thus, CpCo will be replaced by BH with an extra electron, which makes it isolobal to CH. Now, the resulting structure is 9-C, the structural type becoming competitive for the heavier analogues.

Strain energies of l(C-Pb) are estimated by the following homodesmic equation (Table 3).

$$A_3H_6 + 3A_2H_6 = 3A_3H_8 \qquad (1)$$
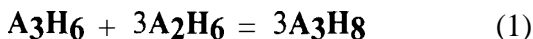
As was explainned in literature, silacyclopropane has higher strain energy than cyclopropane owing to the limited hybridization in Si.[28] The same trend has been observed for the homologues of the group.

Thus, the H-bridged structures 9, 10 and 11 were studied as an alternatives for the homologues of cyclopropane, 1. Among these bridged structures, 9 is found to be minimum for Si to Pb. Structure 10 is a minimum only for Si and Sn, and 11 is not a minimum for C to Pb. Structure 9 is found to be isolobal with B3H9 and $(C_pCoCO)_3$.

Table 3 :

Total energies (au) of A_2H_6 and A_3H_8 and the strain energies from equation 1 (kcal/mol) for 1. The energies are at HF/6-31G* for C and Si and at HF/LANL1DZ for Ge-Pb.

Molecule	A_2H_6	A_3H_8	Strain energy of 1
C	-79.22876	-118.26365	28.7
Si	-581.30495	-871.38646	38.9
Ge	-10.71789	-15.51283	42.7
Sn	-9.91518	-14.31535	40.0
Pb	-10.03646	-14.50258	36.4

Studies on 3-membered rings has shown that the stability of H-bridged alternative structures increases down the 14th group. In the present section this study has been extended to 4-memberd rings. The structures considered in the present study are shown in Fig.2. The bridged structures, 16 and 17, are derived from 15 and 2 in which a set of four hydrogens bridges the planar and puckered A4 ring respectively. Structures 18 and **19** are arrived from the doubly bridged structure 6. The classical planar D_{4h} structure, 15, is a transition state for C-Pb. The path of the imaginary frequency leads to the classical D_{2d} isomer, 2, for C-Sn. Previous calculations at HF level has shown that structure 2 collapses to 15 on optimization for Ge and Sn, and is a minimum. But the present results at MP2 level reveals a small negative frequency (-4.95 and **-16.48** for Ge and Sn respectively), which leads to D_{2d} structure, 2. However, in the case of Pb, the imaginary frequency leads to a C_{4h} structure, **20**.[31] The optimization of D_{2d} structure (2) for Pb collapses to 15. The C_{4v} bridged structure, 16, is a transition state for Si-Pb. The path of the imaginary frequency in 16 gives the puckered C_{2v} bridged sturcture, 17. Thus, classical planar structures, 15, and bridged planar structures, 16 are transition states for Si-Pb. The puckered structures, 2 (with the exception of Pb) and 17, are minimum for Si-Pb. In the case of carbon, the classical structure, 2, is a minimum and the bridged structure, 17, collapses to 21 on optimization. Among the doubly H-bridged structures, 18 is a higher order saddle point for C-Pb. Structure **19** collapses to two ethylenic units (A2H4) on optimization except for Sn. But, **19-Sn** is also a higher order saddle point.
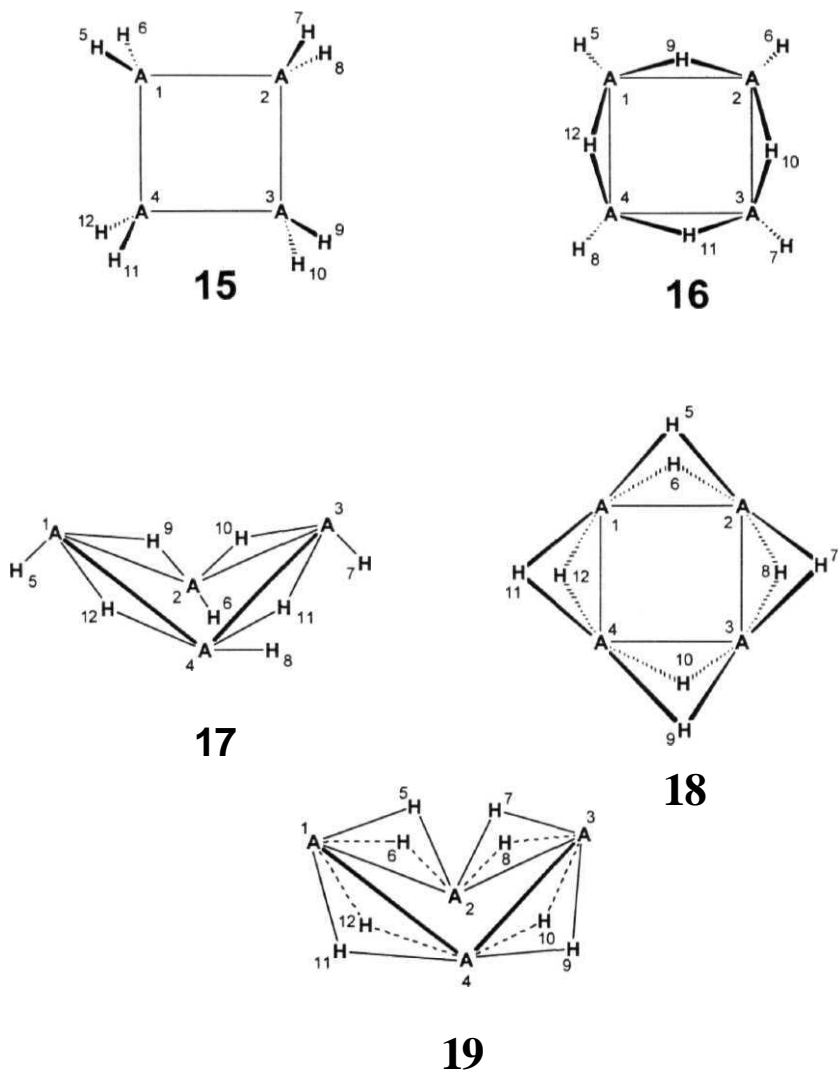
Fig. 2: Structures considered in the present study for A_4H_8 system. The classical system 2 (Section 2.1) is not shown in this figure.

Table 4:

Total energies (in au), zero point energies (ZPE in Kcal/mol) **and** relative energies (RE in kcal/mol) of A_4H_8 system. The values in parentheses are the number of imaginary frequencies.

Molecule	Total energy (HF)	Total energy (MP2)	ZPE	RE
15-C (D_{4h})	-156.09575(1)	-156.61438(1)	71.13	1.8
2-C (D_{2d})	-156.09720 (0)	-156.61799(0)	71.59	0.0
16-C (C_{4v})	-155.57660(4)	-156.15794(4)	55.90	273.8
17-C (C_{2v})	-155.77788(4)	-156.31043(4)	63.04	184.9
18-C (D_{4h})	-155.02277(11)	-155.68712(12)	28.8	543.5
15-Si (D_{4h})	-1160.29787 (1)	-1160.61438(1)	43.96	1.9
2-Si (D_{2d})	-1160.29894 (0)	-1160.61807(0)	44.40	0.0
16-Si (C_{4v})	-1160.06527 (1)	-1160.37533(1)	40.00	148.2
17-Si (C_{2v})	-1160.06840 (0)	-1160.37?53 (0)	40.30	145.8
18-Si (D_{4h})	-1159.96392(3)	-1160.33244 (3)	41.10	176.1
15-Ge (D_{4h})	-19.15310(1)	-19.35010(1)	39.40	0.3
2-Ge (D_{2d})	-19.15310(0)	-19.35120(0)	39.80	0.0
16-Ge (C_{4v})	-19.02071 (1)	-19.21208(1)	36.00	83.7
17-Ge (C_{2v})	-19.02368(0)	-19.21579(0)	36.30	81.7
18-Ge (D_{4h})	-18.64291 (8)	-18.93250(7)	25.27	248.9
15-Sn (D_{4h})	-17.57903 (0)	-17.75721 (1)	34.06	-0.05
2-Sn (D_{2d})	collapsed to **15**	-17.75728(0)	34.16	0.0
16-Sn (C_{4v})	-17.52895(0)	-17.69965(1)	32.40	34.5
17-Sn (C_{2v})	-17.53198(0)	-17.70331 (0)	32.60	32.4
18-Sn (D_{4h})	-17.16127(8)	-17.42965(6)	25.03	196.9
15-Pb (D_{4h})	-17.84731 (1)	-18.03232(1)	31.80	0.0
2-Pb (D_{2d})	collapsed to **15**			
16-Pb (C_{4v})	-17.90034(1)	-18.07201 (1)	29.90	-26.7
17-Pb (C_{2v})	-17.90286(0)	-18.07500(0)	30.10	-28.4
18-Pb (D_{4h})	-17.56280(8)	-17.82337(6)	27.10	126.7
20-Pb (C_{4h})	-17.85039(0)	-18.03300(0)	31.79	-0.4

Table 5:
Important geometrical parameters of the optimized structures at MP2 level (distances in A and angles in degrees).

S.No.	Parameter	Calc. Value
15-C	C(l)-C(2)	1.550
	C(l)-H(5)	1.093
	H(5)-H9	3.481
	H(5)-C(l)-H(6)	107.81
2-C	C(l)-C(2)	1.545
	C(2)-C(4)	2.145
	C(l)-H(5)	1.095
	C(l)-H(6)	1.094
	H(5)-H(9)	2.691
	θ_4	149.23
16-C	**C(l)-C(2)**	1.612
	C(l)-H(5)	1.089
	C(l)-H(9)	1.290
	C(3)-C(l)-H(5)	136.21
	C(l)-C(2)-H(9)	51.40
	C(3)-C(l)-C(2)-H(9)	119.98
18-C	C(l)-C(2)	1.652
	C(l)-H(5)	1.418
	C(3)-C(l)-C(2)-H(5)	**-98.11**
15-Si	Si(l)-Si(2)	2.367
	Si(l)-H(5)	1.490
	H(5)-H(9)	5.093
	H(5)-Si(l)-H(6)	108.31
2-Si	Si(l)-Si(2)	2.355
	Si(2)-Si(4)	3.237
	Si(l)-H(5)	1.491
	Si(l)-H(6)	1.488
	H(9)-H(11)	**3.681**
	θ_4	142.22
16-Si	Si(l)-Si(2)	3.245
	Si(l)-H(5)	1.509
	Si(1)-H(9)	**1.668**
	Si(3)-Si(l)-H(5)	76.53
	Si(l)-Si(2)-H(9)	13.23
	Si(3)-Si(l)-Si(2)-H(9)	97.07

S.No.	Parameter	Calc. Value
17-Si	Si(l)-Si(2)	3.240
	Si(l)-H(5)	1.513
	Si(2)-H(6)	**1.506**
	Si(l)-H(9)	**1.658**
	Si(2)-H(9)	**1.666**
	θ_6	51.78
	θ_7	77.86
	Si(l)-Si(2)-H(9)	12.69
	Si(4)-Si(3)-Si(2)-H(10)	126.57
	θ_5	129.78
18-Si	Si(l)-Si(2)	2.585
	Si(l)-H(5)	**1.683**
	Si(3)-Si(l)-Si(2)-H(6)	38.28
15-Ge	Ge(l)-Ge(2)	2.515
	Ge(l)-H(5)	1.552
	H(5)-Ge(l)-H(6)	108.60
	H(5)-H(9)	5.367
2-Ge	Ge(l)-Ge(2)	2.510
	Ge(2)-Ge(4)	3.513
	Ge(l)-H(5)	1.552
	Ge(l)-H(6)	1.550
	H(9)-H(11)	4.472
	θ_4	156.90
16-Ge	Ge(l)-Ge(2)	3.511
	Ge(I)-H(5)	1.603
	Ge(l)-H(9)	1.769
	Ge(3)-Ge(l)-H(5)	81.73
	Ge(l)-Ge(2)-H(9)	7.15
	Ge(3)-Ge(l)-Ge(2)-H(9)	89.44
17-Ge	Ge(l)-Ge(2)	3.505
	Ge(l)-H(5)	**1.607**
	Ge(2)-H(6)	**1.600**
	Ge(l)-H(9)	1.762
	Ge(2)-H(9)	**1.768**
	θ_6	**52.84**
	θ_7	**83.366**
	Ge(l)-Ge(2)-H(9)	6.94
	Ge(4)-Ge(3)-Ge(2)-**H(10)**	**138.70**
		121.83

Continued..

Table 5: (Continued)

S.No.	Parameter	Calc. Value
18-Ge	Ge(1)-Ge(2)	3.233
	Ge(1)-H(5)	1.919
	Ge(3)-Ge(1)-Ge(2)-H(6)	32.0
15-Sn	Sn(1)-Sn(2)	2.864
	Sn(1)-H(5)	1.722
	H(5)-Sn(1)-H(6)	108.14
	H(5)-H(9)	
2-Sn	Sn(1)-Sn(2)	2.862
	Sn(2)-Sn(4)	4.035
	Sn(1)-H(5)	1.723
	Sn(1)-H(6)	1.721
	H(9)-H(ll)	5.554
	θ_4	167.02
16-Sn	Sn(1)-Sn(2)	3.862
	Sn(1)-H(5)	1.775
	Sn(1)-H(9)	1.942
	Sn(3)-Sn(1)-H(5)	81.91
	Sn(1)-Sn(2)-H(9)	5.95
	Sn(3)-Sn(1)-Sn(2)-H(9)	82.23
17-Sn	Sn(1)-Sn(2)	3.856
	Sn(1)-H(5)	1.779
	Sn(2)-H(6)	1.770
	Sn(1)-H(9)	1.934
	Sn(2)-H(9)	1.942
	θ_6	51.79
	θ_7	83.11
	Sn(1)-Sn(2)-H(9)	6.22
	Sn(4)-Sn(3)-Sn(2)-H(10)	136.58
	θ_5	119.37
18-Sn	Sn(1)-Sn(2)	3.521
	Sn(1)-H(5)	2.083
	Sn(3)-Sn(1)-Sn(2)-H(6)	31.14
15-Pb	Pb(1)-Pb(2)	2.914
	Pb(1)-H(5)	1753
	H(5)-Pb(1)-H(6)	107.40
	H(5)-H(9)	6.197

| S.No.	Parameter	Calc. Value
16-Pb	Pb(1)-Pb(2)	3.983
	Pb(1)-H(5)	1.824
	Pb(1)-H(9)	2.002
	Pb(3)-Pb(1)-H(5)	82.55
	Pb(1)-Pb(2)-H(9)	5.73
	Pb(3)-Pb(1)-Pb(2)-H(9)	88.80
17-Pb	Pb(1)-Pb(2)	3.973
	Pb(1)-H(5)	1.830
	Pb(2)-H(6)	1.819
	Pb(1)-H(9)	1.994
	Pb(2)-H(9)	2.003
	θ_6	52.23
	θ_7	83.83
	Pb(1)-Pb(2)-H(9)	6.21
	Pb(4)-Pb(3)-Pb(2)-H(10)	89.99
	θ_5	120.70
18-Pb	Pb(1)-Pb(2)	3.589
	Pb(1)-H(5)	2.135
	Pb(3)-Pb(1)-Pb(2)-H(6)	31.58
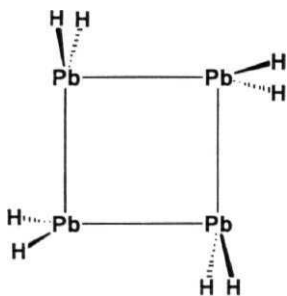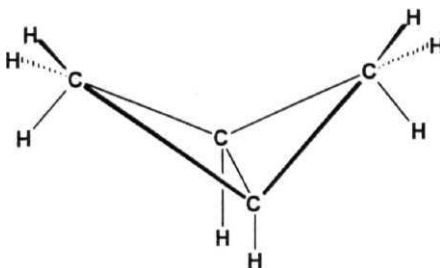
20   **21**

Structure 2 is calculated to be more stable than the bridged structure, 17 for C-Sn. However, the energy difference between 2 and 17 decreases from Si to Sn (Table 4). In the case of Pb, structure 17 is found to be lowest in energy compared to all the other structures. 20 is 28.8 kcal/mol higher in energy than the bridged structure, 17.

The non H-bridged structures 2, 15 and 20 have been well discussed in literature.[27-33] The bond lengths were compared with ethane like structures. The A-A distances in 2 (Table 5) are found to be slightly longer than those in A_2H_6 (C-C: 1.527, Si-Si: 2.353, Ge-Ge: 2.499 and Sn-Sn: 2.843 at HF level).[41] When compared with the 3-membered rings, the A-A bond distance in 2 is elongated (Table 2 and Table 5). The puckering in 2 (64, Scheme 2(a), Table 5) increases from C to Si and then decreases for Ge and Sn. That is to say that the nonplanarity of the structure 2 is more in Si and less in C, Ge and Sn. The bridged structure, 17, has considerably elongated A-A distances compared to the cis-bridged A_2H_4 (Si-Si: 2.603, Ge-Ge: 2.818, Sn-Sn: 3.114 and Pb-Pb: 3.278 at HF level), the cis analog of

$4.^7$ In the case of 16 also, the bridged A-A distances are longer than those in the cis analog of 4. The A-A distances in **17** are slightly shorter compared to those in 16 (Table 5), but longer than the corresponding distances in 3-membered rings (9). The puckering of A4 ring (θ_5, Scheme 2(b), Table 5) in 17 is the lowest for Si. The puckering is nearly constant for Ge, Sn and Pb ($\theta_5 \sim 120.0$). These results are in contrast to what is found in classical structure 2. That is the nonplanarity is more in **2-Si** compared to 2(Ge-Pb) and less in **17-Si** compared to 17(Ge-Pb).

Scheme 2

(a)   **(b)**
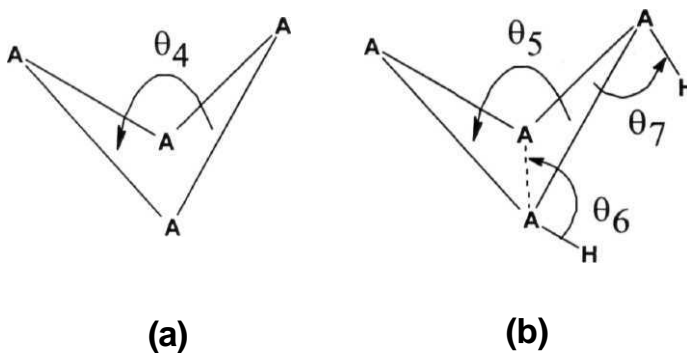
The A-Ht distances increase uniformly in going from 2 to **17** (Table 5). These findings are similar to 3-membered rings. The angle θ_6 (Scheme 2(b)) is found to be interesting in **17.** It is nearly 52° for Si to Pb (Table 5), with the two terminal hydrogens directed towards each other (Fig.3). The angle θ_7 (Scheme 2(b)) has also shown similar trend. It is found to be less than 90° (Table 5). Therefore, the projection of these terminal hydrogens

falls into the 4-membered ring. These findings are similar to that in triply hydrogen bridged A_3H_6 (9, section 2.1), and in 4. In fact, structure 16 is in close resemblance to the 3-membered ring structure, 9. The A-H_t bonds are directed towards a converging point (angle A(3)-A(l)-H(5), Table 5), exactly similar to what was found in 9 (section 2.1). The arrangement of bridging hydrogens in 16 is also interesting. These bridging hydrogens are nearly on the A—A axis with a slight displacement in the perpendicular direction of A4 plane (found by the angles A(3)-A(l)-A(2)-H(9) and A(l)-A(2)-H(9), Table 5).

Inspite of this geometrical arrangement of terminal hydrogens, the H_t---H_t distances (Si: 2.374, Ge: 2.627, Sn: 2.805 and Pb: 2.927A) are clearly not in the range of non-bonded repulsions in 17, except for Si. The H_b---H_b distance in 17-Si is 2.231 A which is within the non-bonded repulsive range,[42] compared to 17-Ge to Pb (Ge: 2.515, Sn: 2.717, Pb: 2.703Å).

The NBO analysis reveals the following bonding features. The bonding in 2 is classical. Whereas, in 17, the bonding can be described by four 3c-2e A-H-A bonds and four lone pairs. The p-orbitals contribute more to the 3c-2e bond, while the lone pairs have predominant s character. The percentage of p-character in 3c-2e bonding is calculated to be 91.9, 95.4, 95.6 and 96.9% in Si, Ge, Sn and Pb respectively. Similarly, the percentage of s-character in lone pairs is 72.5, 77.2, 79.2 and 84.9% in Si, Ge, Sn and Pb respectively. Therefore, the bonding of terminal hydrogens are best described by four 2c-2e bonds involving mainly p-orbitals of A4. The angle between A-Ht axis and the A4 core also supports this bonding description. The bonding in structure 16 is also found to be similar to that of 17, except

that the A4 ring is planar. Four 3c-2e bridged bonds, four 2c-2e $A\text{-}H_t$ bonds and four lone pairs one each on A, are traced by the NBO analysis.

$$A_4H_8 + 4A_2H_6 = 4A_3H_8 \qquad (2)$$
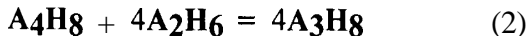
Though the present study is mainly aimed at finding the alternative bridged structures for 4-membered rings, we have estimated the strain in classical structure 2 as well (Eq.2, Table 6).   The strain energy was calculated at HF level due to the limitation on the available computer time. The strain energy of the 4-membered rings is found to decrease from C to Sn, unlike in 3-membered rings, in which the strain energy of heavier analogs of 1 is calculated to be more than that in **1-C**.

Thus the H-bridged structures 16, 17, 18, and 19 were studied as an alternatives for the homologues of cyclobutane, 2. Among these bridged structures only 17 is found to be minima for Si to Pb. In the case of Pb, 17 is lower in energy than the classical structure.

Table 6

Strain energies from equation 2 (kcal/mol) for 2. The energies are at HF/6-31G* for C and Si and at HF/LANL1DZ for Ge-Pb.

Molecule	Strain energy of 2
C	26.58
Si	17.01
Ge	16.73
Sn	13.59
Pb	10.77
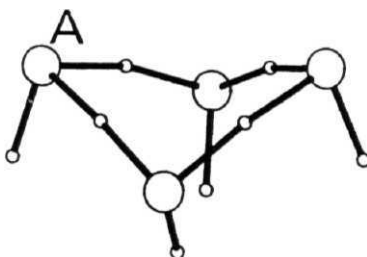
Fig. 3: Optimized geometry of 17 (A is Si-Pb).

References:

1. McQuillin, F.J.; Baird, M.S. *Alicyclic Chemistry* Cambridge University Press: New York, 1983.

2.(a) Dewar, M.J.S. *J. Am. Chem. Soc.* **1984,** *106,* 669.

  (b) Cremer, D.; Kraka, E. *Structure and Reactivity,* Liebman, J.F.; Greenberg, A., Eds.; VCH Publications: New York, 1988, Chapter 3, pp 65.

  (c) Ferguson, L.N. *Highlights of Alicyclic Chemistry,* Franklin: Palisades, NJ, 1973, Part 1, Chapter 3.

  (d) Greenberg, A.; Liebman, J. *Strained Organic Molecules,* Academic: New York, 1978 and references therein.

3.(a) Coffey, S. Ed., *Rodd's Chemistry of Carbon Compounds,* 1967, Vol. II, Part. A., Elsevier: New York.

  (b) Trost, B.M.; Wong, H.N.C.; Lau, K.-L.; Tarn, K.-F. *Topics in Current Chemistry,* 1986, Vo.133.

  (c) Salaün, J.R.Y.; Reipig, H.-U. *Topics in Current Chemistry,* 1988, Vol.144.

4.(a) Newton, M.D. *Applications of Electronic Structure Theory,* Ed. Schaefer III, H.F. Plenum: New York, 1977.

  (b) Wiberg, K.B. *Angew. Chem. Int. Ed. Engl.* **1986,** *25,* 312.

5.(a) Windus, T.L.; Gordon, M.S. *J. Am. Chem. Soc,* **1992,** *114,* 9559.

  (b) Curtiss, L.A.; Raghavachari, K.; Deutsch, P.W.; Pople, J.A. *J. chem. Phys.,* 1991, 95, 2433.

  (c) Karni, M.; Apeloig, Y. *J. Am. Chem. Soc,* **1990,** *112,* 8559.

  (d) Schelyer, P.v.R.; Kost, D. *J. Am. Chem. Soc,* **1988,** *110,* 2105.

  (e) Teramae, H. *J. Am. Chem. Soc,* **1987,** *109,* 4140.

  (f) Olbrich, G. *Chem. Phys. Lett., 1986, 130,* 115.

  (g) Krogh-Jespersen, K. *J. Am. Chem. Soc, 1985, 107,* 537.

  (h) Krogh-Jespersen, K. *J. Phys. Chem.,* **1982,** *86,* 1492.

6. Grev, R.S.; Schaefer III, H.F.; Baines, K.M. *J. Am. Chem. Soc,* **1990,** *112,* 9458.

7.(a) Trinquier, G. *J. Am. Chem. Soc,* **1990,** *112,* 2130.

  (b) Trinquier, G. *J. Am. Chem. Soc,* **1991,** *113,* 144.

  (c) Trinquier, G.; Malrieu, J.P. *J. Am. Chem. Soc,* **1991,** *113,* 8634.

8.(a) West, R. *Angew. chem. Int. Ed. Engl.* 1987, *26,* 1201.

  (b) Raabe, G.; Michl, J. *Chem. Rev.,* **1985,** *85, 419.*

9. Cowley, A.H. *Acc. Chem. Res.* **1984,** *17,* 386.

10.(a) Fink, M.J.; MichalCzyk, M.J.; Haller, K.J.; West, R.; Michl, J. *J. Chem. Soc, Chem. Commun.* 1983, 1010.

(b) Masamune, S.; Murakami, S.; Snow, J.T.; Tobita, H. *Organometallics* 1984, *3,* 333.

11. Hitchcock, P.B.; Lappert, M.F.; Miles, S.J.; Thorne, A.J. *J. Chem. Soc, Chem. Commun.* 1984, 480.

12.(a) Goldberg, D.E.; Harris, D.H.; Lappert, M.F.; Thomas, K.M. *J. Chem. Soc, Chem. Commun.* 1976, 261.

(b) Davidson, P.J.; Harris, D.H.; Lappert, M.F. *J. Chem. Soc, Dalton Trans.* 1976, 2268.

(c) Fjeldberg, T.; Haaland, A.; Lappert, M.F.; Schilling, B.E.R.; Seip, R.; Thorne, A.J. J. *Chem. Soc, Chem. Commun.* 1982, 1407.

13.(a) Grev, R.S.; Schaefer.III, H.F. *J. Chem. Phys.,* 1992, *97,* 7990 and references therein.

(b) Cordonnier, M.; Bogey, M.; Demuynck, C; Destombes, J.L. *J. Chem. Phys.,* 1992, *97,* 7984 and references therein.

(c) Brenda, T.C.; Schaefer.III, H.F. *J. Phys. Chem.,* 1990, *94,* 5593.

14.(a) Palagyi, Z.; Schaefer III, H.F. Kapuy, E. *J. Am. Chem. Soc.* 1993, 775,6901.

(b) Grev, R.S.; Deleeuw, B.J.; Schaefer III, H.F. *Chem. Phy. Lett.* 1990, 765, 257.

15.(a) Bogey, M.; Bolvin, H.; Cordonnier, M.; Demuynck, C; Destombes, J.L.; Csaszar, A.G. *J. Chem. Phys.* 1994, *100,* 8614.

(b) Bogey, M.; Bolvin, H.; Demuynck, C; Destombes, J.L. *Phys. Rev. Lett.* **1991,** *66,* 413.

16.(a) Radom, L.; Hariharan, P.C.; Pople, J. A.; Schleyer, P.v.R. *J. Am. Chem. Soc.* 1976,95, 10.

(b) Li, W.-K.; Riggs, N.V. *J. Mol. Struct.* (THEOCHEM) 1992, *257,* 189, and references therein.

(c) Wong, M.W.; Radom, L. *J. Am. Chem. Soc.* 1993 775, 1507.

(d) Lopez, R.; Sordo, J.A.; Sordo, T.L. *J. Chem. Soc, Chem. Commun.* 1993, 1751.

(e) Maluendes, S.A.; McLean, A.D.; Yamashita, K.; Herbst, E. *J. Chem. Phys.* 1993,99,2812.

17.(a) Korkin, A.A.; Glukhovstev, M.; Schleyer, P.v.R. *Int. J. Quantum. Chem.* 1993,46, 137.

(b) Glukhovtsev, M.N.; Kirienkova, T.V.; Simkin, B.Ya.; Minkin, V.I.; Yudilevich, I.A. *Zh. Org. Khim.* 1989, *25,* 196.

18. Jemmis, E.D.; Srinivas, G.N.; Leszczynski, J.; Kapp, J.; Korkin, A.A.; Schleyer, P.v.R. *J. Am. Chem. Soc.* **1995**, *117*, 11361.

19. Allen, F.H. *Acta. Crystallogr. Sect. B,* 1980, *B36,* 81; 1981, *B37,* 890.

20.(a) Belzner, J.; Detomi, N.; Ihmels, H.; Noltemeyer, M. *Angew. Chem. Int. Ed. Engl.* 1994, 53, 1854.

  (b) Masamune, S.; Hanzawa, Y.; Murakami, S.; Bally, T.; Blount, J.F. *J. Am. Chem. Soc.* 1982, *104,* 1150.

  (c) Dewan, J.C.; Murakami, S.; Snow, J.T.; Collins, S.; Masamune, S. *J. Chem. Soc. Chem. Commun.* **1985**, 892.

  (d) Watanabe, H.; Kato, M.; Okawa, T.; Nagai Y.; Goto, M. *J. Organomet. Chem.* 1984,277,225.

  (e) Schafer, A.; Weidenbruch, M.; Peters, K. Schnering, H.-G.v. *Angew. Chem. Int. Ed. Engl.* 1984, *23,* 302.

21.(a) Masamune, S.; Hanzawa, Y.; Williams, D.J. *J. Am. Chem. Soc.* 1982, 22,6137.

  (b) Weidenbruch, M.; Grimm, F.-T.; Herrndorf, M.; Schaefer, A.; Peters, K.; Schnering, H.-G.v. *J. Organomet. Chem.* 1988, *341,* 335.

22. Masamune, S.; Sita, L.R.; Williams, D.J. *J. Am. Chem. Soc.* 1983, *105,* 630.

23.(a) Alder, R.W.; Colclough, D.; Grams, F.; Orpen, A.G. *Tetrahedron* 1990, *46,* 7933.

  (b) Krujer, G.J.; Boeyens, J.C.A. *J. Phys. Chem.* 1968, *72,* 2120.

  (c) Bock, CM. *J. Am. Chem. Soc.* 1968, *90,* 2748.

  (d) Margulis, T.N. *Acta. Cryst.* **1965**, *19*, 8577.

  (e) Lemoire, H.P.; Livingston, R.L. *J. Am. Chem. Soc.*.1952, *74,* 5732.

  (0 Owen, T.B.; Hoard, J.L. *Acta. Cryst.* 1951, *4,* 172.

24.(a) Kawase, T.; Batcheller, S.A.; Masamune, S. *Chem. Lett.* 1987, 227.

  (b) Masamune, S. *Silicon Chemistry,* Corey, E.R.; Corey, J.Y.; Gasper, P.P., Ed., Chapter 25, 1988, p.257.

  (c) Kabe, Y.; Masamune, S. *Angew. Chem. Int. Ed. Engl.* 1988, *27,* 1725.

25.(a) Richter, M.; Neumann, W. P. *J. Organomet. Chem.* 1969, *20,* 81.

  (b) Lesbre, M.; Mazerolles, P.; Stage, J. *The Organic Compounds of Germanium.* Wiley: New York, 1971.

26.(a) Puff, H.; Bach, C; Schuh, W.; Zimmer, P. *J. Organomet. Chem.* 1986,372,313.

  (b) Belsky, U.K.; Zemlyansky, N.N.; Kolosova, N.D.; Borisova, I.U. *J. Organomet. Chem.* 1981,275,41.

27.(a) Inagaki, S.; Yoshikawa, K.; Hayano, Y. *J. Am. Chem. Soc.* **1993,** 7/5, 3706.

(b) Horner, D.A.; Grev, R.S.; Schaefer III, H.F. *J. Am. Chem. Soc.* **1992,** *114,* 2093.

(c) Nagase, S.; Kobayashi, K.; Nagashima, M. *J. Chem. Soc, Chem. Commun.* **1992,** 1302.

(d) Cremer, D.; Gauss, J.; Cremer, E. *THEOCHEM,* **1988,** *46,* 531.

(e) Cremer, D.; Karaka, E. *J. Am. Chem. Soc.* **1985,** 707, 3800.

(f) Cox, J.D.; Pilcher, G. *Thermochemistry of Organic and Organometallic compounds,* Academic: New York, 1970.

28.(a) Korkin, A.A.; Schleyer, P.v.R. *J. Am. Chem. Soc.* **1992,** *114,* 8720.

(b) Coolidge, M.B.; Hrovat, D.A.; Borden, W.T. *J. Am. Chem. Soc.* 1992, *114,* 2354.

(c) Liang, C; Allen, L.C. *J. Am. Chem. Soc.* **1991,** *113,* 1878.

(d) Sax, A.F.; Kalcher, J. *J. Phys. Chem.* **1991***, 95,* 1768.

(e) Kitchen, D.D.; Jackson, J.E.; Allen. L.C. *J. Am. Chem. Soc.* 1990, *112,* 3408.

(f) Boatz, J.A.; Gordon, M.S. *J. Phys. Chem.* **1989,** *93,* 3025.

(g) Nagase, S.; Nakano, M; Kudo, T. *J. Chem. Soc, Chem. Commun.* **1987,** 60.

(h) Grev, R.S.; Schaefer III, H.F. *J. Am. Chem. Soc.* **1987,** *109,* 6569.

29.(a) Matsunaga, N.; Cundari, T.R.; Schmidt, M.W.; Gordon, M.S. *Theor. Chim. Acta.* **1992,** *83,* 57.

(b) Nagase, S.; Nakano, M. *J. Chem. Soc, Chem. Commun.* **1988,** 1077.

30. Rubio J.; Illas, F. *THEOCHEM,* **1984,** *19*, **131.**

31. Nagase, S. *Polyhedron,* **1991,** *10,* 1299.

32.(a) Wiberg, K.B.; Shobe, D.; Nelson, G.L. *J. Am. Chem. Soc.* **1993,** *115*, 10645.

(b) Carmichael, I. *J. Phys. Chem.* **1993,** *97,* 1789.

(c) Esteban, A.L.; Galache, M.P.; Ruiz, E.; Diez, E.; Bermejo, F.J. *J. Mol. Struct.* **1991,** *245*, 315.

(d) Murray, J.S.; Seminario, J.M.; Politzer, P.; Sjoberg, P. *Int. J. Quant. Chem.* 1990, *S24,* 645.

(e) Cremer, D. *J. Phys. Chem.* **1990,** *94,* 5502.

(f) Boatz, J.A.; Gordon, M.S.; Hilderbrandt, R.L. *J. Am. Chem. Soc.* **1988,** *110*, 352.

(g) Cremer, D.; Gauss, J. *J. Am. Chem. Soc.* **1986,** *108,* 7467.

33.(a) Wu, C.J.; Carter, E.A. *Phys. Rev.* **B. 1992,** *46,* 4651.

(b)   Sax, A.F.; Kalcher, J. *J. Chem. Soc, Chem. Commun.* 1987, 809.

(c)   Grev, R.S.; Schaefer III, H.F. *J. Am. Chem. Soc.* 1987, *109,* 6577.

(d)   Schoeller, W.W.; Dabisch, T. *Inorg. Chem.* 1987, *26,* 1081.

(e)   Sax, A.F. *Chem. Phys. Lett.* 1986, *127,* 163.

34.   Hehre, W.J.; Radom, L.; Schleyer, P.v.R.; Pople, J.A. *Ab initio Molecular orbital Theory,* Wiley: New York, 1986.

35.   M0ller, C; Plesset, M.S. *Phys. Rev.* 1934, *46, 618.*

36.(a) Hariharan, P.C.; Pople, J.A. *Chem. Phys. Lett.* 1972, *66,* 217.

(b)   Francl, M.M.; Pietro, W.J.; Hehre, W.J.; Binkley, J.S.; Gordon, M.S.; DeFrees, D.J.; Pople, J.A. J. *Chem. Phys.* 1982, *77,* 3654.

37.   Hay, P.J.; Wadt, W.R. *J. Chem. Phys.* 1985, *82,* 270.

38.   Pople, J.A.; Raghavachari, K.; Schlegel, H.B.; Binkley, J.S. *Int. J. Quantum. Chem. Symp.* 1979, *13,* 255.

39.   Gaussian 92, Revision A, Frisch, M.J.; Trucks, G.W.; Head-Gordon, M.; Gill, P.M.W.; Wong, M.W.; Foresman, J. B.; Johnson, B. G.; Schlegel, H. B.; Robb, M. A.; Replogle, E.S.; Gomperts, R.; Andres, J.L.; Raghavacharei, K.; Binkley, J.S.; Gonzalez, G.; Martin, R.L.; Fox, D. J.; DeFrees, D.J.; Baker, J.; Stewart, J.J.P; Pople, J.A. Gaussian, Inc., Pittsburgh PA, 1992.

40.(a) Reed, A.E.; Curtiss, L.A.; Weinhold, F. *Chem. Rev.* 1988, *88,* 899.

(b)   Weinhold, F.; Carpenter, J.E. *The Structure of Small Molecules and Ions.* Ed. Naaman, R.; Vager, Z. Plenum: New York, 1988.

41.   Schleyer, P.v.R.; Kaupp, M.; Hampel, F.; Bremer M.; Mislow, K. *J. Am. Chem. Soc.* 1992, *114,* 6791.

42.   Tsuzuki, S.; Scaefer, L.; Goto, H.; Jemmis, E.D.; Hosoya, H.; Tanabe, K.; Osawa, E. *J. Am. Chem. Soc.* 1991, *113,* 4665.

43.(a)McKee, M.L. *J. Am. Chem. Soc.* 1990, *112,* 6753.

(b)   Jemmis, E.D.; Subramanian, G.; Naga Srinivas, G. *J. Am. Chem. Soc.* 1992, *114,* 7939.

(c)   Korkin, A.A.; Schleyer, P.v.R.; McKee, M.L. *Inorg. Chem.* 1995, *34,* 961.

44.(a) Jemmis, E.D.; Prasad, B.V.; Prasad, P.V.A.; Tsuzuki, S.; Tanabe, K. *Proc. Ind. Acad. Sci. (Chem. Sci.)* 1990, *102,* 107.

(b)   Jemmis, E.D.; Prasad, B.V.; Tsuzuke, S.; Tanabe, K. *J. Phys. Chem.* 1990, *94,* 5530.

45.   Hoffmann, R. *Angew. Chem. Int. Ed. Engl.* 1982, *21,* 711.

46.   Robben, M.P.; Geiger, W.E.; Rheingold, A.L. *Inorg. Chem.* 1994, *33,* 5615.

Three structures in case of A_3H_6 and four structures in case of A_4H_8 have been considered for the homologues of cyclopropane (1) and cyclobutane (2) respectively.

The following results have been observed for A_3H_6 system in the present study.

i)   Structure 9 is a minimum for Si to Pb.

ii)   9-Pb is the lowest energy minimum among the structures considered

iii)   In accordance with the calculated geometry of 9, NBO analysis reveals the bonding pattern as three 3c-2e bonds, three 2c-2e AH_t bonds and three lone pairs on the heavier atoms.

iv)   Structure 10 is higher order saddle point for C, Ge and Pb, whereas a minimum for Si and Sn.

v)   Structure **11** is not a minimum for C to Pb.

vi) Strain energy of **1-C** is lower than that of the heavier analogs.

The following results have been observed for A_4H_8 system.

i)   Structure 17 is a minimum for Si to Pb.

ii)   Only in case of Pb, 17 is lower in energy than the classical structure **15-Pb**.

iii)   The NBO analysis reveals the bonding pattern in 17 as four 3c-2e bonds, four 2c-2e AH_t bonds and four lone pairs on the heavier atoms.

iv)   Structure 16 is a transition state whereas 18 is a higher order saddle point for Si to Pb.

v)   Structure 19 collapses upon optimization for C, Si, Ge and Pb.

Chapter 3:   Studies on **Si₃H₃X** and A4H4 Molecules.

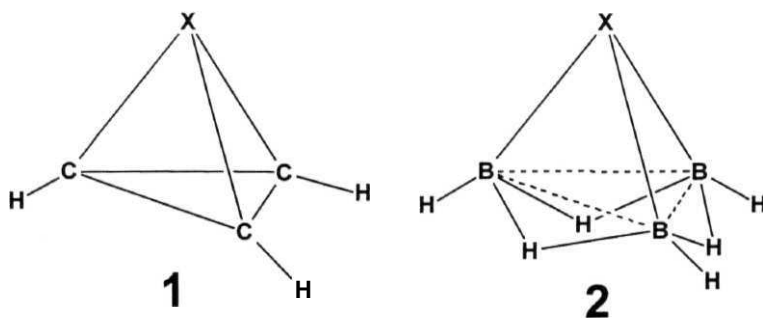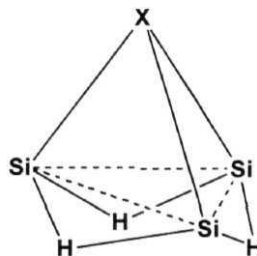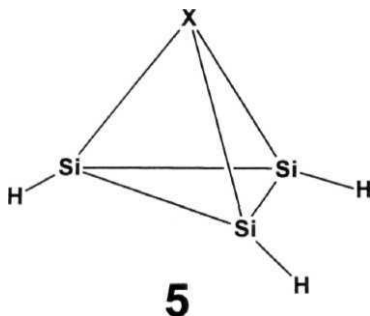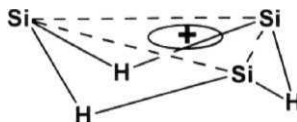# [3.0] *Abstract*

Trigonal pyramidal Si_3H_3X systems have been studied at HF/6-31G*, MP2/6-31G* and Becke3LYP/6-31G* levels. The classical trigonal pyramidal structure 5 is calculated to be a higher order saddle point for $X=BH^-$, CH, NO, SiH, P, PH^+ and PO, whereas it is minima for X=N and NH^+ at the MP2/6-31G* level. An alternative pyramidal structure (**6**, C_{3v}) with three SiHSi 3c-2e bonds is found to be minimum , lower in energy than 5 by 47.7 ($X=BH^-$), 39.1 (X=CH), 31.7 (X=N), 25.0 ($X=NH^+$), 20.6 (X=SiH), 20.7 (X=P), 16.1 ($X=PH^+$) and 18.2 ($X=PO$) kcal/mol. Isosynaptic analogy connects 6 with various triply hydrogen bridged pyramidal structures in organometallics.

The extension of isosynaptic analogy to metal tetrahedrane complexes of the type $H_4Ru_4L_{12}$ leads to various kinds of structures for the tetrahedranes in group 14 (A4H4, A=C, Si, Ge, Sn and Pb). These structures have been studied at HF, MP2 and Becke3LYP levels using 6-31G* basis set for C and Si and LANL1DZ basis set for Ge, Sn and Pb. Among the tetrahedrane structures, the triply hydrogen bridged structure 2 (C_{3v}) is found to be more stable for Si, Ge and Sn. For Pb 8 (C_s) is calculated to be more stable than the other structures considered here. However for C, the classical T_d structure 1 is more stable than all the other tetrahedrane alternatives.

There is a well-developed chemistry based on the smallest carbocyclic π-ligand η^3-$C_3H_3^+$.[1-3] Derivatives of 1 with main group and transition metal fragments (e.g. $C_4(t\text{-}Bu)_4$ (T_d) and $(C_3Ph_3)Co(CO)_3$) are available in the literature.[1,2] An all-boron analog of cyclopropenyl cation $B_3H_6^+$ is calculated to be a stable species.[4] Theoretical studies on pyramidal structures (**2**,C_{3v}) based on the $B_3H_6^+$ ligand have indicated them to be stable species on their potential energy surfaces.[5] There are no reports on trigonal-pyramidal structures based on $Si_3H_3^+$, the trisilacyclopropenyl cation, except for the studies on tetrasilatetrahedranes.[6] The cation $Si_3H_3^+$, found in the gas phase, is calculated to be more stable as trisilacyclopropenium ion (3, D_{3h}) with 2π electron delocalization (Chapter 1).[7,8]

H—Si———————Si—H
          ⊕
          Si—H

Si⇐ - - - - - - - ⊕ - - - - - Si
              H⁻ - - >Si
         H   H

X
Si———————Si—H
H   Si
        H

5

X
Si⇐ - - - - - - - - - - Si
         H - - >Si
    H   H

	a	b	c	d	e	f	g	h	i
X	BH⁻	CH	N	NH⁺	NO	SiH	P	PH⁺	PO
	BH⁻	CH	N	NH⁺	NO	SiH	P	PH⁺	PO

An alternative triply hydrogen bridged structure $(4, C_{3v})$ is also found to be a minimum for $Si_3H_3^+$, but it is 42.0 kcal/mol higher in energy than 3 at the MP2/6-31G level (Chapter 1). There are reasons to believe that the Si_3H_3 ligand should be a more appropriate π-ligand than C_3H_3 on the basis of ring size. C_5H_5 is an ideal η^5 ligand in chemistry because of the ideal claw size of the *n* framework of the C_5H_5 ring for a range of caps from main group and transition metal fragments.[9] The cyclopropenyl cation provides a much smaller span of orbitals. This is compensated to an extent by the large out-of-plane bending of the ring substituents away from the capping group observed in $C_3R_3^+$ π-complexes.[2] The longer SiSi bond length in $Si_3H_3^+$ should reduce this orbital mismatch considerably. The

bridged structure, 4, has an even longer SiSi distance. This brings in the interesting question of relative stabilities of the classical structure, 5, and the bridging structure, 6. Structure 5 can be considered as a homologue of 1, whereas structure 6 can be derived from 2 by replacing the BH group by Si using the isolobal analogy between BH and Si (Chapter 1).[10]

$$\text{Me}$$
$$\text{C}$$
$$(CO)_3 Fe \qquad Fe(CO)_3$$
$$H \qquad Fe \qquad H$$
$$H \qquad (CO)_3$$
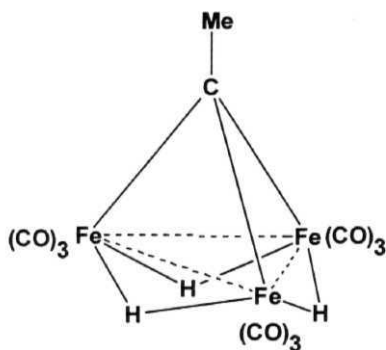
7

The triply hydrogen bridged trigonal-pyramidal structures with metallacycles are known in the literature. For example, 6b (C_{3v}) can be related to $(\mu\text{-H})_3Fe_3(CO)_9(\mu_3\text{-CMe})$ (7) through isolobal analogy.[11] We present here the results of a theoretical study on a series of pyramidal $Si_3H_3(X)$ compounds with BH^- (5a, 6a), CH (5b, 6b), N (5c, 6c), NH^+ (5d, 6d), NO (5e, 6e), SiH (5f, 6f), P (5g, 6g), PH^+ (5h, 6h) and PO (5i, 6i) as capping groups (X) which support our contention that there is more flexibility for 4 in ring-cap bonding. H-bridged structures, 6, are calculated to be more favourable than the classical, 5, in all cases.

Table 1

The total energies (au) and Zero point energies (ZPE, kcal/mol) of structures **5** and **6** for various caps at HF/6-31G*, MP2/6-31G* and at Becke3LYP/6-31G*.

| | HF/6-31G* | | | | MP2/6-31G* | | | | Becke3LYP/6-31G* | | | |
| | Structure 5 | | Structure 6 | | Structure 5 | | Structure 6 | | Structure 5 | | Structure 6 | |
Cap	Total Energy	ZPE	Total Energy	ZPE	Total Energy	ZPE	Total Energy	ZPE	Total Energy	ZPE	Total Energyy	ZPE
BH⁻	-893.58893	22.8	-893.65458	24.1	-893.93912	21.2	-894.01933	24.0	-895.62773	20.7	-895.70808	22.8
CH	-906.75329	26.3	-906.82467	27.4	-907.14051	24.3	-907.20677	26.9	-908.83666	23.3	-908.91038	25.8
N	-922.78286	19.9	-922.84882	19.2	-923.21175	18.1	-923.26361	19.0	-924.91116	17.5	-924.977621	18.0
NH⁺	-923.17848	28.0	-923.22223	28.6	-923.58258	25.7	-923.62580	27.9	-925.29129	25.1	-925.34796	26.9
NO	-997.51493	20.4	-997.58465	21.0	--	--	-998.17220	20.5	-1000.04626	19.1	-1000.07783	18.6
SiH	-1157.82123	23.0	-1157.84049	22.7	-1158.14842	20.5	-1158.18403	22.3	-1160.23571	20.3	-1160.28032	21.2
P	-1209.10052	18.8	-1209.12337	18.5	-1209.45535	16.8	-1209.49043	18.2	-1211.54589	16.5	-1211.59051	17.2
PH⁺	-1209.41746	23.5	-1209.43578	23.5	-1209.75711	21.5	-1209.78535	23.2	-1211.85828	20.8	-1211.90181	22.0
PO	-1283.89647	20.7	-1283.92219	20.4	-1284.43948	18.1	-1284.47116	19.9	-1286.71660	18.0	-1286.76027	18.9

103

Table 2

Relative Energiesa (kcal/mol) of Structure 5 **and** 6 at HF/6-31G*, MP2/6-31G* and at Becke3LYP/6-31G* (the values in the parenthesis are number of imaginary frequencies).

	HF/6-31G*			MP2/6-31G*			Becke3LYP/6-31G*	
Cap	Structure 5	Structure 6		Structure 5	Structure 6		Structure5	Structure 6
BH⁻	40.0(2)	0.0(0)		47.7(2)	0.0(0)		48.6(2)	0.0(0)
CH	43.8(0)	0.0(0)		39.1(2)	0.0(0)		44.0(2)	0.0(0)
N	42.0(0)	0.0(0)		31.7(0)	0.0(0)		41.3(0)	0.0(0)
NH⁺	26.9(0)	0.0(0)		25.0(0)	0.0(0)		34.0(0)	0.0(0)
NO	43.2(2)	0.0(0)		67.3(0)ᵇ	0.0(0)		20.3(2)	0.0(0)
SiH	12.4(0)	0.0(0)		20.6(2)	0.0(0)		27.2(0)	0.0(0)
P	14.6(0)	0.0(0)		20.7(2)	0.0(0)		27.4(0)	0.0(0)
PH⁺	11.5(0)	0.0(0)		16.1(2)	0.0(0)		26.3(2)	0.0(0)
PO	16.4(0)	0.0(0)		18.2(2)	0.0(0)		26.6(0)	0.0(0)

aThe relative energies are calculated after scaling the zero point energy by 0.89 for HF/6-31G* and Becke3LYP/6-31G* levels and by 0.95 for MP2/6-31G* level (ref.12).

bThe structure corresponds to 8 (ref.36).

Geometries of **5a-i** and **6a-i** were optimized under C_{3v} symmetry (except 5f, which has T_d symmetry) at the **HF/6-31G*** level.[12,13] The effect of electron correlation is obtained by further optimizing the structures at the MP2/6-31G* level.[14] The density functional calculations at the **Becke3LYP/6-31G* (B3LYP/6-31G*)** level were also done for comparison of relative energies.[15] The nature of the stationary points was determined by analytical evaluation of the harmonic force constants and vibrational frequencies.[16] All the calculations were carried out using the GAUSSIAN92 program package.[17] The total and relative energies obtained from these calculations are given in Tables 1 and 2. Important geometrical parameters are listed in Tables 3 and 4. The **MP2/6-31G*** results are used in the discussion unless otherwise specified. These are qualitatively similar to those obtained at other levels.

The H-bridged structure, 6, is calculated to be lower in energy than the classical structure 5 at all three levels for all ring-cap combinations (Table 1). The stability of 6 over 5 ranges from 47.7 **kcal/mol** for $X=BH^-$ to 16.1 kcal/mol for $X=PH^+$. Similar trends are seen at the HF and Becke3LYP levels (Table 2). Structure 6 is found to be a minimum with all the caps. However, this is not true for the classical structure, 5, which is a higher order saddle point for BH-, CH, SiH, P, PH^+ and PO caps. Structure 5 is calculated to be a minimum for NH^+ and N. The caps BH~, CH and PH^+ followed the same trend at the Becke3LYP level, whereas, structures with SiH, P and PO caps are shown to be minimum at this level. The classical structure with NO cap (5e) collapses to 8 (C_{3v}) on optimization at the MP2 level. On the other hand, the triply hydrogen bridged structure 6e is a minimum.

8   **9**
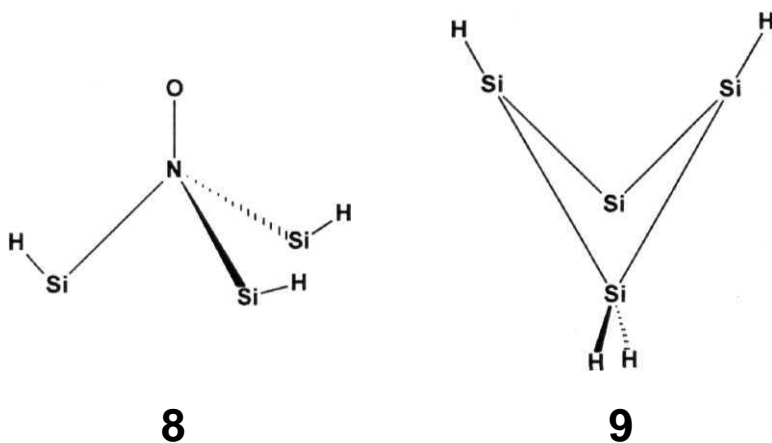
The classical structure, 5f, with SiH cap (one of the nine caps considered in the present study), is tetrasilatetrahedrane. Previous calculations on Si_4H_4 have shown that the tetrasilatetrahedrane is a local minimum at the HF/6-31G* level on the potential energy surface of Si_4H_4.[6] However, Nagase et al predicted that at higher levels two SiSi bonds in 5f can be broken without a barrier to form a four-membered ring isomer.[18] In the present study, the tetrasilatetrahedrane is found to be a second-order saddle point at the MP2 level. The two imaginary frequencies are found to follow the path suggested by Nagase et al to break the two SiSi bonds. However, 5f is calculated to be a minimum at the Becke3LYP level supporting the HF level of calculations. It was also indicated that silyl substitution can stabilize **5f**.[19] The tetrasilatetrahedrane (Si_4R_4) has been synthesized with a "super silyl" group (R = $t\text{-}Bu_3Si$).[20] The C_{3v} isomer of Si_4H_4, 6f, is calculated to be 20.6 kcal/mol (12.4 and 27.2 kcal/mol at the HF and Becke3LYP levels, respectively) more stable than the T_d arrangement, 5f. But, 6f is 28.7 kcal/mol higher in energy than the lowest

energy isomer (9, C_S), reported in the literature for Si_4H_4.[6e,21] The
tetrahedral structure observed for Si_4R_4 experimentally points to the effect
of substituents in controlling the structures; the propensity for bridging does
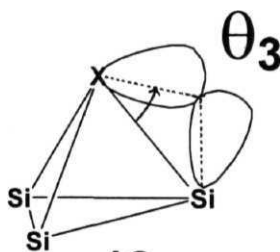not seem to go beyond hydrogens.

The SiSi distances (Table 3) in the classical structure 5 are in the
range of single bonds (2.332A° in trisilacyclopropane (10, D_{3h}) and 2.334A
° in disilane).[22-24] The bridged structure, 6, has considerably shortened
SiSi distances (Table 4) compared to the triply hydrogen bridged
trisilacyclopropane (11, C_{3v}), Si_3H_6 (3.080A^0).[23]

10
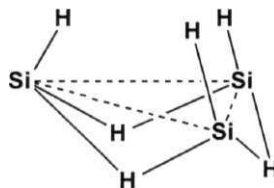
11

12

Table 3

Important geometrical parameters for Si_3H_3X, 5 at MP2/6-31G* level. All the distances are in angstroms and the angles are in degrees.

Cap	X-Si	Si-Si	Si-H	θ_1[a]
BH-	2.051	2.289	1.491	21.1
CH	1.904	2.337	1.489	-31.7
N	1.861	2.286	1.486	-29.5
NH$^+$	1.886	2.298	1.477	-23.7
NO	—	—	—	—
SiH	2.315	2.315	1.478	19.5
P	2.304	2.256	1.479	-2.6
PH$^+$	2.265	2.318	1.475	-2.3
PO	2.272	2.333	1.478	18.6

[a] θ_1 is the angle of deviation of terminal hydrogens from Si_3 plane, positive θ_1 indicates that the hydrogens are bent away from the cap (X)

Table 4

Important geometrical parameters for Si_3H_3X, 6 at MP2/6-31G* level. All the distances are in angstroms and the angles are in degrees.

Cap	X-Si	Si-Si	Si-H	θ_2[a]
BH$^-$	1.988	2.558	1.715	35.1
CH	1.884	2.595	1.698	33.3
N	1.829	2.534	1.706	34.7
NH$^+$	1.879	2.678	1.684	30.9
NO	1.838	2.626	1.706	32.4
SiH	2.283	2.715	1.695	30.0
P	2.257	2.619	1.686	32.1
PH$^+$	2.245	2.842	1.695	27.2
PO	2.230	2.721	1.692	29.5

[a] θ_2 represents the angle between the Si_3 plane and SiHSi plane.

Table 5
The bond bending angle (θ_3, the deviation of hybrid orbital from XSi axis)
in degrees at X at HF/6-31G*//MP2/6-31G* level, from NBO analysis.

Cap	$\theta_3(5)$	$\theta_3(6)$
BH-	29.7	22.8
CH	25.7	18.3
N	19.6	14.5
NH+	25.5	15.3
NO	—	14.5
SiH	32.6	25.4
P	25.1	18.8
PH+	32.6	23.0
PO	32.0	23.9

Table 6
Energy of the reaction ΔE_1 for equation 1 and ΔE_2 for equation 2
at MP2/6-31G* level.

Cap	ΔE_1(kcal/mol)	AE2(kcal/mol)
BH-	-89.7	-129.5
CH	-81.1	-120.9
N	-73.7	-113.5
NH+	-67.1	-106.8
SiH	-62.7	-102.5
P	-62.7	-102.5
PH+	-58.1	-97.9
PO	-60.2	-100.0

NBO analysis shows the bonding in 5 to be classical.[25] The triply hydrogen bridged structure 6 has three each of 2c-2e XSi bonds, SiHSi 3c-2e bond, and lone pairs on the silicon atom of the Si_3H_3 ring. The geometrical constraints in 5 force bent bonds between the cap (X) and Si_3H_3 ring (12). The deviation of the XSi bonds from the internuclear axis (θ_3) at X in 5 and 6 obtained from the NBO analysis is listed in Table 5. θ_3 is smaller in 6 compared to 5. That means the XSi bond becomes more directed in 6 leading to better bonding. The NBO analysis also reveals that the lone pair on divalent Si in 6 is predominantly of s character (~73%). This leaves maximum p-character for XS_1 bonds (~86%). Since the lone pair on Si has greater s character, it looses the directionality and is in the plane of the Si_3 ring rather than in the anticipated direction, away from the cap. Thus the coplanarity of lone pairs on the Si_3 ring pushes the p_π orbital toward X, resulting in better overlap between X and the Si_3H_3 ring.[26] This type of arrangement is absent in 5, leading to poor overlap between X and the Si_3H_3 ring. The Mulliken overlap population between X and Si increases in going from 5 to 6 for all X (0.210. 0.388 for BH-; 0.206, 0.309 for CH; 0.180, 0.253 for N; 0.053, 0.144 for NH^+; -0.001, 0.271 for SiH; 0.132, 0.248 for P; -0.019, 0.178 for PH^+; and 0.011, 0.240 for PO). These changes in overlap population also indicate the better bonding between X and Si_3H_3 ring in 6 compared to 5.

The bonding in 5 and 6 can also be explained by the six interstitial electron rule for three-dimensional delocalization in pyramidal systems.[3] According to this rule, the Si_3H_3 ring provides *3n* electrons and the cap, X, provides three electrons leading to a total of six electrons to fill the three

bonding combinations obtained from the ring and cap orbitals. All X groups considered here are selected on the basis of this interstitial electron rule. The caps BH~, CH, N, and NH$^+$ are selected from the previous theoretical calculations on carbocyclic pyramidal structures.[3] P, PH$^+$, and SiH are selected to see the effect of heavier analogs. The report on interaction between CO and cyclobutadiene[27] suggested the possibility of nitrosyl (NO) and phosphoryl (PO) groups as caps in the present study. The bonding with these caps (NO and PO) is due to the degenerate rc-orbitals of Si_3H_3 and the degenerate π^* orbitals of NO and PO. Therefore, The N-0 (6e: 1.396 A$°$) and P-O (5i: 1.512 A$°$, 6i: 1.517 A$°$) distances in 5 and 6 are close to their respective single bond distances.[28] The changes in B-H, C-H, N-H, Si-H (cap) and P-O bond lengths are found to be minimal between structures 5 and 6.[29] The negative θ_1 (bending of the terminal Si-H bonds toward the cap) in 5b, 5c, 5d, 5g and 5h (Table 3) can be explained by the concept of the compatibility of orbitals in overlap.[3] The relatively less diffuse p_π-orbital on the cap (X) pushes the H_t toward the cap for better interaction.

Structure 6 is related to the triply hydrogen bridged isomer of Si_3H_6 (11).[23] Bridged structure 11 is calculated to be 84.0 kcal/mol higher in energy than the classical structure, 10. Since the three terminal hydrogens are directed toward a converging point along SiH_t axes in 11, these hydrogens can be replaced by a 3-electron donor cap (X) (similar to the replacement of nonbonded hydrogen repulsions in [10]-annulene by a CH_2 bridge[30]) leading to structure 6. In contrast, the classical structure of Si_3H_6 (10) has divergent hydrogens. The advantage in the formation of the

pyramidal molecules with capping X provided by the SiH bond directions in **11** in comparison to those in 10 is reflected in the uniformly lower energy of 6.

Similarly, the "isosynaptic analogy" connects the structural patterns in silicon chemistry with **organometallic** chemistry.[31]   Thus using this analogy, we can relate $(\mu$-H$)_3$Fe$_3$(CO)$_9(\mu_3$-CMe),[11] $(\mu$-H$)_3$Os$_3$(CO)$_9(\mu_3$-CX)   (X=H,   C$_6$H$_5$,   Cl),[32] $(\mu$-H$)_3$Co$_3$Cp$^*(\mu_3$-CMe),[33]   and $(\mu$-H$)_3$Os$_3$(CO)$_9(\mu_3$-CBCl$_2$)[34] with 6b and $(\mu$-H$)_3$Os$_3$(CO)$_9(\mu_3$-BCO)[35] with 6a.
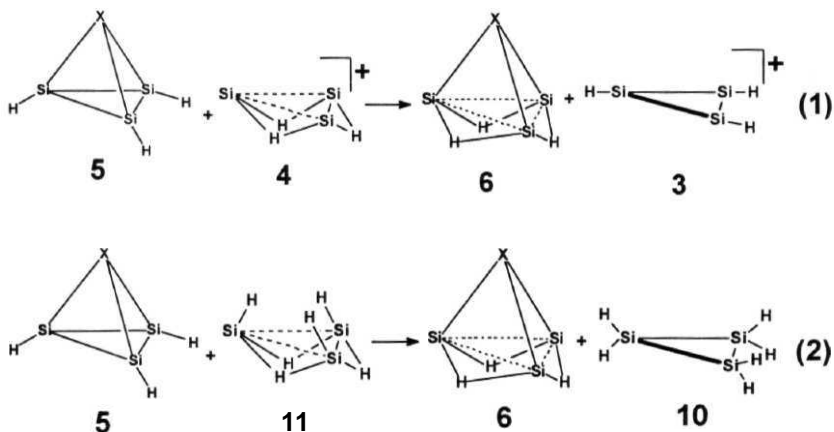
The low relative energies of 5 and 6 hide the enormous advantage of the triply bridging 4 in interacting with X^-. Even though 4 is less stable than 3, 6 obtained by complexing 4 and X^- is more favourable than 5 (Eq.l;Table 6). The strain energies involved in going from 11 to 6 and from

10 to 5 are not the same. An estimate of their difference is obtained from Eq 2. The high **exothermicity** of this equation is also a reflection of the increased strain in 5 in relation to 6. Thus the classical trigonal-pyramidal structure, 5, is found to be relatively more strained compared to the triply hydrogen bridged structure, 6. The **X-Si$_3$H$_3$** binding is more favourable in 6.

Calculations at the **HF/6-31G***, MP2/6-31G* and Becke3LYP/6-31G*** levels shown that the classical pyramidal structure is a second order stationary point for all 5 except for X = N and NH$^+$ at the MP2 level. The **C$_{3v}$** alternatives, 6, are minima and lower in energy than 5.

In the present study the triply hydrogen bridged structure 6f, derived from the organometallic complexes, is found to be more stable than the **T$_d$** structure 5f for **Si$_4$H$_4$**. There are many metal tetrahedrane structures with various topological arrangement of four hydrogens (e.g. H$_4$Ru$_4$(CO)$_{12}$).[37] Using the isosynaptic analogy[31] one can **derive** different variety of structures for group 14 tetrahedranes (A$_4$H$_4$) from these organometallic complexes, which is discussed in section 2 of this chapter.

References

1. (a) Maier, G.; Pfriem, S.; Schafer, U.; Matusch, R. *Angew. Chem. Int. Ed. Engl.* 1978, 77, 520.
   (b) Bally, T.; Masamune, S. *Tetrahedron* **1980,** *36,* 343.
   (c) Maier, G. *Angew. Chem. Int. Ed. Engl.* **1988,** *27,* 309.
2. Chiang, T.; Kerber, R.C.; Kimball, S.D.; Lauther, J.W. *Inorg. Chem.* **1979,** *18,* 1687 and references therein.
3. (a) Jemmis, E.D.; Schleyer, P.v.R. *J. Am. Chem. Soc* **1982,** *104,* 4781.
   (b) Jemmis, E.D. *J. Am. Chem. Soc.* **1982,** *104,* 7017.
4. (a) Jemmis, E.D.; Subramanian, G.; Srinivas, G.N. *J. Am. Chem. Soc.* **1992,** *114,* 7939.
   (b) Korkin, A.A.; Schleyer, P.v.R.; McKee, M.L. *lnorg. Chem.* **1995,** *34,* 961.
5. Jemmis, E.D.; Subramanian, G.; Siinivas, G.N. *Inorg. Chem.* **1994,** 33, 2317.
6. (a) Clabo, D.A.; Schaefer III, H.F. *J. Am. Chem. Soc.* **1986** *108,* 4344.
   (b) Sax, A.F.; Kalcher, J. *J. Chem. Soc, Chem. Commun.* **1987,** 809.
   (c) Nagase, S.; Nakano, M.; Kudo, T. *J. Chem. Soc, Chem. Commun.* **1987,** 60.
   (d) Yates, B.F.; Clabo, D.A.; Schaefer III, H.F. *Chem. Phys. Lett.* **1988,** *143*, 421.
   (e) Yates, B.F.; Schaefer III, H.F. *Chem. Phys. Lett.* **1989,** 755, 563.
7. (a) Stewart, G.W.; Henis, J.M.S.; Gaspar, P.P. *J. Chem. Phys.* **1973,** *58,* 890.
   (b) Korkin, A.A.; Glukhovtsev, M.; Schleyer, P.v.R. *Int. J. Quantum. Chem.* **1993,** *46,* 137.
8. Jemmis, E.D.; Srinivas, G.N.; Leszczynski, J.; Kapp, J.; Korkin, A.A.; Schleyer, P.v.R. *J. Am. Chem. Soc.* **1995,** *117,* 11361.
9. (a) Huheey, J.E.; Keiter, E.A.; Keiter, R.L. *Inorganic Chemistry* 4th ed.; Harper Collins College Publishers: New York 1993.
   (b) Haaland, A.; Martinsen, K.-G.; Schlykov, S.A.; Volden, H.V.; Dohmeier, C; Schnockel, H. *Organometallics* **1995,** *14,* 3116.
   (c) Loos, D.; Schnockel, H.; Gauss, J.; Schneider, V. *Angew. Chem. Int. Ed. Engl.* 1992, 37, 1362.
   (d) Berndt, A.F.; Marsh, R.E. *Acta. Crystallogr.* **1963,** *16*, 118.
10. (a) Jemmis, E.D.; Prasad, B.V.; Prasad, P.V.A.; Tsuzuki, S.; Tanabe, K. *Proc. Ind. Acad. Sci. (Chem. Sci.)* **1990,** 702, 107.

  (b) Jemmis, E.D.; Prasad, B.V.; Tsuzuki, S.; Tanabe, K. *J. Phys. Chem.* **1990,** *94,* 5530.

11.(a) Wong, K.S.; Haller, K.J.; Dutta, T.K.; Chipman, D.M.; Fehlner, T.P. *Inorg. Chem.* **1982,** *21,* 3197.

  (b) Hoffmann, R. *Angew. Chem. Int. Ed. Engl.* **1982,** 27, 711.

12.   Hehre, W.J.; Radom, L.; Schleyer, P.v.R.; Pople, J.A. *Ab initio Molecular Orbital Theory;* Wiley: New York, 1986.

13.(a) Hariharan, P.C.; Pople, J.A. *Chem. Phys. Lett.* **1972,** *66,* 217.

  (b) Francl, M.M.; Pietro, W.J.; Hehre, W.J.; Binkley, J.S.; Gordon, M.S.; DeFrees, D.J.; Pople, J.A. *J. Chem. Phys.* **1982,** *77,* 3654.

14.   M0ller, C; Plesset, M.S. *Phys. Rev.* **1934,** *46,* 618.

15.(a) Becke, A.D. *J. Chem. Phys.* **1993,** *98,* 5648.

  (b) Becke, A.D. *Phys. Rev.* A **1988,** *38,* 3098.

  (c) Lee, C; Yang, W.; Parr, R.G. *Phys. Rev.* B **1988,** *37,* 785.

  (d) Vosko, S.H.; Wilk, L.; Nusair, M. *Can. J. Phys.* **1980,** *58,* 1200.

16.   Pople, J.A.; Raghavachari, K.; Schlegel, H.B.; Binkley, J.S. *Int. J. Quantum Chem. Symp.* **1979,** *13,* 255.

17.   Gaussian 92, Revision A, Frisch, M.J.; Trucks, G.W.; Head-Gordon, M.; Gill, P.M.W.; Wong, M.W.; Foresman, J. B.; Johnson, B. G.; Schlegel, H. B.; Robb, M. A.; Replogle, E.S.; Gomperts, R.; Andres, J.L.; Raghavacharei, K.; Binkley, J.S.; Gonzalez, G.; Martin, R.L.; Fox, D. J.; DeFrees, D.J.; Baker, J.; Stewart, J.J.P; Pople, J.A. Gaussian, Inc., Pittsburgh PA, 1992.

18.   Nagase, S.; Nakano, M. *Angew. Chem. Int. Ed. Engl.* **1988,** *27,* 1081.

19.   Nagase, S.; Kobayashi, K.; Nagast ima, M. *J. Chem. Soc, Chem. Commun.* **1992,** 1302.

20.   Wiberg, N.; Finger, C.M.M.; Polborn, K. *Angew. Chem. Int. Ed. Engl.* **1993,** *32,* 1054.

21.   The MP2/6-31G* energy for structure 9 is -1158.23125 au and the zero-point energy is 23.3 kcal/mol.

22.   Nagase, S.; Kobayashi, K.; Nagashima, M. *J. Chem. Soc, Chem. Commun.* **1992,** 1302.

23.   Srinivas, G.N.; Kiran, B.; Jemmis, E.D. *J. Mol. Str. (THEOCHEM)* **1996,** *361,* 205.

24.   Schleyer, P.v.R.; Kaupp, M.; Hampel, F.; Bremer, M.; Mislow, K. *J. Am. Chem. Soc.* **1992,** *114,* 6791.

25.(a) Read, A.E.; Curtiss, L.A.; Weinhold, F. *Chem. Rev.* **1988,** *88,* 899.

(b) Weinhold, F.; Carpenter, J.E. *The Structure of Small Molecules and Ions;* Naaman, R., Vager, Z., Eds.; Plenum: New York, 1988; p 277.

26. Jemmis, E.D.; Subramanian, G.; Prasad, B.V.; Tsuzuki, S.; Tanabe, K. *Angew. Chem. Int. Ed. Engl.* **1993,** *32,* 865.

27.(a) Maier, G.; Schafer, U.; Sauer, W.; Hartan, H.; Matusch, R.; Oth, J.F.M. *Tetrahedron Lett.* **1978,** 1837.

(b) Glukhovtsev, M.; Schleyer, P.v.R.; Hommes, N.J.R.V.E.; Minkin, V. *Chem. Phys. Lett.* **1993,** *205,* 529.

28. The experimental N-0 and P-0 distances in various compounds are listed in: Allen, F.H.; Kennard, O.; Watson, D.G.; Bramma, L.; Orpen, A.G.; Taylor, R. *J. Chem. Soc, Perkin. Trans.* 2 **1987,** S1-S19.

29. The bond lenths (A) calculated at the MP2/6-31G* level. 5: B-H = 1.194, C-H=1.084, N-H=1.021, P-H=1.402, P-O=1.512. **6:** B-H = 1.189, C-H=1.081, N-H=1.021, Si-H=1.469, P-H=1.394, P-O=1.517.

30. March, J. *Advanced Organic Chemistry,* 4th ed.; Wiely-Interscience: New York, 1992.

31. Epiotis, N.D. *Top. Curr. Chem.* **1989,** *150,* 47.

32.(a) Orpen, A.G.; Koetzle, T.F. *Acta Crystallogr. B (Sir. Sci.)* **1984,** *40,* 606.

(b) Jan, D.Y.; Workman, D.P.; Hsu, L.Y.; Krause, J.A.; Shore, S.G. *Inor. Chem.* 1992,37,5123.

33. Casey, C.P.; Widenhoefer, R.A.; Hallenbeck, S.L.; Hayashi, R.K.; Powell, D.R.; Smith, G.W. *Organometallics* **1994,** *13,* 1521.

34. Jan, D.Y.; Hsu, L.Y.; Workman, D.P.; Shore, S.G. *Organometallics* **1987,** *6,* 1984.

35. Shore, S.G.; Jan, D.Y.; Hsu, L.Y.; Hsu, W.L. *J. Am. Chem. Soc.* **1983,** *105,* 5923.

36. The MP2/6-31G* energy for structure 8 is -998.16338 au and the zero-point energy is 85.5 kcal/mol.

37. Osella, D.; Nervi, C; Ravera, M.; Fiedler, J.; Strelets, V.V. *Organometallics* **1995,** *14,* 2501.

Despite the high strain the structure of **tetrahedrane (1-C)** can be explained by the tetravalent **carbon.** [1] The derivatives of tetrahedrane were prepared experimentally and their structures were solved by X-ray diffraction methods.[2,3] How do the heavier analogs of tetrahedrane in **group-14** behave? The structural differences between ethylene and acetylene with their heavier analogs have been discussed well in literature.[4,5] The H-bridged alternative structures are found to be competitive in stability with classical structures for cyclopropane and cyclobutane (Chapter 2). Hence we reasoned that the H-bridged alternatives may be realistic for the heavier group 14 tetrahedranes. In fact, the triply H-bridged tetrahedrane for Silicon (2-Si) is 20.6 **kcal/mol** more stable than the classical structure at **MP2/6-31G*** level (Section 3.1).
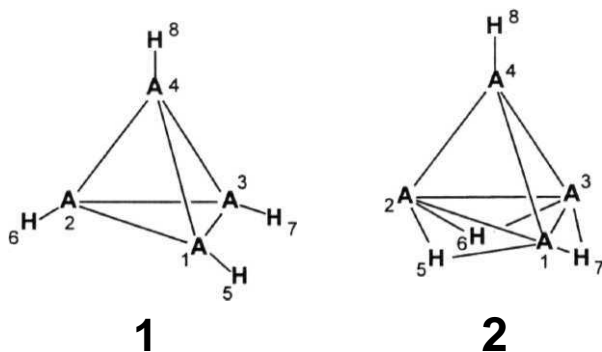
Structure 2 has been derived from **organometallic** complexes using the isolobal analogy.[6"8] There are many metal tetrahedrane structures with

various topological arrangements of four hydrogens. Wilson et **al** reported that the structure of $H_4Ru_4(CO)_{12}$ contains face bridging hydrogens, 3.[9] A D_{2d} structure, 4, where the four hydrogens are bridging the four edges of the tetrahedrane was also found for $H_4Ru_4(CO)_{12}$.[10] In this D_{2d} structure, the two unbridged Ru-Ru bonds are opposite to one another. The compounds $H_4Os_4(CO)_{11}(CNMe)$, $H_4Ru_4(CO)_{10}(PPh_3)_2$, $H_4Ru_4(CO)_{11}[P(OMe)_3]$ and $H_4Ru_4(CO)_8[P(OMe_3)]_4$ exhibit the pseudo D_{2d} symmetry.[10-13] Other than these structures, a C_s structure 5, where the two unbridged Ru-Ru bonds are adjacent to each other is also reported for $H_4Ru_4(CO)_{10}[\mu-\{Ph_2P(CH_2)_nPPh_2\}]$ (n = 1-4), $H_4Ru_4(CO)_{10}[\mu-\{Ph_2PCH_2CH(CH_3)PPh_2\}]$, $H_4Ru_4(CO)_{10}[Ph_2PCH_2CH(CH_3)PPh_2]$ and $H_4Ru_4(CO)_{11}(\eta^1-C=N(CH_3)CH_2CH_2CH_2)$.[14,15] The "Isosynaptic" analogy connects the structural patterns of organometallic compounds with main group compounds.[16] According to this analogy, $Fe(CO)_3$ is very much like Si or Ge with a stereochemically inactive `ns-electron pair'. Therefore, the isosynaptic analogy is represented as shown below.
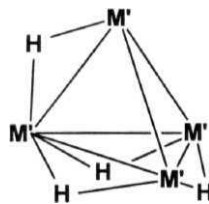
$$Fe(CO)_3 \quad \bigcirc \!\!\!\longrightarrow \quad Si, Ge$$

Further, it has been extended to Ru and Os complexes and shown that $Ru(CO)_3$ and $Os(CO)_3$ are also isosynaptic to Si and Ge.
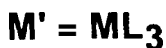
3   4   5

$$M' = ML_3$$
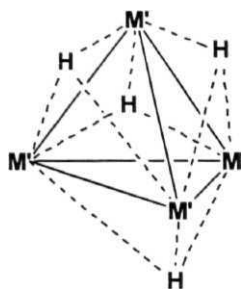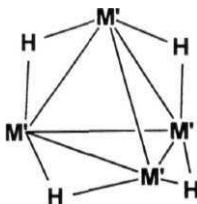
The H-bridged tetrahedranes are derived from **organometallics** in the present study using this isosynaptic analogy. Experimentally, so far only the derivatives **1-C** and **1-Si** are known.[3,17] In both these cases, sterically very bulky substituents have been used. In C4R4, the substituent R is t-Bu group and in Si_4R_4 the substituent R is "super **silyl**" group (Si(t-Bu)3). By keeping these factors in view this chapter deals with the classical as well as H-bridged tetrahedranes of **group-14** analogs.

The geometries of all the structures considered here are optimized at HF level under the symmetry conditions.[18] The electron correlation effects are determined at MP2 level.[19] The density functional calculations at the Becke3LYP (B3LYP) level were also done for comparison of relative energies.[20] For C and Si, **Pople's 6-31G*** basis set was **used.**[21] Molecules involving Ge, Sn and Pb were optimized using the **LANL1DZ** basis set.[22] This basis set uses the valence **double-zeta** (DZ) basis on H and effective core potentials plus DZ on Ge, Sn and Pb. The nature of the stationary

points was determined by harmonic force constants and vibrational frequencies.[23]   All the calculations were carried out using the GAUSSIAN92 program package.[24]   The energy comparisons are at the MP2/6-31G*//MP2/6-31G*+ZPE level for C and Si and at the MP2/LANL1DZ//MP2/LANL1DZ +ZPE level for Ge, Sn and Pb.   Zero point energies were scaled by 0.95.[18]   The natural bond orbital (NBO) analysis at HF level and the geometries at the MP2 level are used in the discussion.[25]
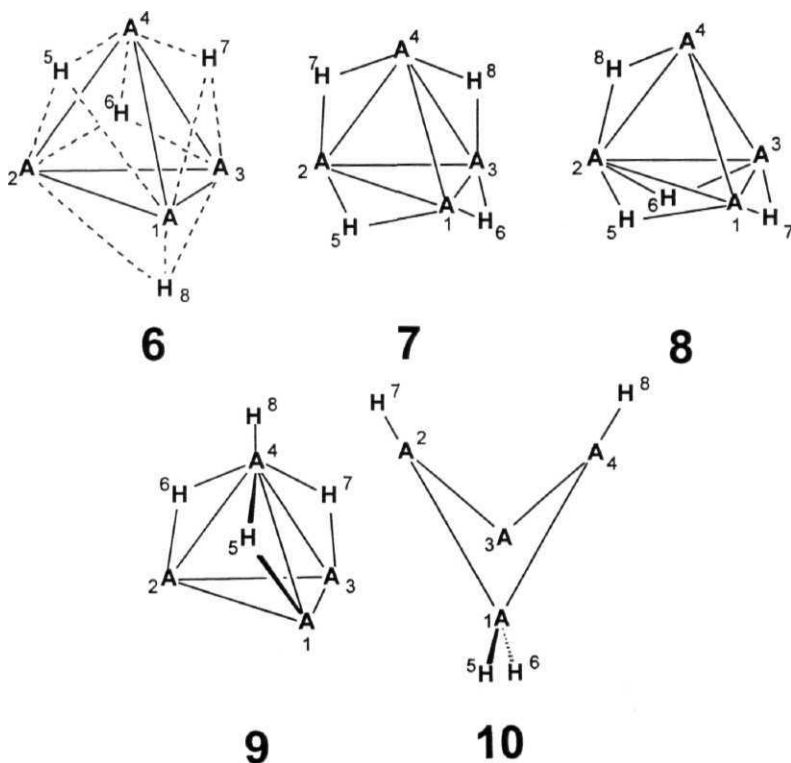

6   **7**   **8**

9   **10**

120

Table 1

Total energies (in au), zero point energies (ZPE in kcal/mol) and relative energies (RE in kcal/mol at MP2 level) of A4H4 system. The values in parantheses are the number of imaginary frequencies.

Molecule	Total energy (HF)	Total energy (B3LYP)	Total energy (MP2)	ZPE	RE
1-C	-153.59789(0)	-154.63669(0)	**-154.10772(0)**	37.87	0.0
2-C	-153.41875(2)	-154.48687(2)	-153.96487(2)	31.89	84.0
6-C	-152.99161(8)	-154.13540(8)	-153.63950(8)	16.97	273.9
7-C	-153.33422(4)	-154.41918(4)	-153.89976(4)	28.24	121.3
8-C	collapsed	-	-	-	-
9-C	collapsed to 1	—	-	--	-
10-C	-153.63033(0)	-154.65329(0)	-154.12560(0)	39.83	-9.5
1-Si	-1157.82123(0)	-1160.23571(0)	-1158.14842(2)	20.50	0.0
2-Si	-1157.84049(0)	-1160.28032(0)	-1158.18403(0)	22.30	-20.6
6-Si	-1157.64615(3)	-1160.14880(2)	-1158.06710(2)	18.95	49.5
7-Si	-1157.80603(0)	-1160.25685(0)	-1158.15218(0)	19.90	-3.0
8-Si	collapsed to 2	-	-	-	-
9-Si	-1157.80173(0)	-1160.23672(2)	-1158.15214(0)	20.63	-2.3
10-Si	-1157.90076(0)	-1160.31371(0)	-1158.23125(0)	23.32	-49.4
1-Ge	-16.68773(3)	-17.33236(3)	-16.88137(0)	17.82	0.0
2-Ge	-16.77372(0)	-17.42525(0)	-16.97021(0)	17.94	-55.6
6-Ge	-16.61891(3)	-17.32140(0)	-16.87285(0)	13.39	1.1
7-Ge	-16.75860(0)	-17.41609(0)	-16.95441(0)	16.74	-46.9
8-Ge	-16.75302(0)	-17.41062(0)	collapsed to 2	..	-
9-Ge	collapsed to **11**	-	-	-	-
10-Ge	-16.80023(0)	-17.43813(0)	-16.99276(0)	19.59	-68.3
11-Ge	-16.75004(0)	-17.37017(0)	-16.91037(0)	17.10	-18.9
1-Sn	-15.16110(3)	-15.78597(3)	**-15.33771(0)**	15.03	0.0
2-Sn	-15.28209(0)	-15.90091(0)	-15.44978(0)	16.22	-69.2
6-Sn	-15.16799(3)	-15.83189(0)	-15.38768(0)	14.02	-32.3
7-Sn	-15.28273(0)	-15.90087(0)	-15.44371(0)	15.63	-66.0
8-Sn	-15.27954(0)	-15.89953(0)	-15.44463(0)	16.18	-66.0
9-Sn	collapsed to 11	-	-	—	-
10-Sn	-15.27378(0)	-15.88918(0)	**-15.44514(0)**	16.61	-66.0
11-Sn	-15.24374(0)	-15.84267(0)	**-15.38714(0)**	14.73	**-31.3**
1-Pb	-15.46302(3)	-16.12865(3)	-15.65437(0)	19.97	0.0
2-Pb	-15.65821(0)	-16.29554(0)	-15.82491(0)	15.08	-111.7
6-Pb	-15.58510(3)	-16.25803(0)	-15.79360(0)	13.84	-93.2
7-Pb	-15.68044(0)	-16.31414(0)	-15.83775(0)	14.74	-120.1
8-Pb	-15.67943(0)	-16.31534(0)	-15.84140(0)	15.20	-121.9
9-Pb	collapsed to **11**	-	-	-	-
10-Pb	-15.63167(0)	-16.26698(0)	-15.79605(0)	14.94	-93.7
11-Pb	-15.61386(0)	-16.23869(0)	**-15.76024(0)**	13.74	-72.4

Table 2:

Important geometrical parameters of the optimized structures at MP2 level (distances in A and angles in degrees).

S.No.	Parameter	Calc. Value
1-C	C-C	1.477
	C-H	1.073
2-C	C(l)-C(2)	1.732
	C(l)-C(4)	1.465
	C(l)-H(5)	1.288
	C(4)-H(8)	1.078
		29.23
6-C	C(l)-C(2)	1.736
	C(l)-H(5)	1.406
7-C	C(l)-C(2)	1.773
	C(l)-C(4)	1.448
	C(l)-H(5)	1.289
10-C	C(l)-C(2)	1.498
	C(2)-C(3)	1.432
	C(l)-H(5)	1.085
	C(2)-H(7)	1.089
	C(2)-C(3)-C(l)-C(4)	143.66
	H(5)-C(l)-H(6)	113.84
1-Si	Si-Si	2.315
	Si-H	1.478
2-Si	**Si(l)-Si(2)**	2.715
	Si(l)-Si(4)	2.283
	Si(l)-H(5)	1.695
	Si(4)-H(8)	1.469
		30.0
6-Si	Si(l)-Si(2)	2.658
	Si(1)-H(5)	1.764
7-Si	Si(l)-Si(2)	2.764
	Si(l)-Si(4)	2.257
	Si(l)-H(5)	1.711
9-Si	Si(l)-Si(2)	2.507
	Si(l)-Si(4)	2.324
	Si(l)-H(5)	1.604
	Si(4)-H(8)	1.473
10-Si	Si(l)-Si(2)	2.314
	Si(2)-Si(3)	2.283
	Si(l)-H(5)	1.483
	Si(2)-H(7)	1.494
	Si(2)-Si(3)-Si(l)-Si(4)	154.72
	H(5)-Si(l)-H(6)	110.90

S.No.	Parameter	Calc. Value
1-Ge	Ge-Ge	2.546
	Ge-H	1.542
2-Ge	Ge(l)-Ge(2)	3.162
	Ge(l)-Ge(4)	2.544
	Ge(l)-H(5)	1.848
	Ge(4)-H(8)	1.529
	θ_1	28.79
6-Ge	Ge(l)-Ge(2)	3.080
	Ge(l)-H(5)	1.964
7-Ge	Ge(l)-Ge(2)	3.152
	Ge(l)-Ge(4)	2.574
	Ge(l)-H(5)	1.839
10-Ge	Ge(l)-Ge(2)	2.505
	Ge(2)-Ge(3)	2.527
	Ge(l)-H(5)	1.548
	Ge(2)-H(7)	1.565
	Ge(2)-Ge(3)-Ge(1)-Ge(4)	159.53
	H(5)-Ge(l)-h(6)	109.92
11-Ge	Ge(l)-Ge(4)	2.572
	Ge(l)-Ge(2)	3.981
	Ge(l)-H(5)	1.615
	Ge(4)-H(8)	1.557
	Ge(4)-H(5)	3.053
1-Sn	Sn-Sn	2.927
	Sn-H	1.719
2-Sn	Sn(l)-Sn(2)	3.555
	Sn(l)-Sn(4)	2.908
	Sn(l)-H(5)	2.010
	Sn(4)-H(8)	1.703
		27.20
6-Sn	Sn(l)-Sn(2)	3.398
	Sn(l)-H(5)	2.126
7-Sn	Sn(l)-Sn(2)	3.605
	Sn(l)-Sn(4)	2.943
	Sn(l)-H(5)	2.010

Continued...

Table 2: (Continued)

S.No.	Parameter	Calc. Value
8-Sn	Sn(1)-Sn(2)	3.573
	Sn(1)-Sn(3)	3.396
	Sn(1)-Sn(4)	3.091
	Sn(2)-Sn(4)	3.580
	Sn(1)-H(5)	2.002
	Sn(1)-H(7)	2.015
	Sn(2)-H(8)	1.900
	Sn(4)-H(8)	2.041
10-Sn	Sn(1)-Sn(2)	2.870
	Sn(2)-Sn(3)	2.889
	Sn(1)-H(5)	1.722
	Sn(1)-H(6)	1.727
	Sn(2)-H(7)	1.742
	H(5)-Sn(1)-H(6)	107.74
	Sn(2)-Sn(3)-Sn(1)-Sn(4)	163.04
11 -Sn	Sn(1)-Sn(4)	2.927
	Sn(1)-Sn(2)	4.601
	Sn(1)-H(5)	1.785
	Sn(4)-H(8)	1.733
	Sn(4)-H(5)	3.436
1-Pb	Pb-Pb	3.111
	Pb-H	1.782
2-Pb	Pb(1)-Pb(2)	3.645
	Pb(1)-Pb(4)	2.978
	Pb(1)-H(5)	2.067
	Pb(4)-H(8)	1.739
		27.64
6-Pb	Pb(1)-Pb(2)	3.460
	Pb(1)-H(5)	2.175
7-Pb	Pb(1)-Pb(2)	3.691
	Pb(1)-Pb(4)	3.013
	Pb(1)-H(5)	2.066
8-Pb	Pb(1)-Pb(2)	3.632
	Pb(1)-Pb(3)	3.456
	Pb(1)-Pb(4)	3.166
	Pb(2)-Pb(4)	3.630
	Pb(1)-H(5)	2.046
	Pb(1)-H(7)	2.070
	Pb(2)-H(8)	1.962
	Pb(4)-H(8)	2.072

S.No.	Parameter	Calc. Value
10-Pb	Pb(1)-Pb(2)	2.985
	Pb(2)-Pb(3)	3.035
	Pb(1)-H(5)	1.768
	Pb(1)-H(6)	1.769
	Pb(2)-H(7)	1.822
	H(5)-Pb(1)-H(6)	103.79
	Pb(2)-Pb(3)-Pb(1)-Pb(4)	170.97
11 -Pb	Pb(1)-Pb(4)	2.985
	Pb(1)-Pb(2)	4.658
	Pb(1)-H(5)	1.834
	Pb(4)-H(8)	1.772
	Pb(4)-H(5)	3.500
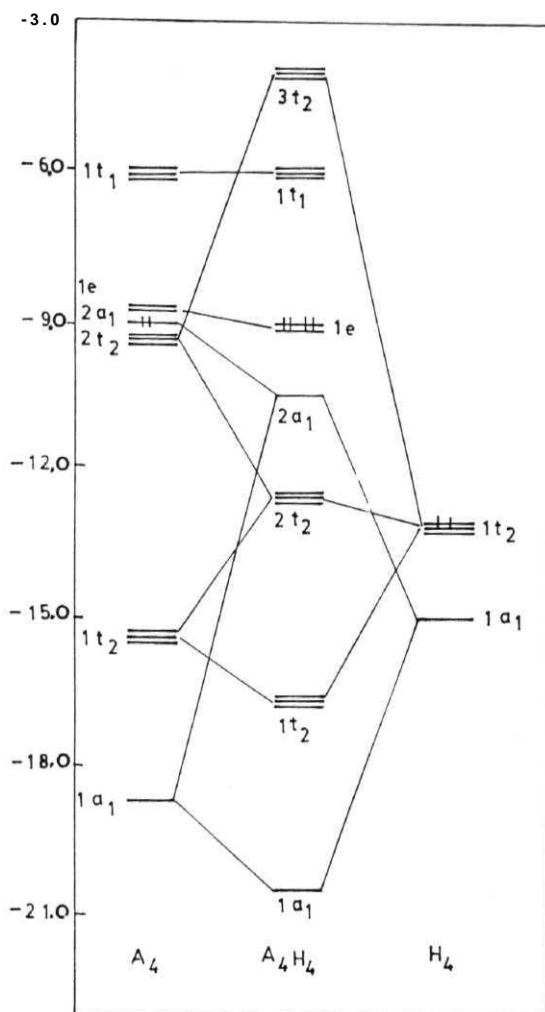
Fig. 1: Interaction diagram between A4 (Td) and H4 (Td) leading to A4H4 (T$_d$).

Structure 2 (C_{3v}) is derived from previous section (3.1). The transition metal structure with face-bridging-hydrogens, 3, suggests isomer 6 (T_d). Similarly, the structures having the edge-bridging-hydrogens, 4 and 5, leads to 7 (D_{2d}) and 8 (C_s) respectively. The triply hydrogen bridged structure, 9 (C_{3v}), is another candidate considered in the present study. The lowest energy structure suggested for Si_4H_4, 10 (C_s), is also included for comparison.[26]

There are many theoretical calculations available in literature on 1-C and 1-Si.[1,26] Structure 1 is a minimum for C-Pb, except for Si, in which it is a second order saddle point. However, the results at HF and B3LYP level are different. Structure 1 is a minimum for C and Si and a third order saddle point for Ge to Pb at these levels. The A-A bond lengths are compared with the ethane like structures (A_2H_6)[27] and 3-membered ring structures.[28] The A-A distances in 1-C and **1-Si** are found to be slightly shorter than those in A_2H_6 and cyclic-A_3H_6 (Chapter 2). But for **1-Ge** to **1-Pb**, the A-A bond distances are elongated compared to A_2H_6 and cyclic-A_3H_6. The bonding in 1 is found to be classical.

The triply H-bridged structure, 2, is more stable than the classical structure 1 by 20.6, 55.6, 69.2, 111.7 kcal/mol for Si-Pb respectively (Table 2). In all of these structure 2 is a minimum. 2-C is a second order saddle point and higher in energy than 1-C. The A-A bridged bonds in **2-Si** to 2-**Pb** are shortened to a large extent (Table 2) compared to the A-A bridged bonds in triply H-bridged cyclopropane analogs (Si: 3.080, Ge: 3.417, Sn: 3.783, Pb: 3.889A, Chapter 2).[28] However, the A-H_b distance in 2 is slightly longer than the corresponding distance in triply H-bridged

cyclopropane. The unbridged A-A distance is slightly shorter than the corresponding distance in the classical structure 1. The **non-planarity** of bridging hydrogens (that is the angle between A3 plane and AHA plane, θ_1) is nearly constant (~28.4°) for **2-Si** to **2-Pb.** The NBO analysis has shown the following bonding in 2: Three 2c-2e classical A-A bonds, three 3c-2e H-bridged A-A bonds and a lone pair on each divalent A.

The T_d structure, 6, where all the four hydrogens bridge the four faces of A4, is a minimum for Ge, Sn and Pb at MP2 and B3LYP level. For C and Si, 6 is a higher order saddle point. **6-Sn** and **6-Pb** are 32.3 and 93.2 **kcal/mol** more stable than **1-Sn** and **1-Pb**. But **6-Ge** is 1.1 **kcal/mol** less stable than **1-Ge**. The A-A distance in 6 is calculated to be shorter than the H-bridged A-A distance in isomer 2 and triply H-bridged A_3H_6 (Table 2). However, the A-H distance is elongated in 6 compared to 2 and A_3H_6 (Table 2). The electronic structure analysis of 6 is done using the fragment molecular orbital method.[29] The molecule is divided into A4 (T_d) and H4 (T_d) fragments. The interaction diagram between A4 and H4 leading to A4H4 (6) is shown in Fig.1. The \a\ orbital of A4 is all-symmetric combination of s-orbitals and the $2a_1$ is a sp-hybridized orbital on heavy atoms pointing towards the centroid of the tetrahedrane. Hence, these two MO's lead to an electron density at the centroid of the A4 tetrahedrane.[30] The $1t_2$ and $2t_2$ MO's of A4 mainly contributes to the formation of the A-A bonds in A4 and by tetrahedral symmetry these lead to significant electron density at the centroid of the tetrahedral faces.[30] Therefore, the \a\ and $1t_2$ orbitals of H4 interacts with the $1a_1, 2a_1, 1t_2$ and $2t_2$ orbitals of A4 leading to $1a_1$, $2a_1$, $1t_2$ and $2t_2$ in A4H4 respectively. Hence these orbitals contribute to the surface bonding of H4 on the A4 tetrahedrane. The $1e$ set

of orbitals of A4 lead to A-A bonds and by symmetry it has null density at the centre of the tetrahedrane face; hence, no interaction with the H4 fragment.

In Structures 7 and 8, the four hydrogens are bridging the edges of A4 cage. The main difference between 7 and 8 is that the **unbridged** A-A bonds in 7 are opposite to one another whereas, in 8, they are adjacent to each other. 7 is a minimum for Si-Pb and is calculated to be more stable than the classical structure, 1, by 3.0, 46.9, 66.0 and 120.1 **kcal/mol** for Si, Ge, Sn and Pb respectively. Structure 8 is minimum for Sn and Pb and collapses to 2 on optimization for Si and Ge. However, 8 exists for Ge-Pb at both HF and B3LYP levels and it is a minimum. On optimization of 8-C, the structure gets dismantled by breaking the H-bridged C-C bonds. **8-Sn** and **7-Sn** are energetically degenerate, whereas, **8-Pb** is 1.8 kcal/mol more stable than **7-Pb.** The H-bridged A-A bond distances for **7-Si** to **7-Pb** are very close to the corresponding distances in 2 (Table 2) and shorter compared to triply H-bridged A_3H_6 structure.[28] However, these distances in **8-Sn** and **8-Pb** are slightly shorter compared to **7-Sn** and **7-Pb** respectively (Table 2). The NBO analysis shows the following bonding in 7: Four **3c-2e** H-bridged A-A bonds, two 2c-2e A-A bonds and a lone pair on each A. Similar type of bonding was observed in **8-Sn** and **8-Pb** also.
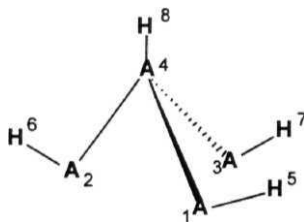
11

The second triply H-bridged structure, 9, is minimum only for Si. For Ge-Pb, 9 collapses to **11** (C_{3v}) on optimization and for C it collapses to 1. **9-Si** is 2.3 kcal/mol more stable than the classical structure 1. The H-bridged Si-Si bonds (2.314Å) are much shorter than what is found in **2-Si** and 7-Si. The unbridged Si-Si bonds (2.507A) are much longer than the unbridged Si-Si bonds in **2-Si** and **7-Si.** The NBO analysis has shown an interesting bonding feature for this isomer. There are three lone pairs one each on Si(l), Si(2) and Si(3). The bonding between Si(4)-H(8) is a classical 2c-2e bond. Other than these, the remaining bonds, Si(l)-H(5)-Si(4), Si(3)-H(7)-Si(4), Si(2)-H(6)-Si(4), Si(4)-Si(l)-Si(2), Si(4)-Si(l)-Si(3) and Si(4)-Si(2)-Si(3) are found to be 3c-2e bonds. This type of bonding picture will lead to longer Si(l)-Si(2), Si(l)-Si(3) and Si(2)-Si(3) bond distances and shorter Si(4)-Si(l), Si(4)-Si(2) and Si(4)-Si(3) bond distances which support the calculated values. Isomer **11** is minimum for Ge, Sn and Pb. It is less stable than 7 and more stable than classical T_d structure 1 (Table 1). The A-A bond in **11-Ge** is slightly longer than that in 1, where as in **11-Sn**, it is equivalent to that in **1** and in **11-Pb** it is less than that in 1 (Table 2). The bonding in **11** is traced to a classical 2c-2e bond between A-A. There are three lone pairs one each on the divalent atom A.

Isomer **10,** which is the lowest energy structure for Si_4H_4, so far, is also computed in the present study.[26] It is a minimum for C, Ge, Sn and Pb as well. **10** is 9.5, 49.4, 68.3, 66.0 and 93.7 **kcal/mol** more stable than 1 for C, Si, Ge, Sn and Pb respectively. Compared to cyclic A_4H_8 (Chapter 2), the A(1)-A(2) bond distance is slightly shorter and the A(2)-A(3) bond distance is slightly longer. The NBO analysis has shown the following bonding features. The four heavy atoms in structure **10** are found to be nearly planar. There are classical 2c-2e bonds between A(1)-A(2), A(2)-A(3), A(3)-A(4) and A(1)-A(4) respectively forming a four membered ring. The bonding of hydrogens with the heavy atoms is also found to be classical 2c-2e type. A(3) is a divalent atom with a lone pair (Fig. 2). The extra two electrons, one each from A(2) and A(4), make use of empty **p-orbital** on A(3), forming a 3c-2e delocalized **π-bond** (Fig. 2).

To conclude, among the tetrahedrane structures considered here, only C has shown the classical T_d structure to be more favourable. In the case of Si and Ge, the triply H-bridged structure, 2, is more favourable among the other bridged structures. But the isomer **10** is 28.8 and 12.7 kcal/mol more stable than 2 for Si and Ge respectively. However, for Sn, 2 is the lowest energy isomer and even lower than **10** by 3.2 kcal/mol. Interestingly **7-Sn, 8-Sn** and **10-Sn** are very close in energy. The situation in Pb is entirely different. The most stable isomer for Pb obtained in the present study is the four H-bridged C_s structure, 8. The D_{2d} structure, 7, and the C_{3v} structure, 2, are 1.8 and 10.2 kcal/mol higher in energy than 8. Compared to **10-Pb**, **8-Pb** is more stable by 28.2 kcal/mol.
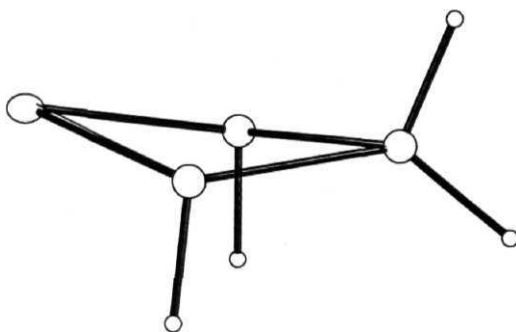
(a)
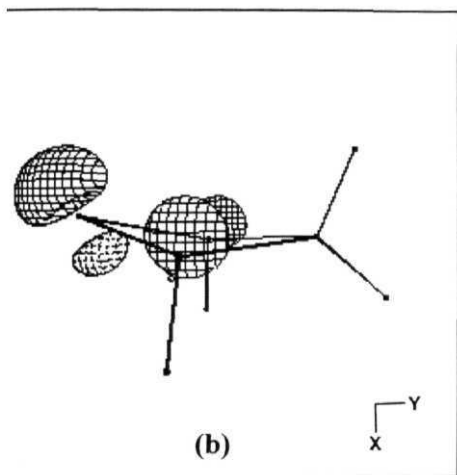
(b)
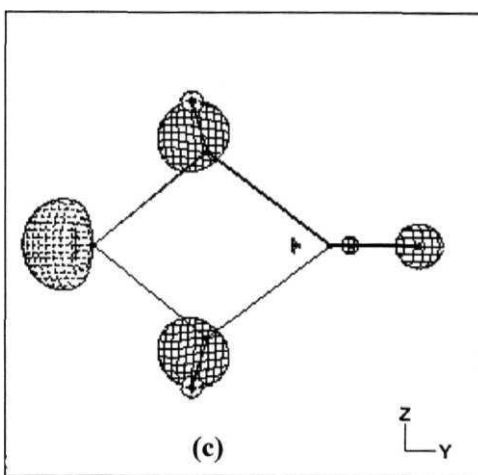
(c)

Fig. 2:   (a) Optimized geometry of A4H4 (10)
    (b) The HOMO, depicting the 3c-2e bond between
       A(2)-A(3)-A(4)
    (c) The HOMO-1 showing the lone pair on A(3).

Thus, the calculations at HF, MP2 and **Becke3LYP** levels have shown that the triply H-bridged tetrahedranes are more stable for Si, Ge and Sn and the four H-bridged tetrahedrane is more stable for Pb, when one considers the H-bridged alternatives for tetrahedranes in group 14. However, for C, the classical T_d structure is more stable.

References

1. (a) Minkin, V.I.; Minyaev, R.M.; Zholanov, Yu.A. "Nonclassical Structures of Organic Compounds" Mir Publishers: Moscow, 1987.

   (b) Hehre, W.J.; Pople, J.A. *J. Am. Chem. Soc.* **1975,** *97,* 6941.

   (c) Kollmar, H.; Carrian, F.; Dewar, M.J.S.; Bingham, R. *J. Am. Chem. Soc.* **1981,** *103,* 5292.

   (d) Grimme, S. *J. Am. Chem. Soc.* **1996,** *118,* 1529.

2. Maier, G.; Pfriem, S.; Schäfer, U.; Matush, R. *Angew. Chem. Int. Ed. Engl.* **1978,** *17,* 520.

3. (a) Maier, G.; Pfriem, S.; Schäfer, U.; Malsch, K.; Matusch, R. *Chem. Ber.* **1981,** *114,* 3965.

   (b) Maier, G.; Wolf, R.; Kalinowski, H.-O.; Boese, R. *Chem. Ber.* **1994,** *127,* 191.

4. (a) Windus, T.L.; Gordon, M.S. *J. Am. Chem. Soc.,* **1992,** *114,* 9559.

   (b) Curtiss, L.A.; Raghavachari, K.; Deutsch, P.W.; Pople, J.A. *J. Chem. Phys.,* **1991,** *95,* 2433.

   (c) Karni, M.; Apeloig, Y. *J. Am. Chem. Soc,* **1990,** 772, 8559.

   (d) Schelyer, P.v.R.; Kost, D. *J. Am. Chem. Soc,* **1988,** 770, 2105.

   (e) Teramae, H. *J. Am. Chem. Soc,* **1987,** *109,* 4140.

   (f) Olbrich, G. *Chem. Phys. Lett.,* **1986,** *130,* 115.

   (g) Krogh-Jespersen, K. *J. Am. Chem. Soc,* **1985,** *107,* 537.

   (h) Krogh-Jespersen, K. *J. Phys. Chem.,* **1982,** *86,* 1492.

   (i) Grev, R.S.; Schaefer III, H.F.; Baines, K.M. *J. Am. Chem. Soc,* **1990,** 772, 9458.

   (j) Trinquier, G. *J. Am. Chem. Soc,* **1990,** 772, 2130.

   (k) Trinquier, G. *J. Am. Chem. Soc,* **1991,** *113,* 144.

   (l) Trinquier, G; Malrieu, J.P. *J. Am. Chem. Soc,* **1991,** 775, 8634.

5. (a) Grev, R.S.; Schaefer.III, H.F. *J. Chem. Phys.,* **1992,** *97,* 7990 and reference therein.

   (b) Cordonnier, M.; Bogey, M.; Demuynck, C; Destombes, J.L. *J. Chem. Phys.,* **1992,** *97,* 7984 and reference therein.

   (c) Brenda, T.C.; Schaefer.III, H.F. *J. Phys. Chem.,* **1990,** *94,* 5593.

   (d) Palagyi, Z.; Schaefer III, H.F. Kapuy, E. *J. Am. Chem. Soc.* **1993,** 775,6901.

   (e) Grev, R.S.; Deleeuw, B.J.; Schaefer III, H.F. *Chem. Phy. Lett.* 1990,765, 257.

6. Jemmis, E.D.; Srinivas, G.N. *J. Am. Chem. Soc* **1996,** *118,* 3738.

7. Wong, K.S.; Haller, K.J.; Dutta, T.K.; Chipman, D.M.; Fehlner, T.P. *Inorg. Chem.* **1982,** 27, 3197.

8. Hoffmann, R. *Angew. Chem. Int. Ed. Engl.* **1982,** *21, 711.*

9. Wilson, R.D.; Bau, R. *J. Am. Chem. Soc.* **1976,** *98,* 4687.

10.(a) Wilson, R.D.; Wu, S.M.; Love, R.A.; Bau, R. *Inorg. Chem.* **1978,** *17,* 1271.

   (b) Osella, D.; Nervi, C; Ravera, M.; Fiedler, J.; Strelets, V.V. *Organometallics* **1995,** *14,* 2501.

11. Churchill, M.R.; Hollander, F.J. *Inorg. Chem.* **1980,** *19,* 306.

12. Wilson, R.D.; Bau, R. *J. Am. Chem. Soc.* **1976,** *98,* 4687.

13. Orpen, A.G.; McMullan, R.K. *J. Chem. Soc, Dalton Trans.* **1983,** 463.

14. Puga, J.; Arce, A.; Braga, D.; Centritto, N.; Grepioni, F.; Castillo, R.; Ascanio, J. *Inorg. Chem.* **1987,** *26,* 867.

15. Day, M.W.; Hajela, S.; Kabir, S.E.; Irving, M.; Mcphillips, T.; Wolf, E.; Hardcastle, K.I.; Rosenbe, R.G.; Milone, L.; Gobetto, R.; Osello, D. *Organometallics* **1991,** *10,* 2743.

16. Epiotis, N.D. *Top. Curr. Chem.* **1989,** *150,* 47.

17. Wiberg, N.; Finger, C.M.M.; Polborn, K. *Angew. Chem. Int. Ed. Engl.* **1993,32,** 1054.

18. Hehre, W.J.; Radom, L.; Schleyer, P.v.R.; Pople, J.A. *Ab initio Molecular Orbital Theory.* Wiley: New York, 1986.

19. Møller, C; Plesset, M.S. *Phys. Rev.* **1934,** *46,* 618.

20.(a) Becke, A.D. *J. Chem. Phys.* **1993,** *98,* 5648.

   (b) Becke, A.D. *Phys. Rev. A* **1988,** *38,* 3098.

   (c) Lee, C; Yang, W.; Parr, R.G. *Phys. Rev.* B **1988,** *37,* 785.

   (d) Vosko, S.H.; Wilk, L.; Nusair, M. *Can. J. Phys.* **1980,** *58,* 1200.

21.(a) Hariharan, P.C.; Pople, J.A. *Chem. Phys. Lett.* **1972,** *66,* 217.

   (b) Francl, M.M.; Pietro, W.J.; Hehre, W.J.; Binkley, J.S.; Gordon, M.S.; DeFrees, D.J.; Pople, J.A. *J. Chem. Phys.* **1982,** *77,* 3654.

22. Hay, P.J.; Wadt, W.R. *J. Chem. Phys.* **1985,** *82,* 270.

23. Pople, J.A.; Raghavachari, K.; Schlegel, H.B.; Binkley, J.S. *Int. J. Quantum Chem. Symp.* **1979,** *13,* 255.

24. Gaussian 92, Revision A, Frisch, M.J.; Trucks, G.W.; Head-Gordon, M.; Gill, P.M.W.; Wong, M.W.; Foresman, J. B.; Johnson, B. G.; Schlegel, H. B.; Robb, M. A.; Replogle, E.S.; Gomperts, R.; Andres, J.L.; Raghavacharei, K.; Binkley, J.S.; Gonzalez, G.; Martin, R.L.;

Fox, D. J.; DeFrees, D.J.; Baker, J.; Stewart, J.J.P; Pople, J.A. Gaussian, Inc., Pittsburgh PA, 1992.

25.(a) Read, A.E.; Curtiss, L.A.; Weinhold, F. *Chem. Rev.* **1988,** *88,* 899.

(b) Weinhold, F.; Carpenter, J.E. *The Structure of Small Molecules and Ions*; Naaman, R., Vager, Z., Eds.; Plenum: New York, 1988; p 277.

26.(a) Clabo, D.A.; Schaefer III, H.F., *J. Am. Chem. Soc.* **1986** *108,* 4344.

(b) Sax, A.F.; Kalcher, J. *J. Chem. Soc, Chem. Commun.* **1987,** 809.

(c) Nagase, S.; Nakano, M.; Kudo, T. *J. Chem. Soc, Chem. Commun.* **1987,** 60.

(d) Yates, B.F.; Clabo, D.A.; Schaefer III, H.F., *Chem. Phys. Lett.* **1988,** 743,421.

(e) Yates, B.F.; Schaefer III, H.F., *Chem. Phys. Lett.* **1989,** *155,* 563.

27. Schleyer, P.v.R.; Kaupp, M.; Hampel, F.; Bremer, M; Mislow, K. *J. Am. Chem. Soc.* **1992,** *114*, 6791.

28.(a) Srinivas, G.N.; Kiran, B.; Jemmis, E.D. *J. Mol. Str.* (THEOCHEM) **1996,** *361,* 205.

(b) Nagase, S.; Kobayashi, K.; Nagashima, M. *J. Chem. Soc, Chem. Commun.* **1992,** 1302.

29.(a) Fujimoto, H.; Hoffmann, R. *J. Phys. Chem.* **1974,** *78,* 1167.

(b) The interaction diagram in Fig.1 is drawn for **6-Sn.** The extended Huckel parameters for Sn: 5s (-16.16, 2.32), 5p (-8.32, 1.94); H: 1s (-13.6, 1.3), Tremel, W.; Hoffmann, R. *Inorg. Chem.* **1987,** *26,* 118.; Jørgensen, K.A.; Wheeler, R.A.; Hoffmann, R. *J. Am. Chem. Soc.* **1987,** *109,* 3240.

30. Hoffmann, R.; Schilling, B.E.R.; Bau, R.; Kaesz, H.D.; Mingos, D.M.P. *J. Am. Chem. Soc.* **1978**, *100*, 6088.

Calculations at HF, MP2 and Becke3LYP levels on Si_3H_3X and A4H4 systems have shown the following results.

Si_3H_3X:

i)   The classical pyramidal structure is a second order saddle point for all 5, except for X=N and NH^+ at the MP2 level.

ii)   The C_{3v} alternatives, 6, are minima and lower in energy than 5.

iii)   Structure 6 is related to B_3H_6X through isolobal analogy.

iv)   The isosynaptic analogy connects 6 with triply H-bridged pyramidal structures in **organometallics**.

v)   The ring-cap interaction, as determined by the isodesmic equation between X^- and $Si_3H_3^+$, in 6 is better than in 5.

vi)   Equation 2 shows that 6 is relatively less strained than 5.

A4H4:

i)   The classical structure 1 is a minimum for C, Ge, Sn and Pb, whereas for Si it is a second order saddle point at MP2 level.

ii)   The triply hydrogen bridged structure 2, is a minimum for Si to Pb and is a more stable structure among the tetrahedranes considered for Si , Ge and Sn.

iii)   The face bridged **isomer** 6 is a minimum for Ge, Sn and Pb.

iv)   Among structures 7 and 8, 7 is a minimum for Si to Pb, whereas 8 is a minimum for Sn and Pb.

v)   In case of Si and Ge, structure 8 collapses to 2 upon optimization.

vi)   Among the structures considered for Pb_4H_4, 8 is the lowest energy minimum.

vii)   Isomer 10 is a minimum for C to Pb.

Chapter 4:   Studies on Ti_8C_{12} Cluster and Transition
          Metal-Containing **Poly-ynes.**

The reactivity centres of Ti_8C_{12} (for the three structures suggested in conformity with experimental observations) have been studied by extended Huckel theory. The C_2 unit can complex with transition metal fragments such as $Pt(PH_3)_2$ with the unusual net result of transferring two electrons to Ti_8C_{12}. The metal centre, Ti can accommodate extra two-electron donors like CO. Model systems are used to explain the carbon and metal environment in Ti_8C_{12}.

Transition metal-containing **poly-ynes** are studied using the tight-binding extended Huckel method. The band gap between valence and conduction bands is found to be dependent both on metal and on the bridging ligand between the two metals. Not only the substitution on phenyl ring but its topology also affects the band gap of the polymer. The cyano substitution on phenyl ring is found to be more effective in reducing the band gaps of these polymers

[4.1] *Electronic Structure study of the reactivity centres in Ti_8C_{12} clusters*

The discovery of fullerenes has given a strong boost to cluster chemistry.[1] Another exciting development in cluster chemistry is the observation of metallocarbohedrenes.[2] During reactions of Ti atoms and hydrocarbons such as CH4, C_2H_2, C_3H_6, C_2H_4 and C_6H_6 in a time of flight mass spectrometer coupled with a laser vaporisation source, a dominant peak at 528 atomic mass units was observed.[2] In order to characterise this "super magic" peak (so called because of its high intensity), a series of studies with varying isotopic labelling was undertaken by Castleman et al.[2] The results showed that the cluster contains 12 carbon atoms but no hydrogens. The remaining mass has been accounted as Ti8 and thus the super magic peak represents $Ti_8C_{12}^+$.[2-4] This was further supported by high resolution distribution pattern analysis. The high intensity of the peak suggested that the neutral Ti_8C_{12} might be equally stable. The intense activity in icosahedral clusters of various kinds led to the first suggestion of a structure based on icosahedron 1 with T_h symmetry (Fig.1) for Ti_8C_{12}.[2,5] The gas phase "titrations" of mass selected Ti_8C_{12} cluster with ND3 in thermal reaction cell revealed that eight equally coordinated Ti sites are present in the cluster. This finding supported the structure 1 with all Ti metals exposed at the cluster surface. This is related to the familiar organic dodecahedrane $C_{20}H_{20}$ provided the twenty hydrogen atoms are removed.[6] The C_{20}, dodecahedrene, is expected to be highly strained species.[7] The pyramidality required at each carbon is considerably larger than that for C_{60}.[8] Replacement of eight carbon atoms of C_{20} by Ti gives Ti_8C_{12}. As a result, the symmetry reduces to T_h. These
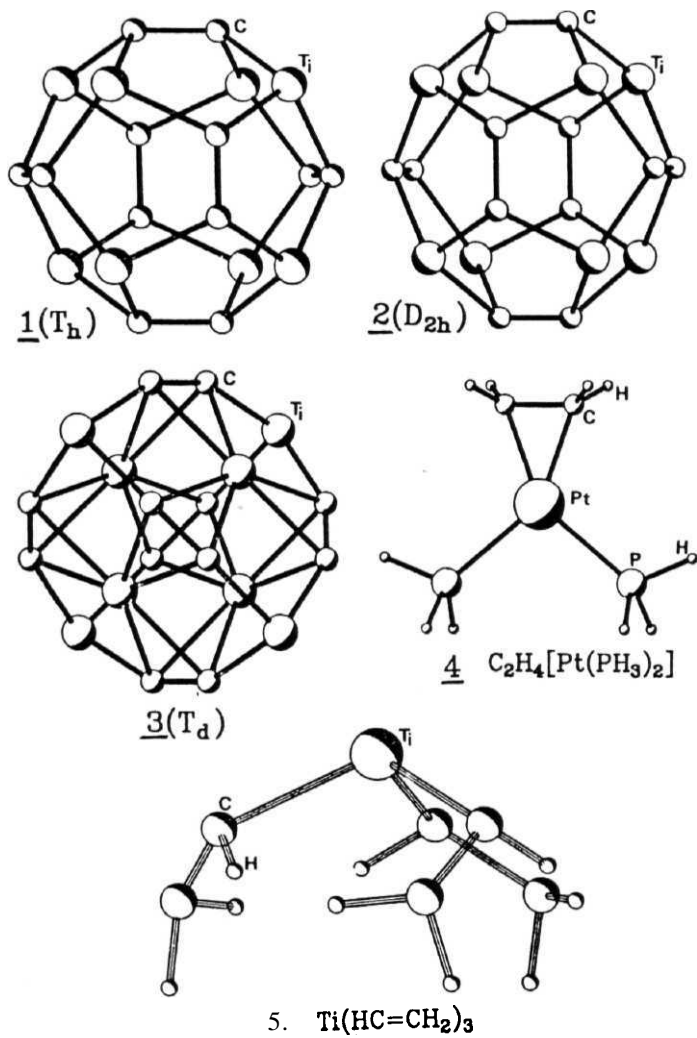
Fig. 1: Ti_8C_{12} in T_h (1), D_{2h} (2) and T_d (3) symmetries, (4) and the model system $Ti(HC=CH_2)_3$ (5).

clusters are named as **metallocarbohedrenes** (Met-Car). Many theoretical studies have been directed to establish the structure of the first Met-Car, a Ti_8C_{12} cluster.[9,21] Geometry optimization with T_h symmetry (1) has shown Ti_8C_{12} to have a triplet state.[9] The **Jahn-Teller** distorted structure with D_{2h} symmetry, 2 (Fig. 1), is calculated to be a singlet and lies lower in energy by about 28.5 kcal/mol than **1**.[10] In another study, a Ti_8 skeleton based on a face-bridged tetrahedron, was **considered**.[11] This structure, 3 (Fig. 1), was optimized to be a minimum in the quintet state, and was found to be lower in energy than 1 by about 300 kcal/mol.[12] These three structures are consistent with the **experimental** observations. Titration with NH_3 and CH_3OH produces $Ti_8C_{12}(NH_3)_8$ and $Ti_8C_{12}(CH_3OH)_8$, detected in mass spectral analysis.[2] Later, the synthesis of Met-Cars has been extended so as to obtain other early transition metals (viz. V_8C_{12}, Zr_8C_{12} and Hf_8C_{12}).[22] Duncan et **al** have reported the observation of chromium, iron and molybdenum Met-Cars.[23] In addition to these, there are also reports on mixed-metal Met-Cars.[24]

There are several interesting features in these structures. The C_2 units in 1 and 2 are similar to those in tetrametalated ethylene with pyramidalized carbon and is reminiscent of the structure of a metal-ethylene **π-complex** with all the substituents of the ethylene bent away from the metal (4).[25] This suggests the possibility of bonding arrangement for an incoming metal fragment to interact with the C_2 in M_8C_{12}. While **isomer** 2 has three different sets of C_2 units (the C-C distances are 1.299, 1.392 and 1.478A), the basic framework in 1 and 2 is the same. Structure 3, a tetracapped tetrahedron, also presents interesting analogies. The C_2 unit is

Table 1.

Extended Huckel Parameters.[25-30]

Atom	Orbital	H_{ii}	ζ_1	ζ_2
Ti	4s	-8.97	1.075	
	4p	-5.44	0.675	
	3d	-10.81	4.500(0.4206)	1.400(0.7839)
Pt	6s	-9.08	2.550	
	6p	-5.48	2.550	
	5d	-12.59	6.010(0.6334)	2.700(0.5513)
C	2s	-21.40	1.625	
	2p	**-11.40**	1.625	
P	3 s	-18.60	1.600	
	3p	-14.00	1.600	
H	**ls**	-13.60	1.300	
0	2s	-32.30	2.275	
	2p	-14.80	2.275	

Table 2.

Important bond lengths of various isomers.[9,11]

Structure	Bond type	Bond length (A)
1	M-M	3.06
	M-C	1.98
	C-C	1.40
2	M-M	3.03
	M-M	3.19
	M-M	3.27
	M-C	2.14
	M-C	2.06
	C-C	1.29
	C-C	1.47
3	M-M	2.86
	M-M	2.90
	C-C	1.34
	M-C	2.19
	M-C	2.93

different from those in 1 and 2, but is similar to one of the minima calculated for tetralithioethylene with two terminal lithiums and two bridging lithiums in the two π-planes.[26]

The metal environment in 1 and 2 can be compared to that in trivinyl metal complex, with the three ligands arranged in a pyramidal fashion. This helps the metal in Met-Cars to accommodate extra ligands. There are two types of metal environments in 3. Four metal atoms form an inner tetrahedron and the other four cap the faces of this inner tetrahedron. Four Ti atoms around one C_2 unit form a butterfly arrangement with the two inner titanium atoms as the hinge. This leads to an outer metal a bonded to three C_2 units and an inner metal having π-interaction with three C_2 units. Keeping these structural possibilities in view, this chapter discusses the interaction of fragments such as $Pt(PH_3)_2$ and carbon monoxide at various sites in the Ti_8C_{12} skeleton. The electronic structure calculations were performed using the fragment molecular orbital approach[27] within the extended Huckel theory[28] with parameters given in Table 1 and 2.

The electronic structure of 1 and 2 was studied previously by *ab initio* MO and density functional theory calculations.[9] But the electronic structure of 3 is not known except the report of the optimized structure.[11] This chapter deals with the electronic structure of 1, 2 and 3 with the main emphasis on assessing the reactivity centres in the cluster.
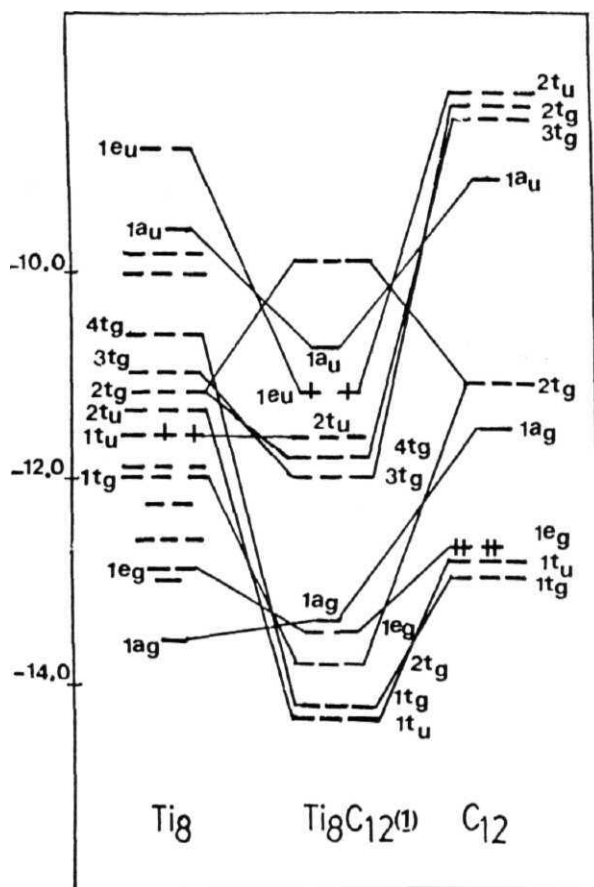
Fig. 2: Interaction diagram between Ti_8 and C_{12} to give the energy levels of Ti_8C_{12} (**1**). T_h symmetry labels are used.

Electronic structure of\ and 2

The electronic structure of 1 is constructed by the interaction of Tig and C_{12} (Fig.2). Only the important interactions are shown. The σ orbitals of C_{12} (2tg and 1ag) interact with Tig fragment leads to 2tg and 1ag, the a bonding orbitals in Ti_8C_{12}. The π bonding combinations between carbon n orbitals (1t_g to leg) and Tig fragment, that is $1t_u$ and $1t_g$ in Ti_8C_{12} are lower in energy than the sigma combination. The second set of 7r-bonding MOs (3tg, 4tg, $1e_u$ and $1a_u$) resulting from carbon n^* orbitals ($1a_u$ to $2t_u$) lie above the a levels in energy. This interaction diagram clearly shows that there is a greater contribution from carbon π^{*} levels at the frontier range. Below this, one finds the carbon a contribution. The HOMO is a doubly degenerate $1e_u$ set with only two electrons and leads to a triplet ground state.

The electronic structure of 2 is not very different from 1. There are three groups of orbitals in 2. The group at HOMO is rich in metal d-orbitals with carbon n^* participation. The second group below this has predominantly carbon p-orbitals of the C-C bond direction along with some contribution from the metal d-orbitals. The third group which is below the second one is mainly contributed by the carbon s-orbitals. In general, these descriptions of the electronic structure of 1 and 2 agree well with the previous theoretical calculations.
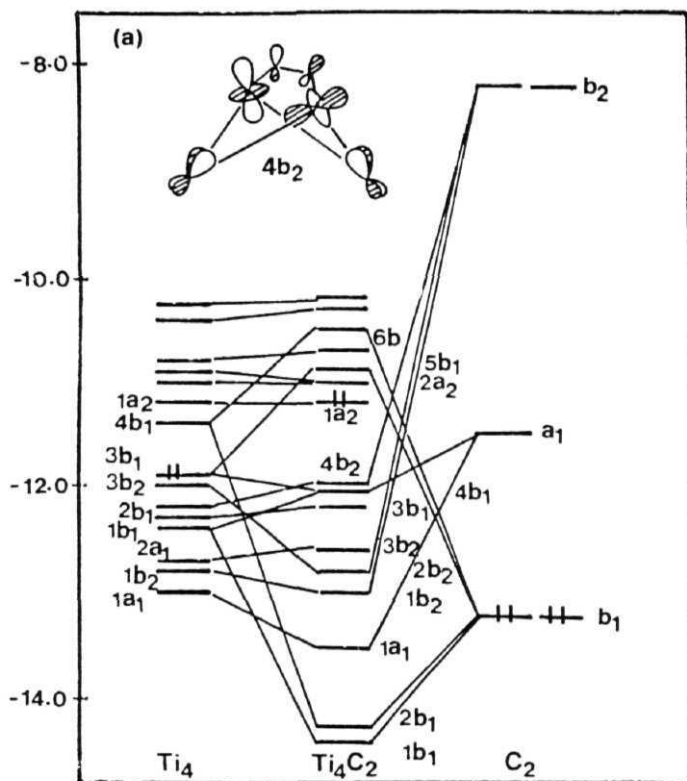
Fig. 3(a): Interaction diagram between Ti_4 and C_2 to give the energy levels of Ti_4C_2 with C_{2v} geometry.

Electronic structure of 3

The coordination around carbon in 3 is different from 1 and 2. To understand this new geometry at the C_2 unit , we have taken a smaller fragment Ti_4C_2 of Ti_8C_{12} (3). The molecular orbitals of Ti_4C_2 are constructed from the fragments Ti_4 (in butterfly geometry) and C_2 (Fig. 3a). The symmetric combination of a and the π^* orbitals of C_2 are empty; whereas, the C-C a, the antisymmetric combination of lone pairs and *n* orbitals are filled in C_2. The molecular orbitals of M4 are similar to those of the butterfly clusters. The long metal-metal distance restricts the energy spread to be small. The π orbitals of C_2 (b_1) interact with \b\ and 4b] of the Ti_4 unit leading to $1b_1$ and $2b_1$ of Ti_4C_2. The non-bonding σ-orbitals of C_2 (a_1) and $1a_1$ of Ti_4 leads to $1a_1$ of Ti_4C_2. These $1b_1$, $2b_1$ and \a\ MOs in Ti_4C_2 are responsible for σ-bonding between the outer Ti and C_2. these interactions mainly lead to 7r-bonding between the inner Ti atoms in the Ti_4 and the C_2 units. The HOMO of Ti_4C_2 is purely metal based arising from $1a_2$, which has *n* anti-bonding interactions between the inner and outer Ti atoms. The interesting feature of this diagram is the HOMO-1 ($4b_2$) of Ti_4C_2, a bonding MO between % orbitals of C_2 and z^2 orbitals on outer Ti atoms.

With this understanding of Ti_4C_2, we proceed to form Ti_8C_4 by taking two Ti_4C_2 units (see Fig.3(b) for MO's of Ti_8C_4). The important developments during dimerization are formation of MOs viz. $1e$, $2a_2 2a_1$, $1b_2$ and 3a,, corresponding to metal-metal bonds. The le and $2a_2$ MOs are responsible for bonding between inner Ti atoms. The MOs $1a_1$, $2a_1$ and $1b_2$ are mainly responsible for bonding between inner and outer Ti atoms.

146

Fig. 3(b): Construction of energy levels of Ti_8C_{12} (3) from Ti_8C_4 and $4C_2$ units. For Ti_8C_4 and $4C_2$'s the D_{2d} symmetry labels are used and T_d symmetry labels are used for Ti_8C_{12}.

The MOs $3a_1$ and $4a_1$ are mainly outer Ti metal-based orbitals. In short, dimerization of Ti_4C_2 brings in metal-metal interactions between inner-inner and inner-outer Ti metals.

Ti_8C_{12}, 3, can now be obtained by adding the remaining C_2 units to Ti_8C_4. Some of the important interactions in the formation of 3 are shown in Fig. 3b. The MOs of $4C_2$ units are given on the right-hand side of the diagram. MOs 1a] and $2a_1$ are symmetric combination of rc-orbitals of C_2 units. 4a] of Ti_8C_4 interacts with $2a_1$ leading to σ-bonding between the outer Ti atoms and C_2. 1e and 2e of the $4C_2$ units are π orbitals which interact with inner Ti atoms in a σ-fashion and with outer metals in a *n*-fashion. The non-bonded σ-orbitals $4a_1$, 3e and $5a_1$ of the C_2 units form mainly σ-bonds with outer metals. The π^* MOs $1b_1$, 4e and 5e of the C_2 units are mainly responsible for a-bonding with inner metals and anti-bonding π-interactions with outer metals. The HOMO of 3 is triply degenerate with two electrons which makes the system susceptible to Jahn-Teller distortion. One way of stabilizing the system is by exciting one electron from $2a_u$ to HOMO, which gives a spin multiplicity of 5.[12]

Oxidation state of metal atoms in Ti_8C_{12}

Each metal atom in 1 may be viewed as a trivinyl derivative. This leads to a +3 oxidation state at the metal with a d^1 configuration. Similarly, each C_2 unit can be viewed as tetrametallated ethylene, that is C_2's exist as C_2^{4-}. The Mulliken charge on the metal atom is +0.41 and on C is -0.27. Isomer 2 can also be viewed in the same way as 1 since the structural features of them are similar. In 2 also, the Mulliken charge on the metal is
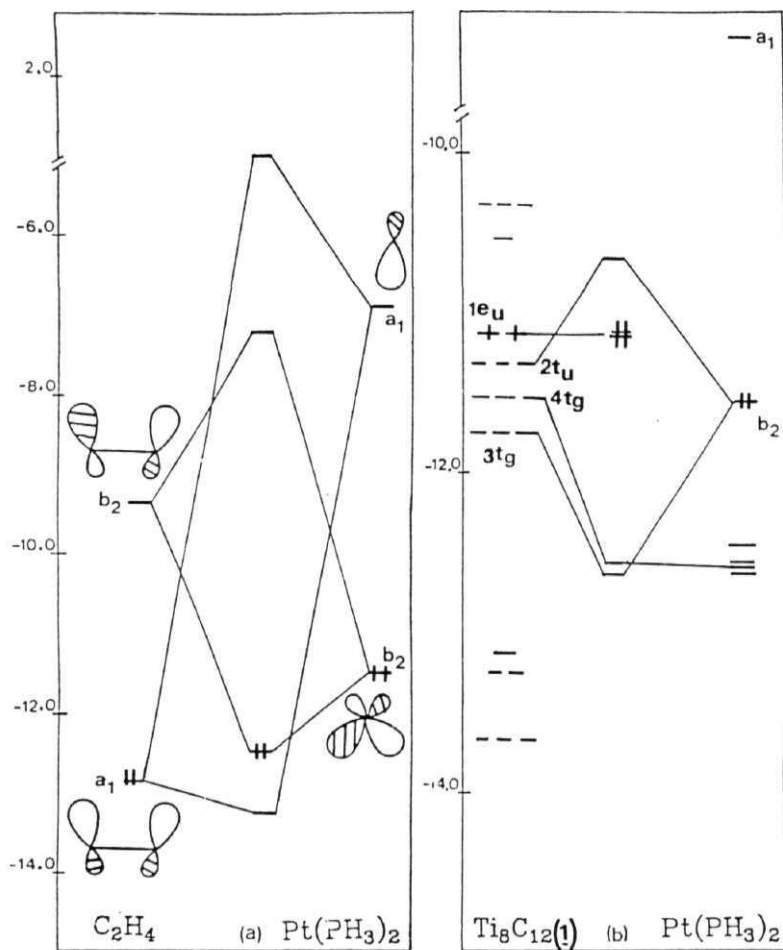
Fig. 4(a) **and** (b): Interaction diagram between (a) C_2H_4 and $Pt(PH_3)_2$, (b) Ti_8C_{12} **(1)** and $Pt(PH_3)_2$.

approximately +0.41. But the C's have charges of magnitude -0.21, -0.26 and -0.34 for the three different carbons.

The oxidation states of the two types of metals in **isomer** 3 are different. Since each metal in the outer tetrahedron is bonded to three C_2 units, the outer metal may have a +3 oxidation state. There are four outer Ti atoms which leads to each C_2 having a -2 charge. This electron counting leaves the inner Ti atoms in a zero oxidation state as the interactions with C_2 units may be treated as 7r-type. But this is not in tune with the calculations which show that the inner Ti atoms have more charge than the outer ones (0.54 Vs 0.11).

Another way of counting electrons leads to the following. Each inner Ti interacts with $3C_2$ units. The metal-carbon distance (2.2A) is very close to that of a σ-bond between them (in **Ti-vinyl** systems the Ti-C single bond distance is 2.2A[29]). Thus, each inner metal is connected to six carbons; whereas, each outer one is connected to three carbons only. Formal oxidation state counting would have led to four outer metals with +3 and each inner metal with +6. But the latter is impossible in an early transition metal. This would also leave each C_2 formally as C_2^{-6} with a C-C single bond. The truth is somewhere in between these extremes. All that can be said safely is that the inner Ti metal is at a higher oxidation state than the outer one. The overlap population between inner Ti-C is 0.26. But between the outer Ti-C it is 0.76 due to the extra π-**bonding**. The C-C overlap population (1.23) shows C-C to be close to a double bond (the C-C bond distance is 1.34A).
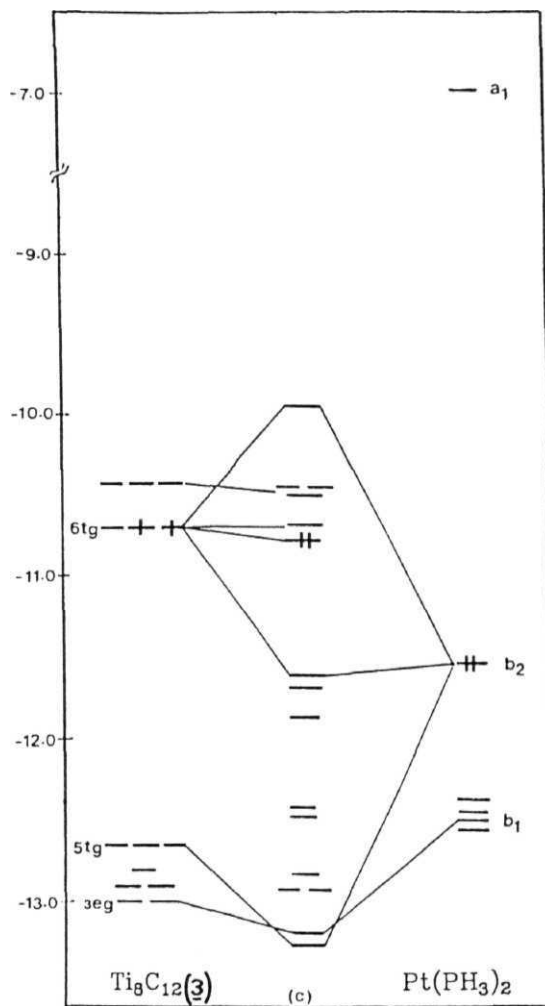
Fig. 4(c): Interaction diagram between Ti_8C_{12} (3) and $Pt(PH_3)_2$.

Carbon environment in Ti_8C_{12}. *Interaction of* C_2 *with* $Pt(PH_3)_2$

The carbons in a transition metal ethylene complex are pyramidalized towards the metal. The C_2 unit in 1 and 2 is pyramidalized in the same way. Even though the C_2 unit in 3 is of a different type, it is also pyramidalized. Thus, the C_2 units in Ti_8C_{12} should act as ethylenes towards transition metal fragments. To study this type of bonding in detail, we have considered the interaction of $Pt(PH_3)_2$ with Ti_8C_{12}. $Pt(PH_3)_2C_2H_4$ is a well known π-complex where the Pt-C bond occurs mainly from the interaction of the π^* (b_2) MO of ethylene (Fig.4(a)) with the hybridized d-orbital (b_2) of $Pt(PH_3)_2$. Fig. 4 gives the interaction diagram between $Pt(PH_3)_2$ (with standard geometry)[29] and isomers 1 and 3. Isomer 2 was left out due to its close resemblance to 1. The equivalent orbital of ethylenic b_2 in 1 is 3tg and $2t_u$. Since 3tg is an occupied orbital unlike b_2 in C_2H_4, the interaction between 3tg and b_2 of $Pt(PH_3)_2$ should have caused destabilization. However, the two electrons fill the degenerate HOMO fully instead of going to an anti-bonding orbital. Thus, $Pt(PH_3)_2$ may be treated as a two-electron donor to Ti_8C_{12} (1).

Structure 2 also has pyramidalized C_2 units. Out of three types of C_2 units, the C_2 unit which has a short C-C bond gives maximum stabilization with $Pt(PH_3)_2$. The interactions between $Pt(PH_3)_2$ and 2 are not very different from 1. The result is donation of electrons from the metal fragment to 2.
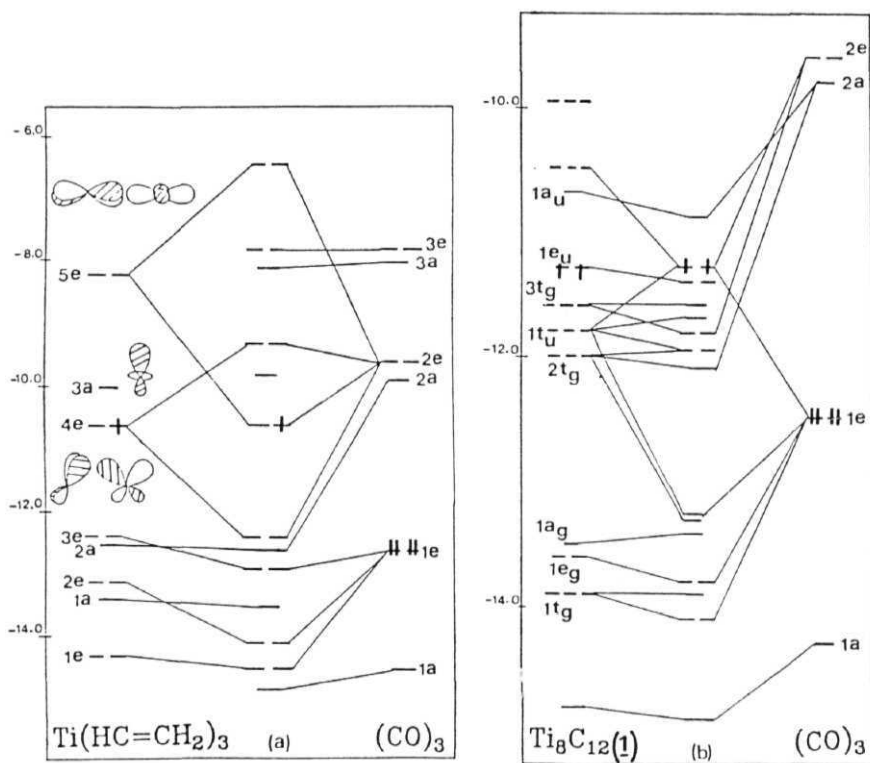
Fig. 5(a) **and** (b): Interaction diagram between (a) Ti(HOCH2)3 and (CO)3, (b) Ti8C12 (**1**) and (CO)3.

Though the geometry around C_2 unit in 3 is different from the other two, it is possible to trace pyramidalized $n*$ orbitals. In 3, the MO 6tg is similar to π^* of C_2H_4 which interacts with the b_2 orbital of $Pt(PH_3)_2$. HOMO-1 of 3 is also of appropriate energy to mix with b_2 of $Pt(PH_3)_2$. Another stabilization in this complex is from the 3eg orbitals of 3 mixing with $b\backslash$ of the metal fragment . $Pt(PH_3)_2$ donates two electrons on complexing with 1, 2 or 3. The two electrons from $Pt(PH_3)_2$ fill the LUMO of 2; whereas, they stabilize the half-filled HOMOs in 1 and 3. Therefore, the C-C overlap population values 1.10, 1.28 and 1.23 are changed to 0.94, 1.10 and 1.08 in 1, 2 and 3 respectively after complexing with $Pt(PH_3)_2$.

Metal environment. Interaction with carbonyls

Our calculations on model system $Ti(CH=CH_2)_3$ (5) has shown that the metal in the non-planar geometry of this complex represents the metal in Ti_8C_{12}. Since we are interested in extra ligand complexion on metal in Ti_8C_{12}, we have studied the complexation of CO on 5. Fig. 5a gives the interaction diagram between 5 and $(CO)_3$ fragments with standard titanium-carbonyl distances.[29]   The angle 80.0° was fixed between carbonyl-titanium-carbonyl. The staggered form which gives pseudo-octahedral geometry is found to be more stable. The hybridized metal orbitals in 5 are 4e, 3a and 5e. The major interactions are between 3e, 4e and 5e set of 5 and 1e and 2e set of $(CO)_3$. The σ interactions occur between 1e and 2e of 5 and le of $(CO)_3$. The symmetric combination of the 7t* orbitals of $(CO)_3$, (that is 3a and 3e) do not have orbitals of right symmetry to mix with 5. There is a stabilization of 10 eV in the formation of the carbon monoxide complex as judged by the change in the sum of one electron energies.
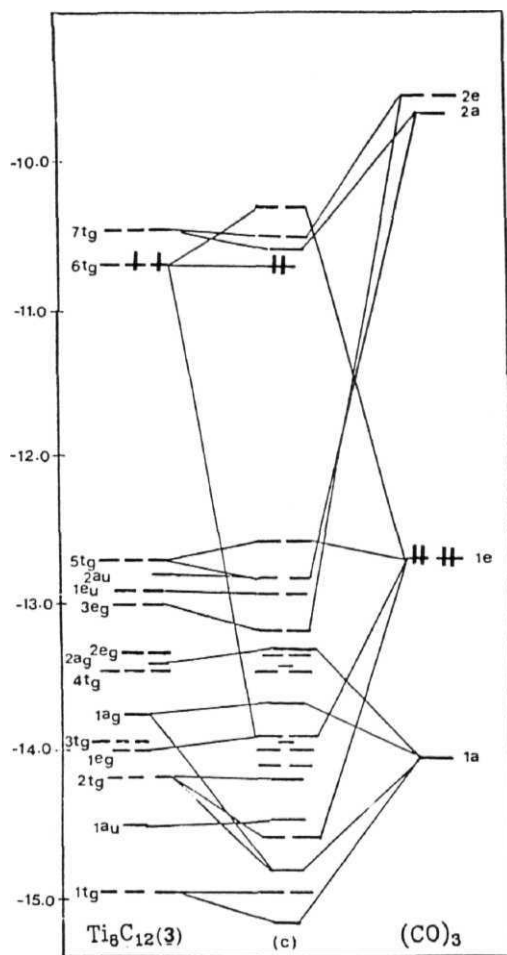
Fig. 5(c): Interaction diagram between Ti_8C_{12} (3) and $(CO)_3$.

The metal contribution in 3tg and 2tg of 1 and 5tg and $2e_g$ orbitals of 3 (which are based on the outer tetrahedron of titaniums) are similar to 5e, 4e and 3e orbitals of 5. Fig. 5 shows the interaction between Ti_8C_{12} (in structures 1 and 3) and $(CO)_3$, which is more or less similar to that between 5 and $(CO)_3$. Isomer 2 also shows an interaction similar to 1. All the Ti metals in 1, 2 and outer Ti metals in 3 have shown enough capacity of complexing with carbonyls. There is an enormous stabilization of 10.20, 10.19 and 11.40 eV for 1, 2 and 3 respectively as calculated from change in the sum of one-electron energies in complexation with $(CO)_3$.

The Mulliken charge on the metal changes drastically on complexation with carbon monoxide. The charges are from +0.41, +0.40 and +0.11 on 1, 2 and 3, to -0.08, -0.33 and -0.68 respectively after complexing with CO. These changes also indicate the electrophilic nature of the metal in the cluster. The outer Ti metal in 3 is most electrophilic, next is the metal in 2 followed by 1. There are changes in overlap population also. The M-M overlap populations of 0.10, 0.11 and 0.18 in 1, 2 and 3 decreases to 0.03, 0.05 and 0.09 respectively after complexing with CO. The M-C overlap population (0.66 and 0.75 in 1 and 3, and 0.53, 0.61 and 0.72 for, medium and long C_2 units in 2) also decreases to 0.45 and 0.59 in 1 and 3, and 0.35, 0.41 and 0.48 for the three C_2 units in 2. In general, this may be considered as a result of donation of electrons from carbonyl to the cluster where predominantly M-C and M-M anti-bonding MOs are at the receiving end.

We conclude that despite the structural differences, all the Ti metals in 1, 2 and outer Ti metals in 3 show the capability of complexing with

COs. It may be possible that by allowing three COs at each metal, the macro-complex $Ti_8(CO)_{24}$ may be obtained. Since we get a high stabilization for each $(CO)3$ unit on one metal, Ti_8C_{12} may be used as a CO absorber.

Thus, in conclusion, the Ti_8C_{12} cluster is a highly electron-deficient species. The cluster is ready to accept electrons from traditional ligands such as CO and also from transition metal fragments. In soot obtained in the experiments of Castleman, Ti_8C_{12} may exist as associated clusters with the interaction of Ti metal in one cluster with C_2 units in the other. Metallocarbohedrens should also be good ligands for forming large clusters.

References

1. (a) Kroto, H.W.; Heath, J.R.; O'Brien, S.C.; Curl, R.F.; Smalley, R.E. *Nature* **1985,** *318,* 162.

(b) Curl, R.F.; Smalley, R.E. *Science* **1988,** *242,* 1017.

(c) Weltner Jr, W.; Van Zee, R.J. *Chem. Rev.* **1989,** *89,* **1713.**

(d) Kroto, H.W.; Allaf, A.W.; Balm, S.P. *Chem. Rev.* **1991,** *91,* 1213.

2. Guo, B.C.; Kerns, K.P.; Castleman, A.W.Jr. *Science* **1992,** *255,* 1411

3. Wei, S.; Guo, B.C.; Purnell, J.; Buzza, S.; Castleman, A.W.Jr. *J. Phys. Chem.* 1992,96,4166.

4. Cartier, S.F.; Chen, Z.Y.; Walder, G.J.; Sleppy, C.R.; Castleman, A.W.Jr. *Science* **1993,** *260,* 195.

5. Pauling, L.J. *Proc. Natl. Acad. Sci.* U.S.A. **1992,** *89,* 3081.

6. (a) Scamehorn, C.A.; Hermiller, S.M.; Pitzer, R.M. *J. Chem. Phys.* **1986,** *84,* 833.

(b) Disch, R.L.; Schulman, J.M.; Sabio, M.L. *J. Am. Chem. Soc.* **1985,** 707, 1904.

(c) Schulman, J.M.; Disch, R.L. *J. Am. Chem. Soc.* **1984,** *106,* 1202.

(d) Paquette, L.A.; Ternansky, R.J.; Balogh, D.W.; Kentgen, G. *J. Am. Chem. Soc.* **1983,** *105,* 5446.

(e) Paquette, L.A.; Balogh, D.W. *J. Am. Chem. Soc.* **1982,** *104,* 77A.

(f) Christoph, G.G.; Engel, P.; Usha, R.; Balogh, D.W.; Paquette, L.A. *J. Am. Chem. Soc.* **1982,** *104,* 784.

(g) Paquette, L.A.; Balogh, D.W.; Usha, R.; Kountz, D.; Christoph, G.G. *Science* **1981,** *211,* 575.

7. (a) Strout, D.L.; Odom, G.K.; Scuseria, G.E.; Pople, J.A.; Johnson, B.G.; Gill, P.M.W. *Chem. Phys. Lett.* **1993,** *214,* 357.

(b) Kurita, N.; Kobayashi, K.; Kumahora, H.; Tago, K.; Ozawa, K. *Chem. Phys. Lett.* **1992,** *188,* 181.

(c) Feyereisen, M.; Gutowski, M.; Simons, J.; Almlof, J. *J. Chem. Phys.* **1992,** *96,* 2926.

(d) Parasuk, V.; Almlof, J. *Chem. Phys. Lett.* **1991,** *184,* 187.

8. Haddon, R.C.; Raghavachari, K. *Buckmisterfullerenes* Billups, W.E.; Cioufolini, M.A. Eds. VCH: New York, 1993.

9. (a) Grimes, R.W.; Gale, J.D. *J. Chem. Soc, Chem. Commun.* **1992,** 1222.

(b) Lin, Z.; Hall, M.B. *J. Am. Chem. Soc.* **1992,** *114,* 10054.

(c) Reddy, B.V.; Khanna, S.N.; Jena, P. *Science* **1992,** *258,* 1640.

(d) Hay, P.J. *J. Phys. Chem.* **1993,** *97,* 3081.

(e)   Mathfessel, M.; Schilfgaarde, V.M.; Scheffer, M. *Phys. Rev. Lett.* **1993,** *70,* 29.

(f)   Reddy, B.V.; Khanna, S.N. *Chem. Phys. Lett.* **1993,** *209,* 104.

10.   Marie-Madeleine, R.; de Vall, P.; Benard, M. *J. Am. Chem. Soc.* **1992,** *114,* 9696.

11.   Dance, I. *J. Chem. Soc, Chem. Commun.* **1992,** 1779.

12.   Marie-Madeleine, R.; Benard, M.; Henriet, C; Bo, C; Poblet, J. *J. Chem. Soc, Chem. Commun.* 1993, 1182.

13.   Ceulemans, A.; Fowler, P.W. *J. Chem. Soc, Faraday Trans.* **1992,** *88,* 2797.

14.   Methfessel, M.; van Schilfgaarde, M.; Scheffer, M. *Phys. Rev. Lett.* **1993,** *71,* 209.

15.   Rantala, T.T.; Jelski, P.A.; Bowser, J.R.; Xia, X.; George, T.F.Z. *Phys.* D **1993,** *26,* 255.

16.   Liu, J.N.; Gu, B.L. *J. Phys.: Condens. Matter.* 1993, 5, 4785.

17.   Chen, H.; Feyereisen, M.; Long, X.P.; Fitzgerald, G. *Phys. Rev. Lett.* **1993,** *71,* 1732.

18.   Lou, L.; Guo, T.; Nordlander, P.; Smalley, R.E. *J. Chem. Phys.* **1993,** 99,5301.

19.   Lin, Z.; Hall, M.B. *J. Am. Chem. Soc* 1993, *115,* 11165.

20.   Lou, L.; Nordlander, P. *Chem. Phys. Lett.* **1994,** *224,* 439.

21.   Rohmer, M.M.; Benard, M.; Henriet, C; Bo, C; Poblet, J.M. *J. Am. Chem. Soc.* **1995,** *117,* 508.

22.(a) Yeh, C.S.; Afzaal, S.; Lee, S.A.; Byun, Y.G.; Freiser, B.S. *J. Am. Chem. Soc* **1994,** *116,* 8806.

  (b) Guo, B.C.; Wei, S.; Purnell, J.; Buzza, S.; Castleman, A.W.Jr. *Science* 1992,255,515.

  (c) Wei, S.; Guo, B.C.; Purnell, J.; Buzza, S.; Castleman, A.W.Jr. *Science* **1992,** *256,* 818.

  (d) Chen, Z.Y.; Guo, B.C.; May, B.D.; Cartier, S.F.; Castleman, A.W.Jr. *Chem. Phys. Lett.* **1992,** 795, 118.

  (e) Byun, Y.G.; Freiser, B.S. *J. Am. Chem. Soc.* **1996,** 775, 3681.

23.   Pilgrim, J.S.; Duncan, M.A. *J. Am. Chem. Soc.* **1993,** *115,* 6958.

24.   Cartier, S.F.; May, B.D.; Castleman, A.W.Jr. *J. Chem. Phys.* **1994,** *100,* 5384.

25.   Albright, T.A.; Hoffmann, R.; Thibeault, J.C.; Thorn, D.L. *J. Am. Chem. Soc.* **1979,** 707,3801.

26. Schleyer, P.v.R.; Dorigo, A.E.; Nicolaas, J.R.; Eikema, H.V.; Krogh-Jespersen, K. *Angew. Chem. Int. Ed Engl.* **1992,** *31,* 1602.

27. Fujimoto, H.; Hoffmann, R. *J. Phys. Chem.* **1974,** *78,* 1167.

28.(a) Hoffmann, R.; Lipscomb, W.N. *J Chem. Phys.* **1962,** *36,* 2179.

   (b) Hoffmann, R. *J. Chem. Phys.* **1963,** *39,* 1397.

29. Orpen, A.G.; Brammer, L.; Allen, F.H.; Kennard, O.; Waston, D.G.; Taylor, R. *J. Chem. Soc, Dalton. Trans,* **1989,** S1.

30. Joseph, W.L.; Hoffmann, R. *J. Am. Chem. Soc.* **1976,** *98,* 1729.

[4.2] *Electronic Structure Studies on Transition Metal-containing* **Poly-ynes**

The search for polymers for specific applications has been an active field of research for many years.[1] Polymer chemistry has become an interdisciplinary field which includes purely organic polymers, inorganic complexes and also organic charge transfer salts.[1,2] These polymers find many practical applications, e.g. photovoltaic devices based on poly-acetylene2 and $(SN)_x$ films,[3] current and optical switching in thin films of Cu(tetracyanoquinodimethane),[4] high density rechargeable batteries,[5] molecular-based electronic devices,[6] stabilization of n-type silicon photoelectrochemical cells[7] in material science and switchable ion conducting membrane[8] and controlled release of drugs from microelectrodes[9] in biological science.

Recently, interest in the search for low-band-gap polymers has increased due to its conductivity and good non-linear optical properties.[10] Among the conjugated polymers, poly(isothionaphthene) was known to have one of the smallest energy gap ($E=1.0$ eV) found experimentally." Theoretical calculations based on the model of Longuet-Higgins and Salem (LHS) have shown the band gaps to be of about 0.7 eV and 0.5 eV for poly (bis-isothionaphthene-methine) and poly (isonaphthothiophene-thiophene) respectively.[12]

Conjugated polymers incorporating transition metal atoms in the main skeleton has attracted much attention in recent years.[13] In expectation of the interesting physical properties associated with a long conjugated

Scheme 1

$[Pt(PH_3)_2$—Y—C≡C—$]_n$

1

$[Pd(PH_3)_2$—Y—C≡C—$]_n$

2

$[Ni(PH_3)_2$—Y—C≡C—$]_n$

3

$[Fe(PH_3)_4$—Y—C≡C—$]_n$

4

a) Y : none   b) Y : C≡C   c) Y : C≡C——C≡C

d) Y : C≡C—⟨benzene⟩—

e) Y : C≡C—⟨benzene with CN⟩—

f) Y : C≡C—⟨benzene with CN, CN⟩—

g) Y : C≡C—⟨benzene with CN, CN⟩—

h) Y : C≡C—⟨benzene with CN, CN, CN, CN⟩—

i) Y : C≡C—⟨benzene with NH_2, NH_2⟩—
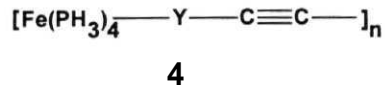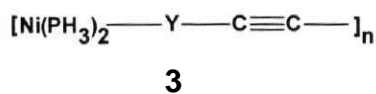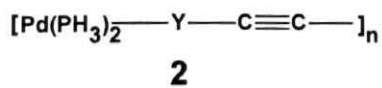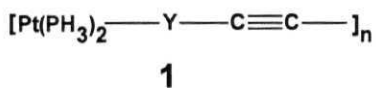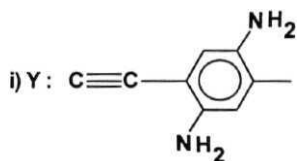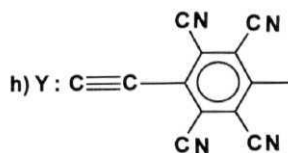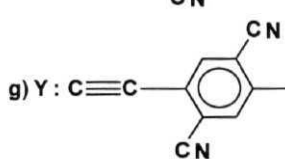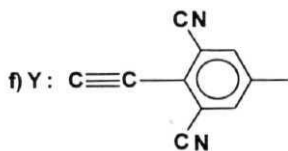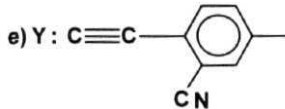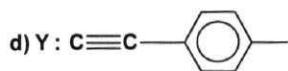
structure due to $d\pi$(metal)-$p\pi$(acetylenic carbon) interaction, novel straight-link oligomers composed of metal atoms of the platinum group and conjugated poly-yne systems have been synthesized.[14]

Hagihara et al have prepared the polymers mainly of the type $[M(PBu_3)_2(-C\equiv C-(R)-C\equiv C-)]_n$ where n>200, M = Ni, Pd, Pt; R=none, p-C_6H_4 etc.[14] They analyzed the electronic spectra of the three polymers $[trans-M(PBu_3)_2-C\equiv C-)]_n$ (M = Ni, Pd and Pt) and assigned the lowest energy bands to metal to ligand charge transfer transitions which have λ_{max} values of 342, 382 and 414nm (that is 3.6, 3.2 and 3.0 eV) respectively.[15] Later, the preparation of these metal poly-yne polymers have been extended from group 10 to group 8 and 9.[16,17]

To explain the conductivity and other physical properties of these polymers, one has to know the electronic structure of these materials. To the best of our knowledge, there is only one electronic structure discussion of these polymers so far.[18] In the present study, we have tried to decrease the band gap by changing the metal-metal distance (by chapging the various connecting ligands in the polymer back bone), and examined some substituents on the bridging ligands.

We have taken polymers $[-C\equiv C-Y-M(PH_3)_m]_n$ where Y - none, $C=C$, p-$C_6H_4-C\equiv C$; M = Pt, Pd, Ni and m = 2 for Pt, Pd, Ni and 4 for Fe to study the electronic structure (Scheme 1). The band structures, density of states (DOS) and crystal orbital overlap populations (COOP) have been calculated using the tight-binding extended Huckel method[19] (parameters are listed in Table 1 and 2).

Table 1

Extended Huckel parameters that are used in the present study[20].

Atom	Orbital	H_{ii} (eV)	ζ_1	$c_,$	ζ_2	C_2
Pt	6s	-11.64	2.554			
	6p	-7.01	2.554			
	5d	-12.27	6.013	0.6334	2.696	0.5513
Pd	5 s	-7.32	2.19			
	5p	-3.45	2.152			
	4d	-12.02	5.983	0.5535	2.613	**0.6770**
N.	4s	-8.86	2.10			
	4p	-4.90	2.10			
	3d	-12.99	5.75	0.5683	2.00	0.6292
Fe	4 s	-9.6372	1.575			
	4p	-5.89379	1.90			
	3d	-11.6686	5.35	0.5366	1.80	0.6678
P	3s	-18.60	1.880			
	3p	-14.00	1.630			
N	2s	-26.00	1.950			
	2p	-13.40	1.950			
C	2s	-21.40	1.625			
	2p	-11.40	1.625			
II	1s	-13.60	1.300			

Table 2

Imortant bond lengths used in the present study.[21]

Parameter	Bond length (Å)
Fe-C	1.920
Pt-C	1.992
Pd-C	1.953
Ni-C	1.880
Fe-P	2.246
Pt-P	2.275
Pd-P	2.338
Ni-P	2.196
P-H	1.380
C≡C	1.188
C-C(in phenyl ring)	1.399
(sp) C—⬡	1.400
NC—⬡	1.380
H₂N—⬡	1.355
C≡N	1.138
N-H	1.032
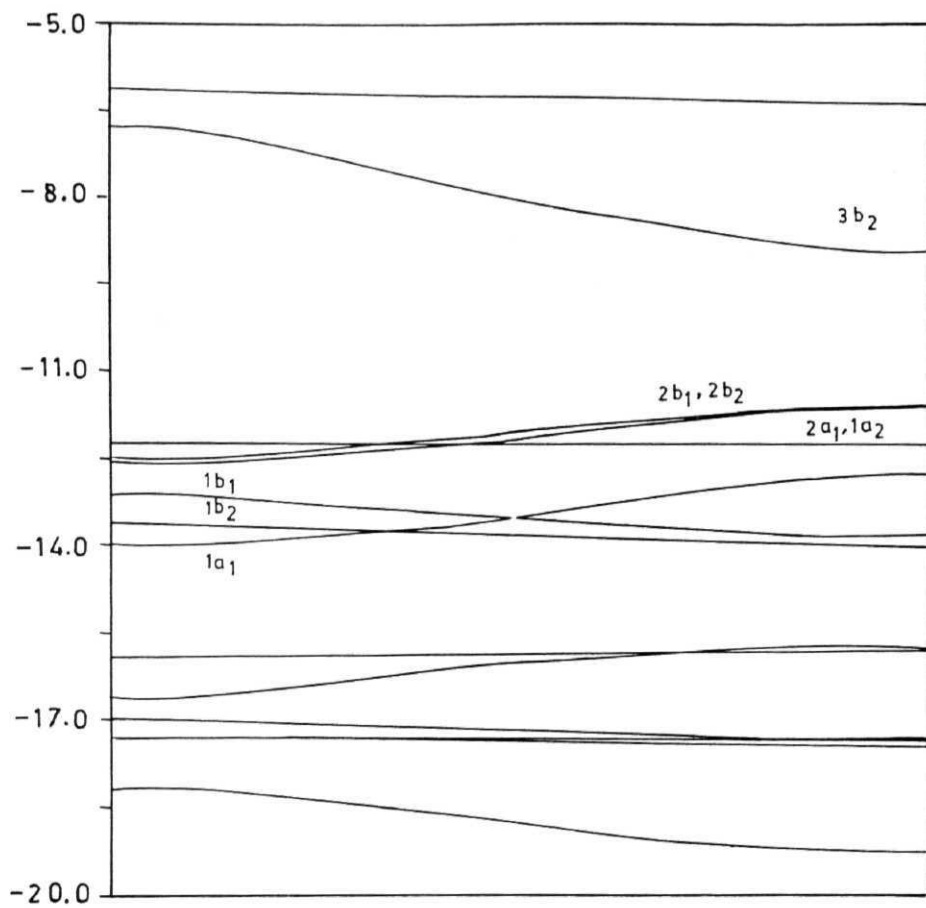
Fig. l(a): Energy bands of the model polymer $[Pt(PH_3)_2\text{-}C\equiv C\text{-}]_n$.

Band structure of **Pt** *polymers*

The development of bands from the molecular energy levels for the Pt polymers in our study agrees well with the previous calculations.[18] Hence only the electronic structure of these polymers are discussed in this chapter. The band structure, density of states and the crystal orbital overlap populations for the polymer la are given in **Fig.1a-e**. The projected DOS has shown that the valence bands and conduction bands are rich in contribution from metal (Fig.1b). There is a predominant participation of ligand in both the bands (Fig.1c). Scheme-2 gives the crystal orbitals corresponding to unoccupied and occupied bands of the model polymer la at k = 0 (zone center) and k = rc/a (zone edge).

The lowest unoccupied band, $3b_2$, is ligand *n* mixed with the metal z at the zone center (k=0) in anti-bonding fashion and *n** of ligand mixed with metal z at zone edge (k=7r/a) in a bonding fashion (Fig. 1, Scheme 2). The anti-bonding interactions decrease and **development** of bonding interactions increase between the metal and the ligand as k changes from 0 to π /a. The Pt-C crystal orbital overlap population (**Fig.1d**) shows that the bonding interactions are much stronger than the anti-bonding interactions. The crystal orbital overlap population between the two carbons of acetylene shows that it is of anti-bonding type (Fig.le). In summary, the unoccupied band, $3b_2$, is a ligand *n*,* in bonding fashion with the metal z orbital.

At the Fermi level, the valence bands $2b_1$ and $2b_2$ are metal xy and yz anti-bonding bands with very little energy difference between them.

Scheme 2
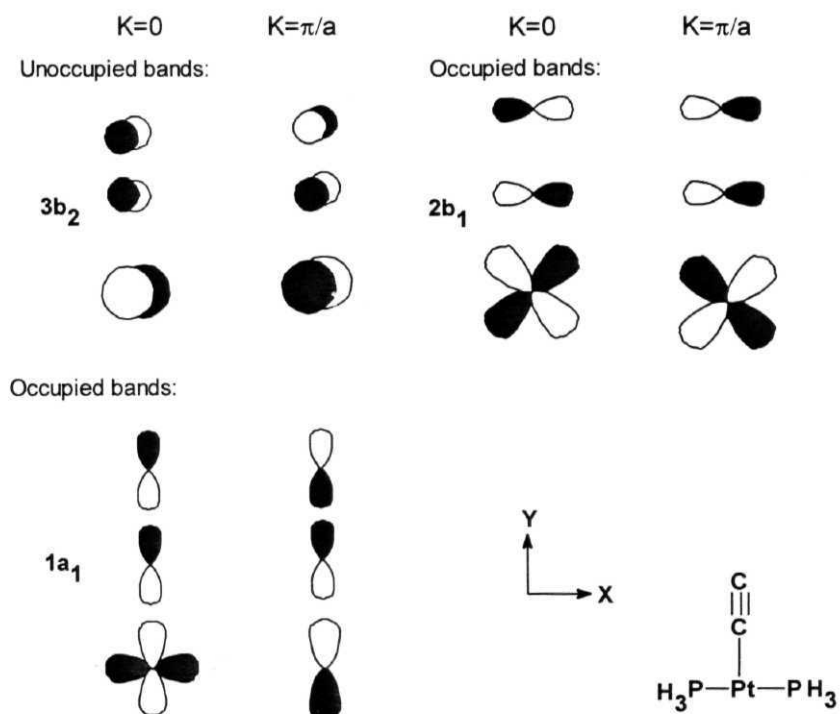
Ligand π_1 and π_2 orbitals mix with the metal xy and yz (Scheme 2). These interactions are very weak bonding type at zone center (k=0), and ligand is in π^* character (Scheme 2). While at zone edge the ligand π orbitals interact with metal orbitals in an anti-bonding fashion. The crystal orbital overlap population shows strong anti-bonding between platinum and carbon and bonding between the two carbons of the acetylene (Fig.1d,e). This indicates that the nature of the polymer at the Fermi level is π anti-bonding between ligand and the metal with a bonding interaction within the ligand (acetylene).

$2a_1$ and $1a_2$ bands are flat without any change in the slope of the bands, as k changes from 0 to π/a (Fig.1a). These two bands are purely metal based xz and z^2 whose symmetry does not allow any interaction with the bridging ligand for polymer propagation. This makes these bands to be uneffected throughout the Brillouin zone.

$1b_1$ and $1b_2$ are the pure ligand π bands at the zone center. There is development of bonding interaction between these ligand n and metal xy and yz as k changes from 0 to π/a. This makes these bands to get stabilized at the zone edge. The band $1a_1$ is a bonding interaction between metal x^2-y^2 and ligand a orbital at zone center; while, at zone edge it is bonding with metal y. As the metal p orbitals are relatively high in energy than the metal d-orbitals, this band goes up in energy at zone edge. Pt-C and C-C (acetylene) crystal orbital overlap populations show the bonding nature within the energy range of these three bands (Fig.1d,e).
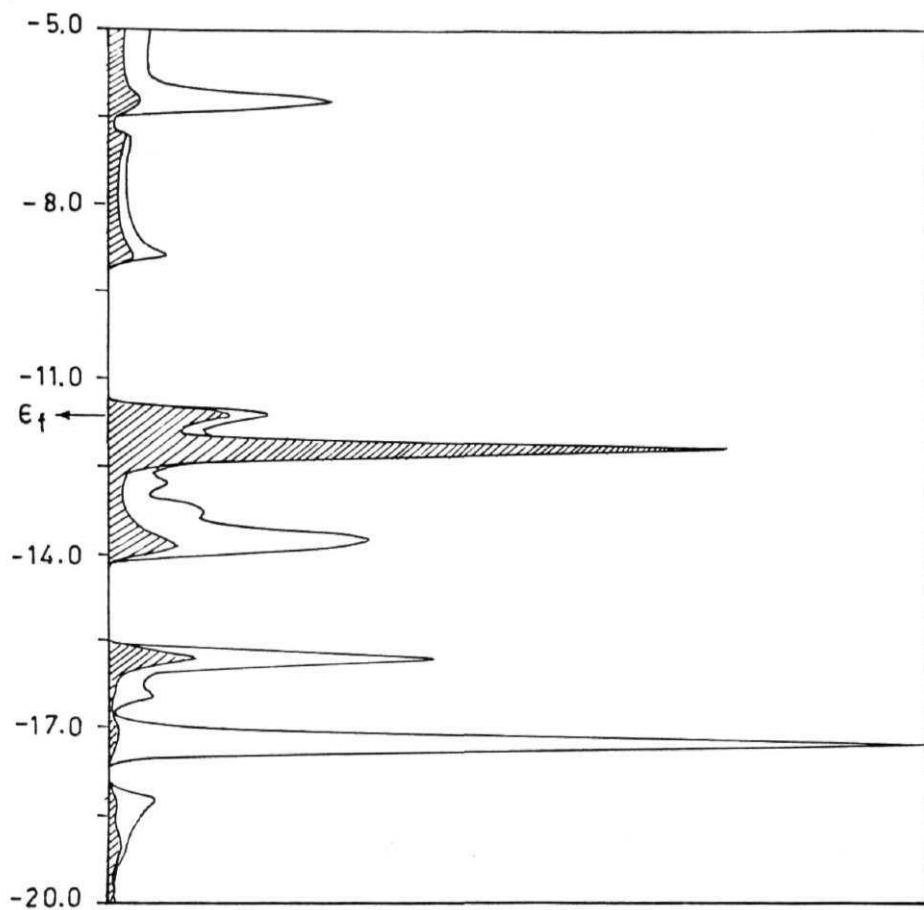
Fig. 1(b): Projected DOS of Pt (shaded part) in $[Pt(PH_3)_2-C≡C-]_n$ polymer.

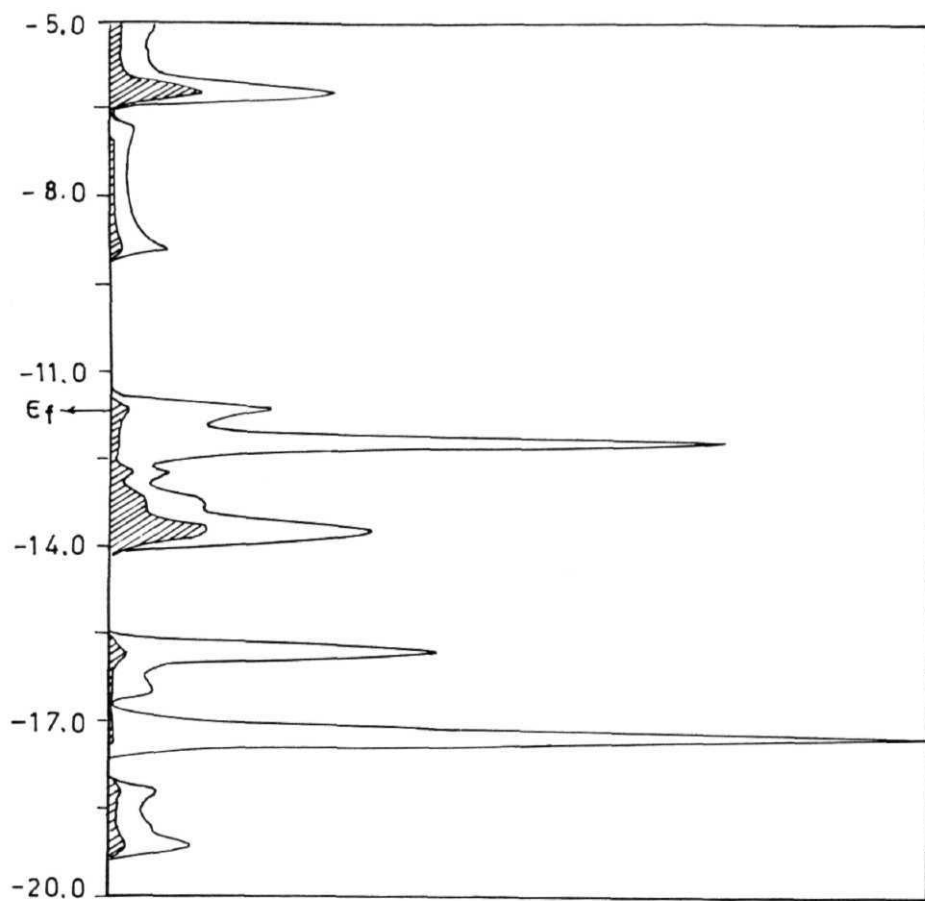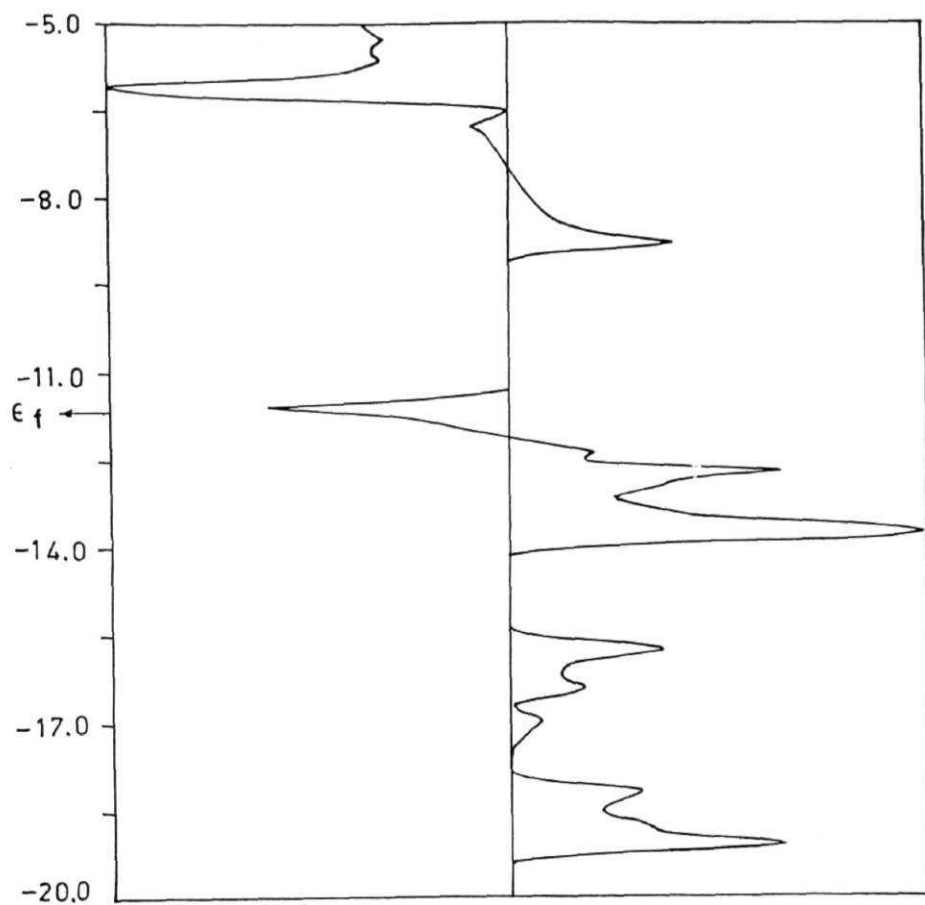Fig. 1(c): Projected DOS of acetylenic carbon (shaded part) in [Pt(PH$_3$)$_2$-C≡C-]$_n$ polymer.

Fig. l(d): The crystal orbital overlap population between Pt and acetylenic carbon in $[Pt(PH_3)_2-C{\equiv}C-]_n$ polymer. ε_f denotes Fermi energy level.
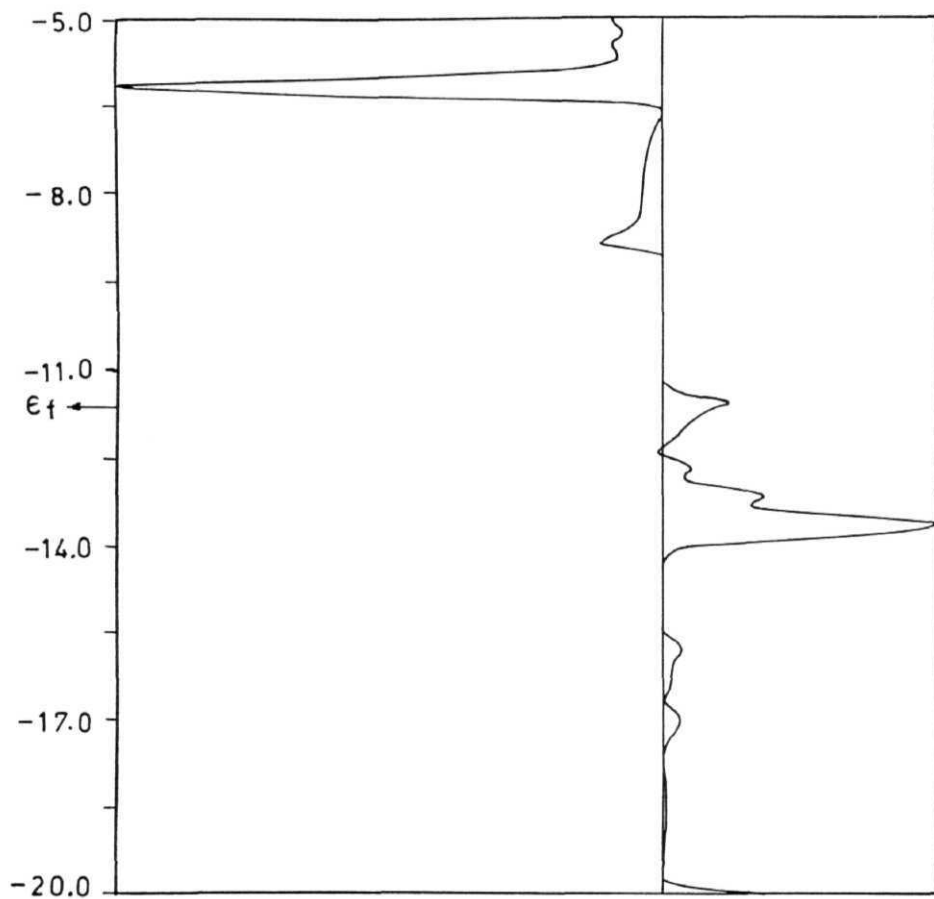
Fig. l(e): The crystal orbital overlap population of C≡C in
[Pt(PH3)2-C≡C-]n polymer. sf denotes Fermi energy level.

So far, we have discussed the band structures of model platinum mono acetylenic polymer $[Pt(PH_3)_2-C\equiv C-]_n$ 1a. Now, let us increase the unit cell size and the distance between the metals in the polymer by increasing the length of the bridging ligand. For this purpose, the polymers that have been taken are **1b** and **1c** (Scheme 1). **1b** is a model for experimentally prepared polymer $[Pt(PBu_3)_2-C\equiv C-C\equiv C-]_n$ known as diacetylenic polymer.[15] Similarly, 1c is also a model for experimentally known triacetylenic polymer $[Pt(PBu_3)_2-C\equiv C-C\equiv C-C\equiv C-]_n$.[15]

The projected DOS of platinum is more at the Fermi level in lb similar to that of polymer la. The Pt-C and C-C crystal orbital overlap populations are also similar to that of la. The band structures of this polymer may be described as if the second half of the band structure of Fig.1 were folded onto its first half. Since the unit cell for lb is not exactly double of that of la, there are large adjustments in folding back. This folding back appears only for the bands in which the acetylenic participation is large. As the unit cell of lb does not contain another platinum, the bands which are mainly metal based were not affected. The lowest unoccupied band is ligand n^* and the valence bands are metal xy and yz anti-bonding degenerate bands at the Fermi level. The crystal orbital overlap population of acetylenic π-orbitals has shown its participation at conduction band as well as at valence band. The crystal orbitals are same as in Scheme 2 except by increased number of carbons. These results are in tune with the experimental findings for $[-Pt(PBu_3)_2-C\equiv C-C\equiv C-]_n$, the lowest energy band in the electronic spectra is the metal to ligand charge transfer.[15]

Polymer **1c** also shows the similar trend, the unoccupied band is based on ligand π^* and the valence bands are predominantly from the metal xy and yz antibonding combinations. The crystal orbital overlap population of acetylenic π-orbitals has also shown similar results like polymer **1b**. Crystal orbitals for this polymer are similar to that of Scheme 2, except for increased number of carbons.

In the process of changing the bridging ligand, we have done the calculations for the polymers **1d, 1e, 1f, 1g, 1h** and **1i** (Scheme 1). All these polymers have shown results similar to that of 1a. The results of **1d** agree well with the previous calculations.[18] The conduction band is ligand π mixed with the metal z in bonding fashion. Valence band is not degenerate in these cases as the C_2 symmetry is missing in these polymers. In all these polymers, metal based yz interacting with ligand n is the valence band at the Fermi level. All cyano substituted polymers have lost their anti-bonding interactions between metal yz and ligand n and have become non-bonding as the valence band runs from k = 0 to k = n/a. In the case of amino substituted polymer, the metal particioation was lost in valence band and it became pure ligand n band as k changes from 0 to n/a. These are the important changes of these polymers when compared to the polymer 1a.

Band structures of Pd *and* Ni *polymers*

To examine the effect of metal on the electronic structure of these polymers, we have done some calculations with Ni and Pd in group 10. The polymers that have been taken are 2a, 2b, 2d and 3a, 3b, 3d in the nickle group (Scheme 1).

The lowest unoccupied bands of palladium polymer, 2a, are ligand $n*$ in bonding interactions with the metal z and ligand σ_u in anti-bonding interactions with metal x^2-y^2 ($3a_1$). Similarly, in the case of Ni (3a), the lowest unoccupied band is ligand π^* in bonding interaction with metal z which is similar to 1a. The $3a_1$ band is stabilized from k = 0 to k = π/a in all the polymers 1a, 2a and 3a. It is ligand σ_u mixing with metal at the zone center; while, ligand σ_u is mixing with metal x^2-y^2 at zone edge. In the case of palladium (2a), $3a_1$ is stabilized more as k changes from 0 to n/a and mixes with $3b_2$ at zone edge. The valence bands are degenerate xy, yz for 2a and 3a at Fermi level as in the case of 1a. In both the cases, the $1a_1$ band rose in energy from k = 0 to k = π/a similar to that of 1a. For 2a the increase in energy of $1a_1$ is to such an extent that it reaches between $2a_1$ (z^2) and $1a_2$ (xz) at zone edge. While, in the case of 3a, \a\, further rises and is above the $2a_1$ and $1a_2$ and below 2b\ and $2b_2$. This shows that the change in energy of $1a_1$ from zone center to zone edge increases from platinum to nickel (1.3, 1.6 and 1.7 eV for platinum, palladium and nickel respectively). This is may be due to the following: the band $1a_1$ is ligand σ p_y in bonding interaction with metal x^2-y^2 at zone center. At zone edge, it is σ_g in bonding interaction with metal y. The sp hybridization also increases in acetylene as we go from 1a to 3a.

The lowest unoccupied bands and valence bands of 2b and 3b are similar to those of **1b**. $2a_1$ (z^2) and $1a_2$ (xz) are not degenerate in nickel (3b) and palladium (2b) polymers; while it is degenerate in platinum polymer (1b). The conduction and valence bands of polymers 2d and 3d

are also similar to those of **1d**. The polymers **1d**, 2d and 3d have narrow energy bands when compared to 1a, 2a, 3a and **1b**, 2b and 3b.

Band structures of Fe polymers

In the process of studying the acetylenic polymers with different metals we have taken some acetylenic polymers of iron to analyze their band structures. Since iron is much cheaper than the platinum group metals, the polymers of iron will be much more attractive commercially.

Band structures, density of states and crystal orbital overlap populations of polymer 4a are given in Fig.2a-e. Scheme 3 gives the crystal orbitals corresponding to unoccupied and valence band of the polymer 4a at $k = 0$ (zone center) and $k = 7t/a$ (zone edge). Projected DOS of iron is rich in valence bands; whereas, the projected DOS of ligand n is rich in conduction band (Fig.2b,c).

The lowest unoccupied band, 3e, is doubly degenerate iigand n^* at Fermi level. Crystal orbital overlap population of acetylene shows that it is strongly anti-bonding at conduction band (Fig.2e). Similarly, the Fe-C crystal orbital overlap population is also strongly anti-bonding (Fig.2d). The π^* orbitals of ligand mix with metal xz and yz in an anti-bonding fashion at zone center (k=0). Metal participation decreases as k changes from 0 to π/a; and finally, at zone edge, it disappears leaving 3e as the pure ligand n^* (scheme 3).
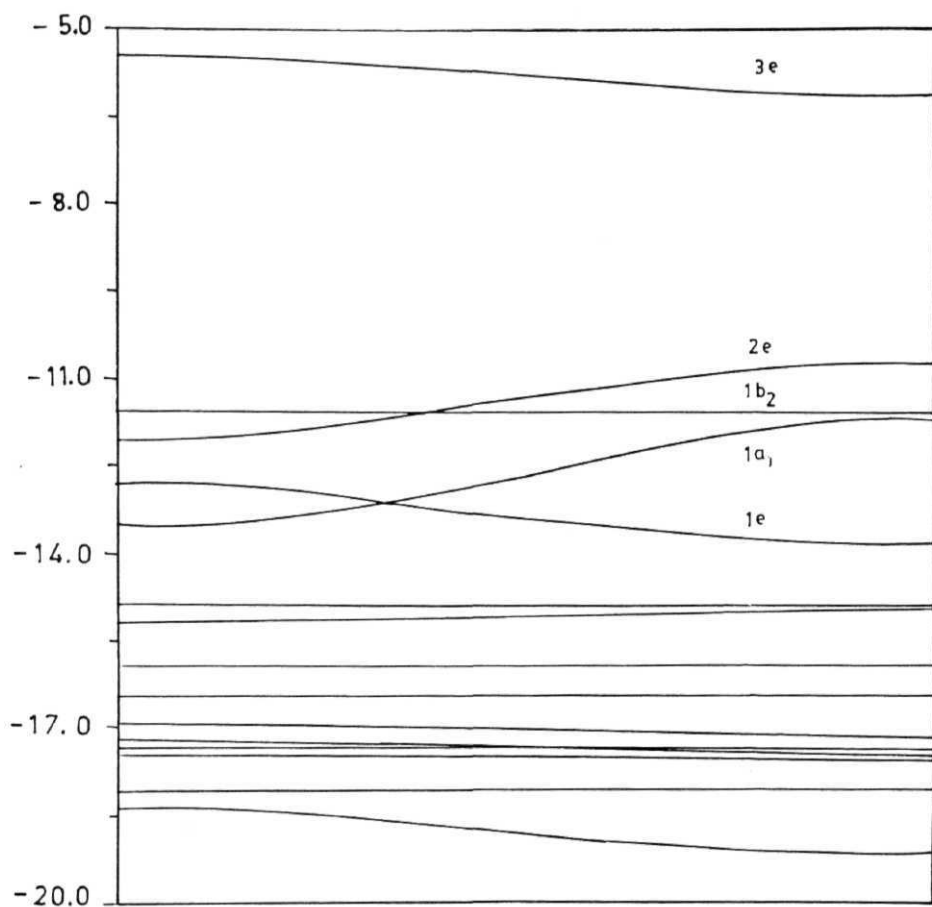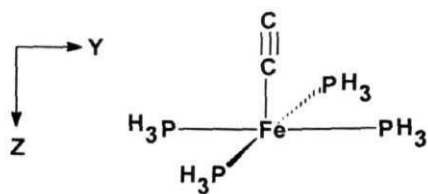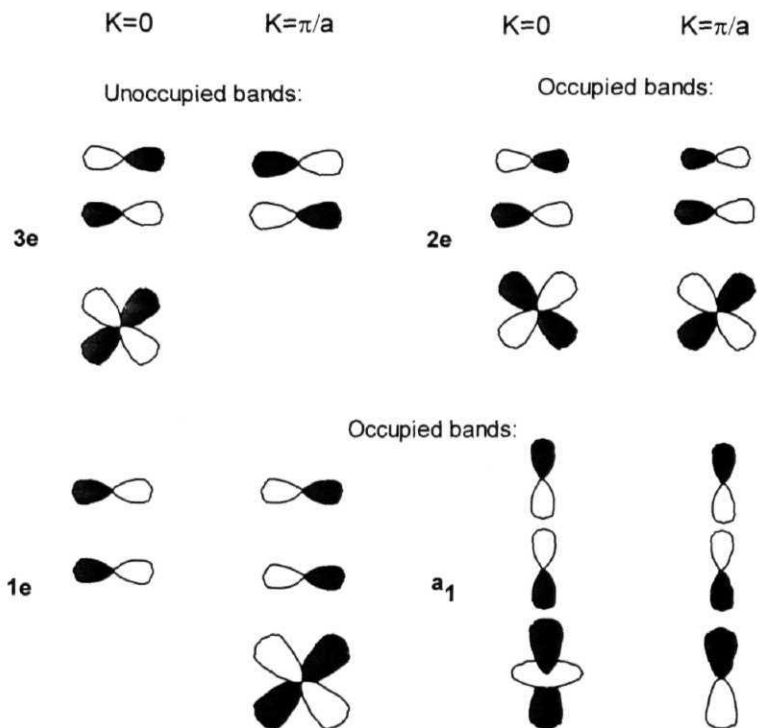
Fig. 2(a): The energy bands of the Polymer $[Fe(PH_3)_4\text{-}C{\equiv}C\text{-}]_n$.

Scheme 3
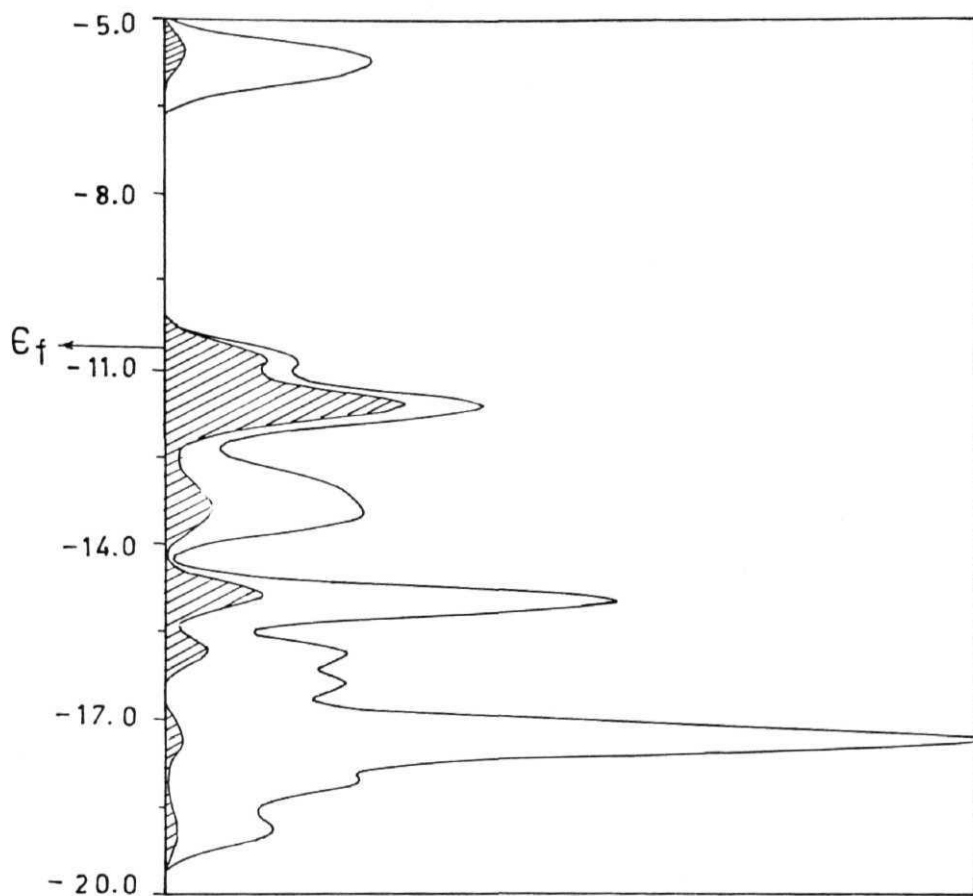
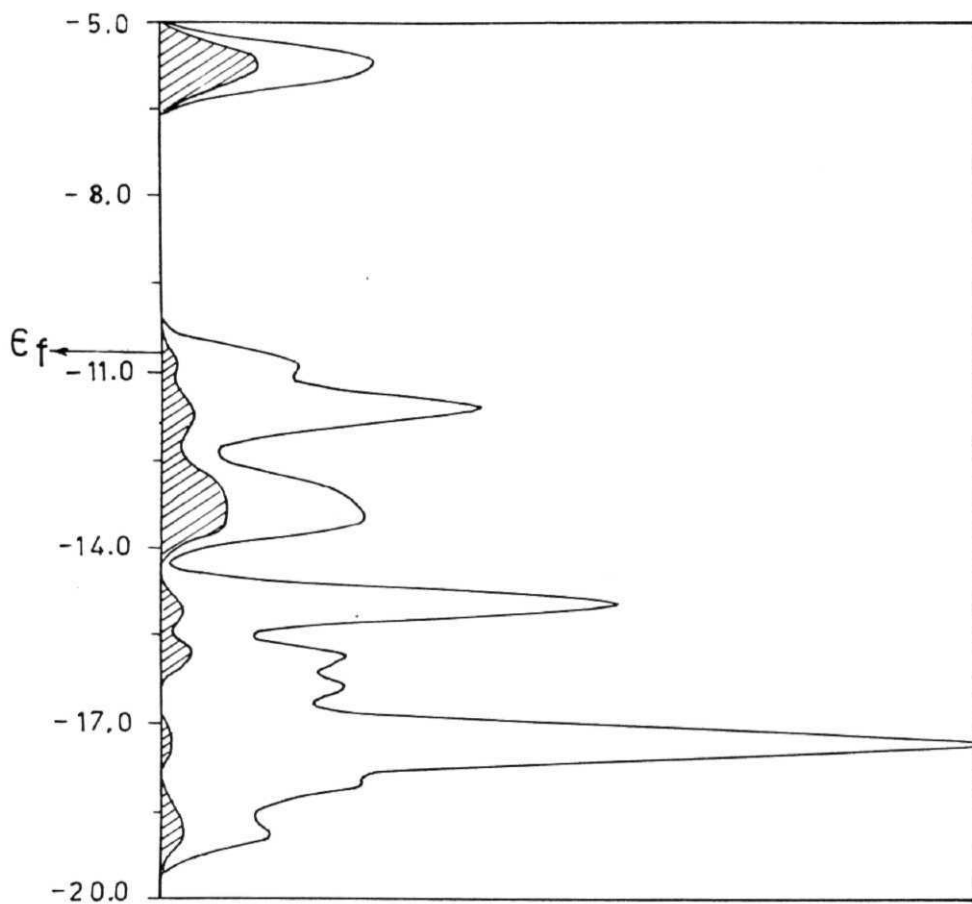Fig. 2(b): The projected DOS of Fe (shaded part) in $[Fe(PH_3)_4-C{\equiv}C-]_n$ polymer.

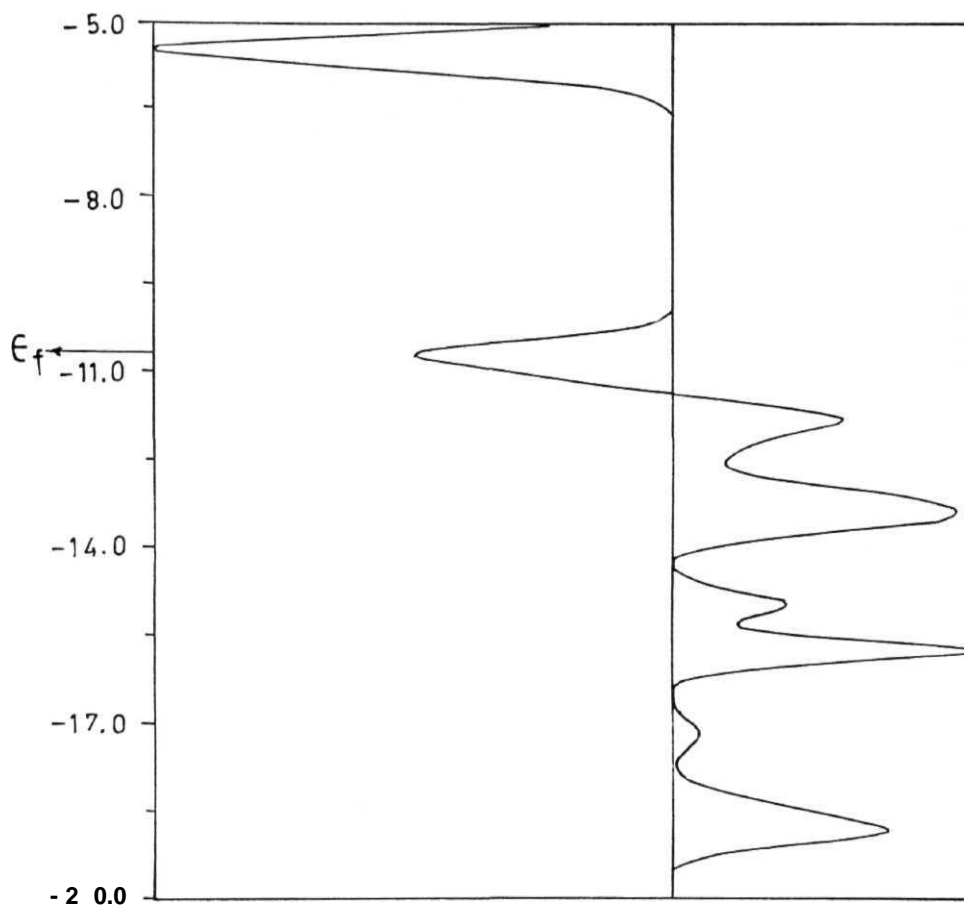Fig. 2(c): The projected DOS of acetylenic carbon (shaded part) in $[Fe(PH_3)_4\text{-}C{\equiv}C\text{-}]_n$ polymer.

Fig. 2(d): The crystal orbital overlap population between Fe and acetylenic carbon in $[Fe(PH_3)_4-C\equiv C-]_n$ polymer. Ef denotes the Fermi energy level.
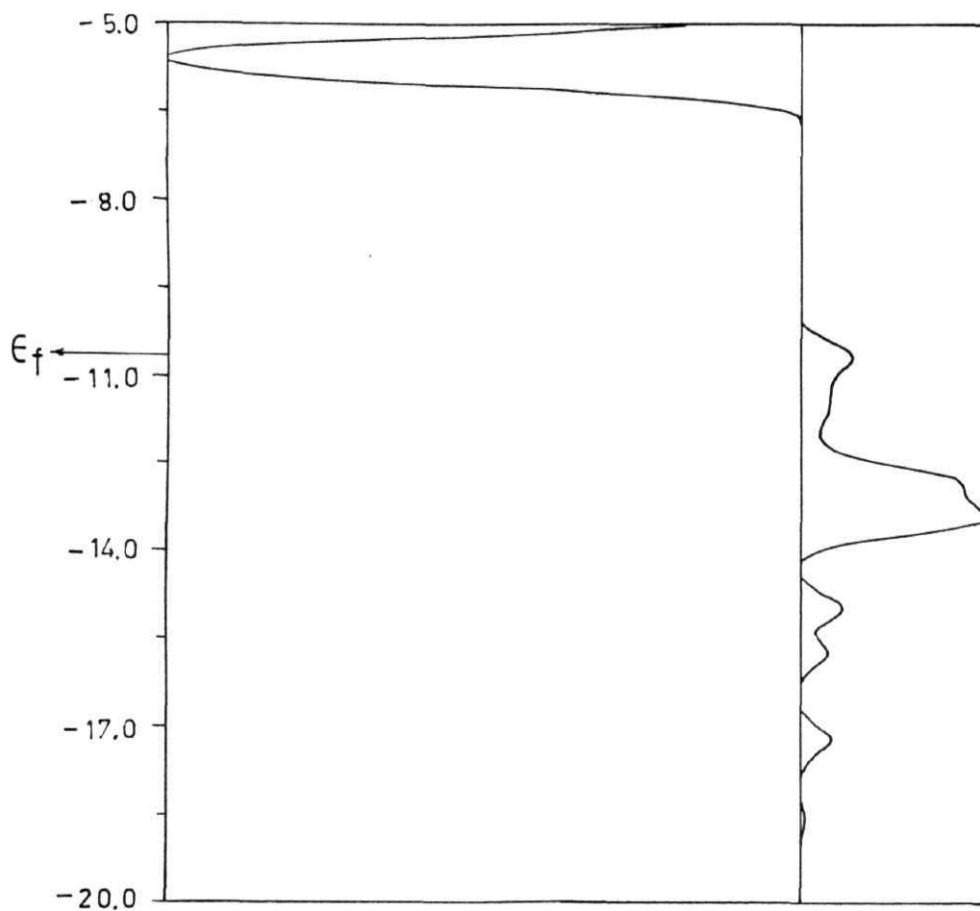
Fig. 2(e): The crystal orbital overlap population of C≡C in [Fe(PH₃)₄-C≡C-]ₙ polymer.   ef denotes the Fermi energy level.

At Fermi level, the valence band 2e is doubly degenerate with metal xz, yz anti-bonding combinations. Ligand π_1^* and π_2^* mix with metal xz, yz in bonding fashion at zone center (k=0). On the other hand, ligand $n \setminus$ and π_2 mix with metal xz, yz in anti-bonding fashion at the zone edge (k= *n/a)* (scheme 3). The Fe-C crystal orbital overlap population has shown that it is strong anti-bonding between iron and carbon (Fig.2d). The crystal orbital overlap population between the two carbons in acetylene is bonding type (Fig.2e); that is, the *n* bonding between metal, and ligand and the *n* anti-bonding within the acetylene which is shown at the zone center is very transient. The anti-bonding interactions between the metal and the ligand and the bonding interactions within the acetylene will be dominant as k changes from 0 to π/a. In summary, the valence band is rich in metal participation and is anti-bonding with ligand *n* orbitals.

Pure metal (xy) band $1b_2$ is not effected as k changes from 0 to *n/a.* The doubly degenerate ligand π band (1e) runs down in energy from zone center to zone edge. It is pure ligand π at k = 0; at k = *n/a,* ligand *n* mixes with metal xz and yz in bonding fashion (scheme 3). Projected DOS of iron shows that the participation is less in this band (Fig.2b). Fe-C and C-C crystal orbital overlap populations support bonding interactions within acetylene and between metal and ligand (Fig.2d,e). The $1a_1$ band is pushed up in energy when k changes from 0 to *n/a.* At the zone center, metal z^2 interacts with ligand σp_y, while at the zone edge metal p_y mixes with ligand σp_y (Scheme 3).

As in the case of platinum, we have increased the unit cell size by increasing the number of acetylene groups in the polymer for bridging
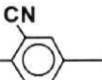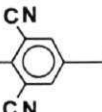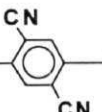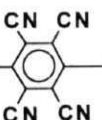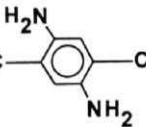
184

ligands. The polymers that have been taken in this process are di and tri-acetylenic polymers 4b and 4c (Scheme 1). Similar to that of polymer 4a, the metal participation is rich in valence band and ligand π participation is rich in conduction band. Lowest unoccupied bands are doubly degenerate ligand π^* and valence bands are doubly degenerate metal xz and yz antibonding bands at Fermi level. This is similar to those found for mono acetylenic polymer, 4a.

In the process of changing the bridging ligands in the polymers, we have taken 4d, 4g and 4i (Scheme 1) for calculations to see the effect of the substituents in the 8th group. The results in 4d are similar to the previously known calculations.[18] In these polymers, the valence and conduction bands are not degenerate as in 4a, due to the loss of C_{4v} symmetry. At the Fermi level, the characteristics of the conduction and valence bands are similar to those of 4a. The conduction band is ligand n^* and the valence band is having an antibonding interaction between the ligand π and the metal xz. The valence band has lost its metal participation as k changes from 0 to n/a in the case of 4i; while, in the case of 4d and 4g, the antibonding interactions between metal and ligand have changed to nonbonding interactions. These results are very much similar to that of the platinum analogues.

Band gap as a function of bridging ligand and metal

The band gaps for various polymers are given in Table 3. Experimental results (wherever available) have been given in parentheses for substituted systems. The band gap decreases as we go from mono

Table 3: Calculated Band gaps for various polymers in the present study.

Unit cell	Band gap (eV)			
	Pt	**Pd**	**Ni**	**Fe**
M—C≡C	2.7	3.7	3.8	4.6
M—C≡C—C≡C	2.4 (3.0)[a]	2.9 (3.2)	3.1 (3.6)	3.0
M—C≡C—C≡C—C≡C	2.2 (2.7)	2.5	2.6	2.4
M—C≡C—⟨benzene⟩—C≡C	2.1	2.4	2.5	2.2
M—C≡C—⟨benzene, CN⟩—C≡C	2.0	–	–	–
M—C≡C—⟨benzene, CN, CN⟩—C≡C	1.9	–	–	–
M—C≡C—⟨benzene, CN, CN⟩—C≡C	1.7	1.7	1.9	1.3
M—C≡C—⟨benzene, CN CN, CN CN⟩—C≡C	1.6	–	–	–
M—C≡C—⟨benzene, H_2N, NH_2⟩—C≡C	1.8	2.1	2.0	2.0

[a]The values in parentheses are experimental results (ref. 15)

acetylene (1a) to diacetylene (1b) and then to triacetylenic (1c) polymers. That is, by increasing the distance between the metals in the polymer the band gap is getting decreased. The lowest charge transfer electronic spectra of polymer $[Pt(PBu_3)_2-C_4-]_n$ has been found at 414 nm (3.0 eV)[15]. For triacetylenic polymer, the minimum excitation energy is 2.7 eV.[15] Our calculations have shown that the band gap for diacetylenic and triacetylenic model polymers is 2.4 eV and 2.2 eV respectively, indicating general agreement with the experimental results. Among the conjugated polymers, band gaps have been decreased by C=C back bone alteration and substituents.[12] We have seen the same effect in the polymers **1d, 1e, 1f**, 1g, **1h** and **1i**. When one acetylenic group in substituted by benzene in triacetylenic polymer, the band gap decreases from 2.2 eV to 2.1 eV. However, it is not a large decrease. Substitution of one cyano group on benzene ring in 1e decreases the energy gap to 2.0eV. If two cyano groups are at **meta** position **(1f),** the band gap is 1.9eV. When the two cyano groups are para to each other (1g), the decrease in band gap is large (the gap is 1.7eV). This shows that not only the substituents but also the topology of the substituents effect the band gaps. The band gap for tttracyano substituted phenyl polymer, 1h, is not up to the expectation. **Amino** substituents (1i) also have caused small band gaps; but, the changes are not as dramatic as for cyano substituents. Ni and Pd also have shown the same trend as Pt.

The band gap for **1f** is 1.9eV; while, for 1g it is 1.7eV. The only difference between the two polymers is the topology of cyano groups. In **1f,** the cyano groups are in meta position to each other; whereas, in 1g, cyano groups are in para position to each other. The change in the band structure

for these polymers is stabilization of conduction band. The conduction band of lg is lower in energy compared to the conduction band of **1f** at Fermi level. The decrease in energy of conduction band from **1f** to lg is 0.2eV. This is the difference that has been projected in the band gaps. The main change that has effected the conduction band of these two polymers is overlap between the phenyl and cyano groups. The overlap is more in lg compared to that of **1f**. The crystal orbital overlap population for lg is 1.0; whereas, for **1f** it is 0.5. This supports the decrease in energy of conduction band at Fermi level in lg compared to that of **1f**.

In the case of Fe polymers, the decrease of band gap is sharp as we change the bridging ligands. From mono acetylenic polymer to diacetylenic polymer, the decrease in band gap is 1.6 eV. From diacetylenic to triacetylenic, the change is 0.6 eV. But, from 4c to 4d, the change is only 0.2eV. In the Fe polymers also, the substituents on phenyl groups have effected the band gaps. Two cyano groups in para to each other on phenyl, lg, has the band gap of 1.3 eV; whereas, for **amino** groups, 4i, the band gap is 2.0 eV.

Thus, present studies show that in the $[Pt(PH_3)_2-C\equiv C-]_n$ polymer the valence band is mainly metal based and the conduction band mostly ligand based. Other polymers of the Pt with increased number of C_2 units have also shown similar results. Therefore, the lowest energy band in the electronic spectra is the metal to ligand charge transfer, which is in tune with the experimental finding. Ni and Pd also have shown similar results. In the case of Fe polymer (4a) the conduction band is purely ligand based π^* and the valence band is rich in metal participation showing the

similarities with the polymer la. When the bridging ligands are changed from one C_2 unit to two and three C_2 units, there is a general decrease in the band-gap. Not only the substitution on phenyl ring but also the topology of the substitution on phenyl ring also effects the band gap of the polymer. The cyano substitution is found to be more effective in reducing the band gaps of the polymer.

References

1 .(a) *Proceedings of the International Conference of Synthetic Metals.* Labes, U.U. Ed. *Mol. Cryst. Liq. Cryst.* **1985,** vol. 117-121, parts A-E.

   (b) *Extended Linear Chain Compounds.* Miller, J.S. Ed. Plenum: New York, 1982 Vol. 1-3.

2.(a) Williams, D.J. *Angew. Chem. Int. Ed. Eng.* **1984** *23,* 690.

   (b) Chisholm, M.H. *Angew. Chem. Int. Ed Engl.* **1991,** *30,* 673.

2.(a) Tsukamoto, J.; Ohigashi, H.; Matsumura, K.; Takahashi, A. *Synth. Met. 1982,4,* 177.

   (b) Weinberger, B.R.; Akhtar, M; Gan, S.C. *Synth. Met.* **1982,** *4,* 187.

3.   Cohen, M.J.; Harris, J.S. *Appl. Phys. Lett.* **1978,** *33,* 812.

4.   Potember, R.S.; Poehler, T.O; Benson, R.C. *Appl. Phys. Lett.* **1982,** *41,* 548.

5.(a) Kaneto, K.; Maxfield, M.; Nairns, D.P.; MacDiarmid, A.G.; Heeger, A.J. *J. Chem. Soc, Faraday Trans.* 1 **1982,** *78,* 3417.

   (b) Nigrey, J.P.; MacDiarmid, A.G.; Heeger, A.J. *Mol. Cryst. Liq. Cryst.* **1982,** Si, 1341.

   (c) Shacklette, L.W.; Elsenbaumer, R.L.; Chance, R.R.; Sowa, J.M.; Ivory, D.M.; Miller, G.G.; Baughman, R.H. *J. Chem. Sco., Chem. Commun.* 1982,6,361.

6.(a) Chidsey, C.E.D.; Murray, R.W. *Science* **1986,** *231,* 25.

   (b) Kittleson, G.P.; White, H.S.; Wrighton, M.S. *J. Am. Chem. Soc.* **1984,** *106,* 7389.

7.   Frank, A.J.; Honda, K. *J. Phys. Chem.* **1982,** *86,* 1933.

8.(a) Burgmayer, P.; Murray, R.W. *J. Phys. Chem.* **1984,** *88,* 2515.

   (b) Burgmayer, P.; Murray, R.W. *J. Electoanal. Chem.* **1983,** *147,* 339.

9.   Zinger, B.; Miller, L.L. *J. Am. Chem. Soc.* **1984,** *106,* 6861.

10.(a) Wu, W.; Kivelson, S. *Synth. Met.* **1989,** *28,* D575.

   (b) Marder, T.B.; Lesley, G.; Yuan, Z.; Fyfe, H.B.; Chow, P.; Stringer, G.; Jobe, I.R.; Taylor, N.J.; Williams, I.D.; Kurtz, S.K. *ACS Symp. Ser.* **1991,** *No. 455,605.*

   (c) Porter, P.L.; Guha, S.; Kang, K.; Frazier, C.C. *Polymer* **1991,** *32,* 1756.

   (d) Prasad, P.N.; Williams, D.J. *Introduction to Nonlinear Optical Effects in Molecules and Polymers;* Wiley-Interscience: New York, 1991.

11. Kabayashi, M.; Colaneri, N.; Boysel, M.; Wudl, F.; Heeger, A.J. *J. Chem. Phys.* **1985,** *82,* 5717.

12. Kurti, J.; Surjan, P.R.; Kertesz, M. *J. Am. Chem. Soc.* **1991,** *113,* 9865.

13. Hagihara, N.; Sonogashira, K.; Takahashi, S. *Adv. Poly. Sci.* **1980,** *41,* 149.

14. Sonogahira, K.; Ohga, K.; Takahashi, S.; Hagihara, N. *J. Organomet. Chem.* **1980,** *188,* 237.

15. Johnson, B.F.G.; Kakkar, A.K.; Khan, M.S.; Lewis, J.; Dray, A.E.; Friend, R.H.; Wittmann, F. *J. Mater. Chem.* **1991,** *1,*485.

16. (a) Johnson, B.F.G.; Kakkar, A.K.; Khan, M.S.; Lewis, J. *J. Organomet. Chem.* **1991,** *401,* C12.

   (b) Davies, S.J.; Johnson, B.F.G.; Khan, M.S.; Lewis, J. *J. Chem. Soc, Chem. Commun.* **1991,** 187.

   (c) Fyfe, H.B.; Mlekuz, M.; Zargarian, D.; Taylor, N.J.; Marder, T.B. *J. Chem. Soc, Chem. Commun.* **1991,** 188.

   (d) Khan, M.S.; Davies, S.J.; Kakkar, A.K.; Schwartz, D.; Lin, B.; Johnson, B.F.G.; Lewis, J. *J. Organomet. Chem.* **1992,** *424,* 87.

17. (a) Chow, P.; Zargarian, D.; Taylor, N.J.; Marder, T.B. *J. Chem. Soc, Chem. Commun.* **1989,** 1545.

   (b) Field, L.D.; George, A.V.; Hambley, T.W.; Malouf, E.Y.; Young, D.J. *J. Chem Soc, Chem. Commun.* **1990,** 931.

   (c) Davies, S.J.; Johnson, B.F.G.; Lewis, J.; Khan, M.S. *J. Organomet. Chem.* **1991,** *401,* C43.

   (d) Akita, M.; Terada, M.; Oyama, S.; Moro-oka, Y. *Organometallics* 1990,9,816.

   (e) Onitsuka, K.; Ogawa, H.; Joh, T.; Takahashi, S.; Yamamoto, Y.; Yamazaki, H. *J. Chem. Soc, Dalton Trans.* **1991,** 1531.

   (f) Wong, A.; Kang, P.C.W.; Tagge, C.D.; Leon, D.R. *Organometallics* **1990,** *9,* 1992.

   (g) Chukwu, R.; Hunter, A.D.; Santarsiero, B.D.; Bott, S.G.; Atwood, J. L.; Chassaignac, J. *Organometallics* **1992,** *11,* 589.

   (h) Dray, A.E.; Wittmann, F.; Friend, R.H.; Donald, A.M.; Khan, M.S.; Lewis, J.; Johnson, B.F.G. *Synth. Met.* **1991,** *41-43,* 871.

18. Frapper, G.; Kertesz, M. *Inorg. Chem.* **1993,** *32,* 732.

19. (a) Andre, J.-M. *J. Chem. Phys.* **1969,** *50,* 1536.

   (b) Andre, J.-M. *Electronic Structure of Polymers and Molecular Crystals.* Andhre, J.-M.; Ladik, J. Eds. Plenum: New York, 1974.

191

(c) Hoffmann, R. *J. Chem. Phys.* **1963,** *39,* 1397.

(d) Hoffmann, R.; Lipscomb, W.N. *J. Chem. Phys.* **1962,** *36,* 2179.

(e) Hoffmann, R.; Lipscomb, W.N. *J. Chem. Phys.* **1963,** *37,* 2872.

(f) Hoffmann, R. *Angew. Chem. Int. Ed. Engl.* **1987,** *26,* 846.

20.(a) Albright, T.A.; Hofmann, P.; Hoffmann, R. *J. Am. Chem. Soc.* **1977,** *99,* 7546.

(b) Elian, M.; Hoffmann, R. *Inorg. Chem.* **1975,** *14,* 1058.

(c) Schilling, B.E.R.; Hoffmann, R. *J. Am. Chem. Soc.* **1979,** *101,* 3456.

21. Orpen, A.G.; Brammer, L.; Allen, F.H.; Kennard, O.; Waston, D.G.; Taylor, R. *J. Chem. Soc, Dalton. Trans,* **1989,** S1.

Theoretical calculations using extended Huckel method on Ti_8C_{12} has shown the following results.

i) Ti_8C_{12} cluster is found to be highly electron deficient species.

ii)   The C_2 units in structures 1, 2 and 3 interacts with the transition metal fragment $Pt(PH_3)_2$, with a net effect of electron transfer from $Pt(PH_3)_2$ to Ti_8C_{12}.

iii)   Despite the structural differences all the Ti metals in 1, 2 and outer Ti metals in 3 showed the capability of complexing with CO's.

iv)   Due to the high electron deficient nature, Ti_8C_{12} may exist as associated clusters in soot.

The band structure calculations on metal-containing **poly-yne** polymers have shown the following results.

i)   The valence band is found to be metal based and the conduction band is found to be mainly ligand based, hence the lowest energy band in the electronic spectra is the metal to ligand charge transfer which is in accordance with the experimental findings.

ii)   The band gap between valence and conduction bands depends on both the metal and the ligand.

iii)   The calculated band gaps in model polymers **1b, 1c,** 2b and 3b have reproduced the general trends found in experiments.

iv)   The dicyano substitution on phenyl ring is found to be more effective in decreasing the band gap of these polymers.

Vitae

Mr. G. Naga Srinivas was born on 10th May, 1967 at Penugonda, Andhra Pradesh. Following his schooling in his native, he completed his B.Sc. degree in S.K.B.R. College, Amalapuram. Later, he joined the School of Chemistry, University of Hyderabad, Hyderabad for his M.Sc., and M.Phil degree. Subsequently, he joined for the Ph.D programme in 1990. He has been UGC JRF and SRF since 1989 and is presently continuing as a DST SRF.

List of Publications

1. E.D. Jemmis and **G. Naga Srinivas** (1996)
   Contrasting stabilities of classical and bridged pyramidal Si_3H_3X molecules (X = BH^-, CH, N, NH^+, NO, SiH, P, PH^+ and PO).
   J. Am. Chem. Soc, 1996, **118,** 3738-3742

2. **G. Naga Srinivas,** B. Kiran and E.D. Jemmis (1996)
   H-Bridged alternatives to the homologues of Cyclopropane
   J. Mol. Str. (THEOCHEM) 1996, **361,** 205-210.

3. E.D. Jemmis, **G. Naga Srinivas, J.** Leszczynski, J. Kapp, A.A. Korkin and P.v.R. Schleyer (1995)
   Group 14 analogs of the cyclopropenium ion: Do they favor classical aromatic structures?
   J. Am. Chem. Soc, 1995, **117,** 11361-11362.

4. E.D. Jemmis, G. Subramanian and **G. Naga Srinivas** (1994)
Pyramidal structures with a B_3H_6 ring. Possibility of terminal
hydrogens opposite the capping group.
Inorg. Chem., 1994, 33, **2317-2319.**

5. **G. Naga Srinivas,** H. Srinivas and E.D. Jemmis (1994)
Electronic structure study of the reactivity centers in Ti_8C_{12} clusters.
Proc. Indian. Acad. Sci. (Chem. Sci.), 1994, **106, 169-181.**

6. E.D. Jemmis, G. Subramanian and **G. Naga Srinivas** (1992)
Boron analogs of cyclopropenyl cation: $B_3H_6^+$, the first nonplanar
2π aromatic.
J. Am. Chem. Soc, 1992, **114,** 7939-7941.

7. **G. Naga Srinivas** and T.P. RadhaKrishnan (1991)
Structure-resonance calculation of the ionization potential of
saturated hydrocarbons.
J. Mol. Str.(THEOCHEM), 1991, **246,** 289-300.

{Manuscripts under preparation)
8. E.D. Jemmis, **G. Naga Srinivas, A.A. Korkin** and P.v.R. Schleyer
An *ab initio* MO study of the isomers of $Si_3H_3^+$.

9. E.D. Jemmis and **G. Naga Srinivas**
H-Bridged structures for tetrahedranes A4H4 (A = C, Si, Ge, Sn and
Pb) through isolobal and isosynaptic analogies.

10. E.D. Jemmis and **G. Naga Srinivas**
    Heavier analogs of Cyclobutane.

11. E.D. Jemmis, **G. Naga Srinivas** and M. McKee
    Sandwich compounds in Silicon chemistry.